Univerzita Karlova v Praze

Přírodovědecká fakulta

Studijní program: Biochemie

Studijní obor: Biochemie

Bc. Sandra Lettlová

Úloha signalizační dráhy Hippo v regulaci metabolismu nádorových buněk

Role of the Hippo Signalling Pathway in Tumour Cell Metabolism

Diplomová práce

Vedoucí diplomové práce: Prof. RNDr. Marie Stiborová, DrSc.

Školitel: Prof. Ing. Jiří Neužil, CSc.

Praha, 2013

Prohlášení:

Prohlašuji, že jsem závěrečnou práci zpracovala samostatně a že jsem uvedla všechny použité informační zdroje a literaturu. Tato práce ani její podstatná část nebyla předložena k získání jiného nebo stejného akademického titulu.

V Praze,

.....

Podpis

Poděkování

Na tomto místě bych ráda poděkovala svému školiteli Prof. Ing. Jiřímu Neužilovi, CSc. za zadání tématu diplomové práce, odborné vedení a laskavý přístup při jejím zpracování a také vedoucí mojí práce Prof. RNDr. Marii Stiborové, DrSc. za ochotu a vstřícnost. Zvláštní dík pak patří Mgr. Jaroslavu Truksovi, Ph.D. za metodické vedení a cenné rady při zpracování diplomové práce. V neposlední řadě také děkuji i všem kolegům z Laboratoře molekulární terapie za jejich pomoc při experimentální práci, velkou podporu a příjemnou pracovní atmosféru.

Abstract

Vitamine E analogues α-tocopheryl succinate (α-TOS) and mitochondrially targeted vitamine E succinate (MitoVES) are anti-cancer agents from the group of "mitocans", the compounds acting via mitochondria which present a promising invariant target for cancer cell therapy. α-TOS and MitoVES induce apoptosis selectively in various cancer cell types involving generation of reactive oxygen species (ROS). Generated superoxid anion radicals in response to α-TOS and MitoVES are believed to be converted into hydrogen peroxide that is known to activate Mammalian sterile 20-like kinase (Mst1), the central component of Hippo signalling pathway, that presents an universal size control mechanism in all metazoans and its deregulation is linked to tumourigenesis. MitoVES and α-TOS were both reported to activate Mst1 that phosphorylates Forkhead box O1 (FoxO1) transcription factor resulting in its transport to nucleus where induce the expression of pro-apoptotic genes, including *NOXA*, and thus promote apoptosis. The target of Hippo signalling pathway is transcriptional co-activator Yes-associated protein (Yap) which was found in *Drosophila melanogaster* to regulate the expression of transcription factor c-Myc which is known as the most prominent human oncogene. This thesis focused on involvement of Hippo signalling pathway in regulation of *C-MYC* gene expression and the clarification of the influence of altered c-Myc expression on the expression c-Myc target genes that are involved in the metabolism of glucose and glutamine (*SCL38A3*, *ENO1, HK2* and *GLUT1)* in response to α-TOS, MitoVES and hydrogen peroxide treatment. For this purpose a Jurkat cancer cell line was used. Obtained data show that α-TOS, MitoVES and hydrogen peroxide induce Mst1 activation followed by Yap nuclear export and cytoplasmic degradation, and downregulation of c-Myc mRNA and protein expression. Moreover, the activation of Mst1 does not correspond to ROS generation in case of α-TOS suggesting for some ROS-independent mechanism of Mst1 activation. Since Yap and c-Myc increased activity contributes to wide range of human cancers their inactivation may present, next to the Mst1-FoxO1-*NOXA* pathway, another possible mechanism of α-TOS and MitoVES anti-tumourigenic action. Moreover, MitoVES causes massive dissipation of mitochondrial inner membrane potential, increased glucose uptake and lactate production suggesting for glycolytic switch during mitochondria impairement. Unfortunately, statistically significant effect of both analogues and hydrogen peroxide on c-Myc target

genes *SCL38A3* and *ENO1* was not observed under used experimental conditions, only *HK2* and *GLUT1* showed a statistically significant slight decrease. (In English)

Key words: Vitamin E analogues, c-Myc, mitochondria, Mst1, reactive oxygen species, Yap

Abstrakt

Analogy vitaminu E, α-tokoferyl sukcinát (α-TOS) a mitochondriálně cílený vitamin E sukcinát (MitoVES), jsou látky s protinádorovým účinkem ze skupiny "mitokanů", která se vyznačuje tím, že účinkuje prostřednictvím mitochondrií, jenž představují nadějný cíl protinádorové léčby. α-TOS a MitoVES selektivně indukují apoptózu v různých typech nádorových buněk pomocí generace reaktivních forem kyslíku (ROS). Generovaný superoxidový anion radikál je přeměněn na peroxid vodíku, který je znám jako aktivátor „Mammalian sterile 20-like kinase“ (Mst1). Mst1-kináza je součástí signalizační dráhy Hippo, která představuje mechanismus zodpovědný za správný vývoj a velikost orgánů u mnohobuněčných organismů a její deregulace je spojena s vývojem nádorového onemocnění. α-TOS a MitoVES aktivují Mst1-kinázu, která dále fosforyluje transkripční faktor „Forkhead box O1“ (FoxO1), což vede k jeho transportu do jádra, kde aktivuje expresi pro-apoptotických genů, mezi nimiž je i gen pro „*Phorbol-12-myristate-13-acetate-induced protein 1“ (NOXA)*, a tím indukuje apoptózu. Cílem signalizační dráhy Hippo je transkripční ko-aktivátor „Yes-associated protein“ (Yap), jenž u *Drosophila melanogaster* reguluje expresi transkripčního faktoru a významného lidského onkogenu c-Myc. Diplomová práce je zaměřena na objasnění vlivu signalizační dráhy Hippo na regulaci exprese genu *C-MYC* a jím ovlivněných cílových genů podílejících se na metabolismu glukózy a glutaminu (*SCL38A3*, *ENO1*, *HK2* a *GLUT1*) za použití α-TOSu, MitoVESu a peroxidu vodíku jako induktorů dráhy Hippo. Pro tento účel byla použita buněčná linie Jurkat. Získané výsledky ukazují, že α-TOS, MitoVES a peroxid vodíku aktivují Mst1-kinázu, poté následuje fosforylace, jaderný export a cytoplazmatická degradace proteinu Yap, a také snížení exprese genu *C-MYC* a jeho proteinu. Navíc, aktivace Mst1 neodpovídá v případě α-TOS generaci ROS, což poukazuje na mechanismus aktivace Mst1, který je na ROS nezávislý. Vzhledem k tomu, že zvýšená aktivita proteinů Yap a c-Myc přispívá ke vzniku nádorových onemocnění, jejich inaktivace může být vedle dráhy Mst1-FoxO1-*NOXA* dalším možným mechanismem, kterým α-TOS a MitoVES potlačují nádorový růst. Kromě toho, MitoVES indukuje masivní „disipaci“ mitochondriálního membránového potenciálu a také nárůst ve vychytávání glukózy korelujícího se zvýšenou produkcí laktátu naznačující adaptaci buněk při pozměněné funkci mitochondrií získáváním energie metabolismem glukózy. Bohužel, statisticky významný účinek obou analogů a peroxidu vodíku na expresi genů regulovaných

proteinem c-Myc nebyl za použitých experimentálních podmínek pozorován u *SCL38A3* a *ENO1*, statisticky významný slabý pokles byl zaznamenám pouze u *HK2* a *GLUT1*. (In English)

Key words: Analogy vitaminu E, c-Myc, mitochondrie, Mst1, reaktivní formy kyslíku, Yap

Content

List of abbreviations

AIF	Apoptosis inducing factor
ANT	Adenine nucleotide transporter
APS	Ammonium peroxodisulphate
ATB	Antibiotic
Bak	Bcl-2 homologous antagonist/killer
Bax	Bcl-2–associated X protein
Bcl	B cell lymphoma
Bcl-x_L	Bcl-extra large
BH	Bcl-2 homology domains
Bid	BH3-interacting domain death agonist
BIS	N,N-methylen-bis-akrylamid
BSA	Bovine serum albumin
CAD	Caspase-activated DNase
CI-IV	Mitochondrial complex I-IV
CK1δ/ε	Casein kinase 1 δ/ε
CoA	Coenzyme A
Cyt c	Cytochrome c
DCF-DA	2´,7´-dichlorodihydrofluorescein diacetate
DISC	Death-inducing signalling complex
dMyc	Diminutive Myc
DR	Death receptor
Ds	Cadherin-like protein Dachsous
Endo G	Endonuclease G
Eno1	Enolase1
ETC	Electron transport chain
Ex	Expanded protein
FADD	Fas-associated death domain
Fat	Fat-like cadherin-related tumour suppressor homologue
FBS	Fetal bovine serum
FERM	4,1 protein/Ezrin/Radixin/Moesin domain
FITC	Fluorescein isothiocyanate

Fj	Four-jointed kinase
FoxO	Forkhead box O
FRMD	FERM domain-containing protein
GLS	Glutaminase
Glut1	Glucose transporter type 1
HEPES	4-(2-Hydroxyethyl)piperazine-1-ethanesulfonic acid
HIF-1α	Hypoxia-inducible factor-1α
HK	Hexokinase
Hpo	Hippo kinase
HtrA2	High temperature requirement protein A2
IAP	Inhibitor of apoptosis
IgG	Immunoglobulin type G
IMM	Inner mitochondrial membrane
Lats1	Large tumour suppressor 1
LDH	Lactate dehydrogenase
LPA	Linear polyacrylamide
Mats	MOB kinase activator-like 1
Mcl-1	Myeloid leukemia cell differentiation protein
Mer	Moesin/ezrin/radixin homologue 2 known as Merlin
MitoVES	Mitochondrially targeted vitamin E succinate
Mob1	MOB kinase activator 1A and 1B
MOMP	Mitochondrial outer membrane permeabilization
Mst1	Mammalian sterile 20-like kinase 1
mtDNA	mitochondrial DNA
2-NBDG	2-(N-(7-Nitrobenz-2-oxa-1,3-diazol-4-yl)Amino)-2-Deoxyglucose
NF2	Neurofibromin
Noxa	Phorbol-12-myristate-13-acetate-induced protein 1
NP40	Nonidet P 40
OAA	Oxaloacetic acid
OMM	Outer mitochondrial membrane
p53	Tumour suppressor protein 53
PBS	Phosphate buffered saline
PI	Propidium iodide

PP2A	Protein phosphatase 2A
Puma	p53 upregulated modulator of apoptosis
qPCR	Quantitative PCR
RIPA	Radio-Immunoprecipitation Assay
ROS	Reactive oxygen species
RPLP0	Human ribosomal protein large P0
RT	Room temperature
S.E.M.	Standard error of the mean
Sav	Salvador protein
$SCF^{\beta\text{-}TRCP}$	SKP1-CUL1-F-box protein E3 ubiquitin ligase with the substrate recognition component F-box/WD repeat-containing protein 1A β-TRCP
Sd	Scalloped
SDH	Succinate dehydrogenase
SDS	Sodium dodecyl sulphate
SLC38A5	sodium-coupled neutral amino acid transporter 5
Smac/DIABLO	Second mitochondria-derived activator of caspases/direct inhibitor of apoptosis-binding protein with a low isoelectric point
SMase	Sphingomyelinase
tBid	Truncated Bid
TBS	TRIS buffered saline
TCA	Tricarboxylic acid
TE	Buffer containing 10 mM Tris and 100 mM EDTA, pH 8.0
TEAD/TEF	Transcriptional enhancer factors containing the TEA/ATTS DNA-binding domain
TEMED	N,N,N´,N´-tetramethylethylendiamin
TMRM	Tetramethylrhodamine methyl ester perchlorate
TNF	Tumour necrosis factor
TPP^{+}	Triphenylphosphonium cation
TRIS	Tris(hydroxymethyl)aminomethan
UbQ	Ubiquinone
VDAC	Voltage-dependent anion channel
VE	Vitamin E

Wts	Warts kinase
XIAP	X-linked IAP
Yap	Yes-associated protein
Yki	Yorkie
α -TOS	α-Tocopheryl succinate
α-KG	α-Ketoglutarate
α-TOH	α-Tocopherol
$\Delta\psi_m$	Mitochondrial inner trans-membrane potential

I. LITERATURE SURVEY

I.1. Introduction into cancer

I.1.1. Cancer definition

Cancer is the term for broad spectrum of diseases with common features involving abnormal cell division without control. Fast-proliferating cancer cells can also spread from the original site to other body parts where they form secondary tumours, metastases, which are often the cause of death. In economically developed countries, cancer is a leading cause of death. The burden of cancer incidence is a result of population growth and aging, environment and adoption of cancer supporting lifestyle such as lack of physical activity, obesity, bad diet, smoking and stress (Jemal *et al.*, 2011). It is estimated that the total of 1,638,910 new cancer cases and 577,190 deaths from cancer occurred in the United States in 2012, where one of four deaths is due to cancer (Siegel *et al.*, 2012). Although cancer was primary the disease of the aging population, it is increasingly diagnosed also in young people at present. Cancer is often very hard to cure with unpredictable outcome; for some types of cancer, e.g. malignant mesothelioma, there is no cure at the moment. The understanding of transformation of normal cells into cancer cells, properties and metabolism of cancer cells can help us to develop new anti-cancer agents, which will selectively kill cancer cells while they will be non-toxic to normal cells.

I.1.2. General characteristics of cancer cells

Since cancer develops from various mutations in the genome, one can say that cancer is, at least partially, a genetic disease. Development of a malignant tumour is hardly caused by a single genetic mutation and, rather, it is a multi-step process of subsequent alterations in many genes. Genes whose mutations contribute to the malignant transformation are called oncogenes and tumour suppressor genes. Products of oncogenes are proteins acting as transcription factors, chromatin re-modelling proteins, growth factors

and their receptors, signal transducers, and apoptosis regulators promoting cell proliferation and inhibiting cell differentiation and apoptosis. Oncogenic mutations usually lead to altered protein expression, which means that protein is produced in abnormal amounts; mutations can also result in the formation of a protein in its activated form. These and other processes are the starting point of the tumourigenic switch leading to transformation (Croce, 2008). On the other hand, protein products of tumour suppressor genes act as inhibitors of tumour progression and as activators of apoptosis, and are often inactivated in cancers. They regulate diverse cellular functions involving cell cycle checkpoint responses, detection and repair of DNA damage, protein ubiquitination and degradation, mitogenic signalling, cell differenciation and apoptosis induction. Whereas activation of oncogenes is genetically dominant, only one mutated allele is sufficient to cause the effect, tumor suppressor genes are recessive requiring inactivation of both alleles to inhibit their beneficial functions (Sherr, 2004).

To develop into a malignant tumour, cell has to undergo several alterations which together dictate the malignant growth. First of all, cancer cells must be able to sustain proliferative signalling. Normal cells require mitogenic growth signals to proliferate. Cancer cells overcome this need by several ways. They produce growth factor ligands themselves or stimulate normal cells to produce them. Receptor signalling can be also enhanced by elevated numbers of receptors on the cell surface or by alterations of such receptors in a way that facilitates ligand-independent receptor activation. Ligand-independent receptor activation and thus activation of certain signalling pathways regulating cell division is often mediated by mutations in the key components as tyrosine kinase, serin/threonine kinases, G-proteins or transcription factors. In addition to sustained proliferation, cancer cells must also evade the function of growth suppressors and the mechanism of contact inhibition. Growth supressors are represented by the two most common and often inactivated tumour suppressor genes encoding the retinoblastoma-associated protein (Rb) and the tumour suppressor protein 53 (p53). Both are important gatekeepers of the cell cycle progression, and their inactivation enables persistent proliferation. Furthermore, upon DNA damage, p53 can also arrest cell cycle progression, and when this damage is irreversible it induces apoptosis. Thus, mutations in the *P53* gene encoding p53 is also responsible for resisting cell death in cancer cells, and this occurs in more than 50% cases of human cancers. Apoptosis can also be diminished by increased expression of anti-apoptotic proteins or a decrease in the expression of pro-apoptotic

proteins from B cell lymphoma 2 (Bcl-2) protein family. Since normal cells can undergo only limited number of divisions, cancer cells must acquire the ability of immortal replication in order to form a tumour. They do so by the expression of telomerase, an enzyme that extends the ends of the telomeric DNA enabling thus its limitless replication. As the tumour formation progresses, cancer cells must induce angiogenesis, the formation of new blood vessels, which supply the increasing cell mass with nutrients and oxygen and also function to drain away the metabolic wastes and carbon dioxide. The hallmark of a malignant tumour is invasion and metastasis. It is a highly complex process when cancer cells leave the primary tumour and spread through blood stream and lymphatic system, and 'settle' in distant parts of the body where they create secondary tumours (Hanahan and Weinberg, 2000).

Two other major attributes of cancer cells arise from the above described six core hallmarks of cancer. Since the basic property of cancer cells is their constant proliferation, they must modify their energetic metabolism to accomplish the high energetic demands of growth and division. The details of cancer cell metabolism are discussed later in the section I.5. The next important characteristic of cancer cells is their ability to evade their killing by cells of the immune system. Although the alterations in cells leading to malignancy are originally recognized by the immune system, after some time the selective immune pressure develops a variant of cancer cells which escape from the check of the immune system and give rise to the formation of a carcinoma (Hanahan and Weinberg, 2011).

I.2. Apoptosis – the programmed cell death

I.2.1. The biological significance of apoptosis

The programmed cell death, apoptosis, is a conserved mechanism by which multicellular organisms remove unwanted or damaged cells. It is an inherent part of animal development, where it ensures the proper organ function by maintaining the tissue architecture. The classical example is correct separation of fingers during embryogenesis. Those are originally connected by webbing which is removed by the process of programmed cell death. The human body produces millions of new cells every day and a

similar amount of cells is eliminated by apoptosis to maintain homeostasis. Apoptosis also represents an important body defence mechanism. It is involved in the development of the immune system. Immature T lymphocytes bearing receptor that reacts with antigens normally present in the body are deleted by apoptosis. Virus-infected cells undergo apoptosis to prevent virus replication or DNA-damaged cells undergo apoptosis to prevent pathological states, such as cancer (Voet and Voet, 2004).

Apoptosis represents controlled cell elimination without any harm to the neighbouring cells and tissues. During the process, cells become rounded and lose its contact with surrounding cells. This is accompanied by plasma membrane blebbing that culminates in separation of small vesicles referred to as apoptotic bodies. These are characterized by the mobilization of phosphatidylserine to the outer leaflet of the plasma membrane, which is mobilized from the inner leaflet upon apoptotic stimuli to induce phagocytosis of apoptotic bodies by macrophages (Taylor et al., 2008). Therefore, apoptosis causes removal of cells without any inflammation, and selective induction of apoptosis in cancer cells is a sought after property of anti-cancer agents. Apoptosis is transmitted via the extrinsic or intrinsic pathways discussed in the following sections.

I.2.2. Molecular mechanisms of apoptosis

A hallmark of apoptosis is caspases activation. Caspases are cysteine-dependent aspartate specific proteases, which cleave substrates after aspartate using cystein side chain as a nucleophile during the peptide bond hydrolysis. Caspases can be divided into groups according to their function as initiator caspases (caspase-2, -8, -9, -10), effector caspases (caspase-3, -6, -7) and inflammatory caspases (caspase-1, -4, -5). They are expressed in organisms as inactive enzymes called pro-caspases, which are activated upon catalytic cleavage. The initiator caspases act upstream to effector caspases and mediate their activation (Pop and Salvesen, 2009). Upon activation of effector caspases, the cell crosses the so called “point of no return”, which means that it can no longer be rescued and is committed to die. Effector caspases cleave proteins referred to as “death substrate”. Examples of death substrate include components of the cytoskeleton, the nuclear membrane, cell-cell adherent junctions, proteins involved in translation and transcription

and in the processing of the ribosomal RNA. An important hallmark of apoptotic cell death is DNA fragmentation facilitated by caspase-activated DNase (CAD) (Taylor et al., 2008).

I.2.3. Extrinsic and intrinsic pathways of apoptosis leading to caspase activation

The extrinsic pathway of apoptosis is activated in response to the stimulation of trans-membrane receptors from the tumour necrosis factor (TNF) receptor gene superfamily called death receptors (DR). The best characterized DRs and their "death ligands" are the Fas receptor with its Fas ligand, TNF receptor-1 with its ligand TNF-α, and DR4 and DR5 with the TNF-related apoptosis-inducing ligand (TRAIL). Upon binding of death ligands, DRs trimerize and their intracellular domains, referred as death domains, recruit adaptor proteins, such as the Fas-associated death domain (FADD). FADD further binds caspases-8 or -10, which results in formation of death-inducing signalling complex (DISC) leading to the autocatalytic activation of caspases (Ashe and Berry, 2003). DISC can be inhibited by the cellular protein FLIP through competition with caspase-8 for binding to FADD (Budd et al., 2006). Apoptosis induction can be also inhibited by the action of members of the inhibitor of apoptosis proteins (IAP) family, particularly the X-linked IAP (XIAP) which is known to block caspase activation by binding to caspase-3, -7 and -9 (Fig. 1, page21) (Deveraux et al., 1997).

Activation of the intrinsic pathway of apoptosis is usually preceded by certain stress stimuli such as DNA damage, viral or bacterial infection, oxidative stress, ionizing radiation, chemotherapeutics (and many more), leading to mitochondrial outer membrane permeabilization (MOMP) and mitochondria destabilisation (Green and Kroemer, 2004). This event is followed by the release of cytochrome c (cyt c) from the mitochondrial inter-membrane space into the cytosol. In mitochondria, cyt c functions as an electron shuttle between complex III (CIII) and CIV in the respiratory chain, but once in the cytosol, this molecule initiates caspase activation (Garrido et al., 2006). In the presence of ATP and even more effectively in the presence of deoxy ATP, cyt c in the cytosol mediates the allosteric activation and hepta-oligomerization of the adaptor protein known as the apoptosis-protease activating factor 1 (Apaf-1) to form the complex referred to as apoptosome. It serves as an adaptor complex recruiting seven molecules of pro-caspases-9

and positioning them in close proximity with each other, whereby promoting their autocatalytic cleavage and activation. Activated caspase-9 then cleaves effector caspases, causing their activation (Fig. 1, page 21) (Garrido et al., 2006).

Together with cyt c, other apoptotic proteins such as the second mitochondria-derived activator of caspases/direct inhibitor of apoptosis-binding protein with a low isoelectric point (Smac/DIABLO), high temperature requirement protein A2 (HtrA2), apoptosis-inducing factor (AIF), endonuclease G (Endo G) and CAD, are mobilized into the cytosol. The serine protease HtrA2 and Smac/DIABLO suppress the inhibitory activity of IAP members by interacting with the IAP-binding N-terminus. AIF and Endo G translocate into the nucleus where they promote DNA fragmentation, whereby inducing apoptosis in a caspase-independent manner in contrast to CAD that acts following caspase activation (Elmore, 2007).

MOMP is mediated by the formation of a pore in the outer mitochondrial membrane (OMM). This is facilitated by the action of proteins from the Bcl-2 family, which can interact with each other via their Bcl-2 homology domains (BH). These proteins are divided according to their function and structure into two groups, the anti-apoptotic and pro-apoptotic proteins. Members of the anti-apoptotic protein group are Bcl-2, Bcl-extra large (Bcl-x_L), Bcl-2-related protein A1 and induced myeloid leukemia cell differentiation protein (Mcl-1). All of them contain four BH domains (BH1-4) and one trans-membrane domain, by which are integrated within the OMM. They control the integrity of OMM by rendering inactive the pro-apoptotic proteins Bcl-2 homologous antagonist/killer (Bak) and Bcl-2–associated X protein (Bax). Bak and Bax contain three BH domains (BH1-3) and also a trans-membrane domain. Upon activation, these two proteins undergo conformational change and homo/hetero-oligomerize to form a pore in the OMM. The pro-apoptotic group of Bcl-2 family further contains a subgroup of BH3-only proteins. Among them are phorbol-12-myristate-13-acetate-induced protein 1 (Noxa), p53 upregulated modulator of apoptosis (Puma), Bcl2-interacting mediator of cell death (Bim), Bcl2 antagonist of cell death (Bad), BH3-interacting domain death agonist (Bid). BH3-only proteins can interact with anti-apoptotic proteins and release Bak and Bax from their sequestration or directly activate Bak and Bax to form a pore in the MOM (Chipuk et al., 2010). The connection between extrinsic and intrinsic pathways is presented by the BH3-only protein Bid, which is in some cases cleaved by activated caspase-8. Truncated Bid

(tBid) then activates Bax, which then translocates to the MOM (Fig. 1) (Lovell et al., 2008).

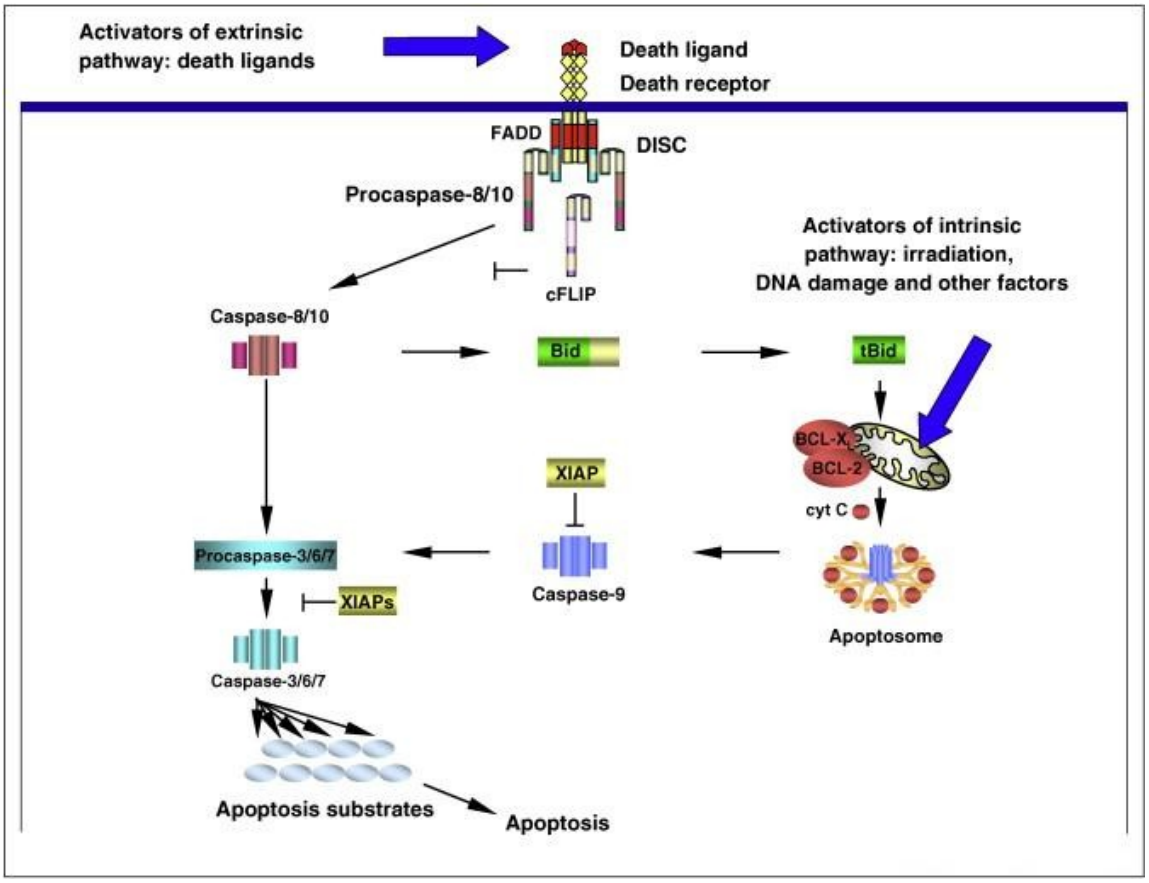

Figure 1. Scheme of the extrinsic and intrinsic apoptotic pathways showing the inhibitors of apoptosis XIAP and cFLIP (taken from Lavrik, 2010)

I.3. Mitochondria as target for cancer therapy

I.3.1. Importance of an invariant target for cancer therapy

Cancer cells, as described above, undergo many alterations which together result in their specific malignant phenotype. It is known that a number of mutations in a number of genes are typical for individual cancer types. However, recent research has shown that these mutations differ also among patients with the same type of tumour (Parsons et al., 2008; Jones et al., 2012). Moreover, the differences in mutations were found within the same tumour in one patient (Gerlinger et al., 2012), making the idea of a design of a drug

that would be efficient across the landscape of the neoplastic disease a considerable challenge. Each cellular process seems to be regulated in a highly complex manner and thus various mutations can contribute to cancer development, highlighting the complexity of the pathology. Thus, it seems to be unlikely to cure cancer by targeting a single signalling pathway. Rather, there is a need to find a target which is invariant, and by using this concept, design drugs that will effectively kill cancer cells and thus inhibit tumour growth in the context of different cancer types.

Mitochondria have recently emerged as such a promising target for anti-cancer therapy. They were found to be functional in the vast majority of cancer cells, further-more cancer cells are susceptible to drugs acting on mitochondria (Galluzzi et al., 2010). Mitochondria are essential cell organelles containing enzymes participating in important metabolic processes such as oxidative decarboxylation of pyruvate, the tricarboxylic acid cycle, oxidative phosphorylation and fatty acid oxidation. Thus mitochondria present the site of oxidative metabolism. At the same time, as described earlier, the mitochondrial inter-membrane space also contain a heterogeneous class of proteins that mediate apoptosis; therefore mitochondria are organelles also responsible for apoptotic cell death induction and cell faith determination (Voet and Voet, 2004). Targeting mitochondria enable these mediators of apoptosis to circumvent the mutation in DNA that makes cancer cells resistant to established anti-cancer therapy, epitomized by the often inactivated *P53*.

Such group of agents targeting mitochondria in cancer cells is represented by ‘mitocans’. These are chemical compounds, some of which are used as anti-cancer agents, which act via mitochondria to induce the apoptotic cell death, often selectively in tumour cells. By targeting mitochondria, mitocans cause the mitochondrial destabilization, which leads to the release of apoptosis-promoting proteins into the cytosol and activation of the intrinsic apoptotic pathways (Neuzil et al., 2007a).

I.3.2. The broad spectrum of mitocans and their classification

Mitocans present a broad group of small molecules that act by several ways to destabilize mitochondria. These agents can be grouped into eight classes based on their site and level of action from the outside through the inside mitochondrial membrane into the

mitochondrial matrix. The classification of mitocans and their representative members are summarized in Table 1 (page 24).

The first class of mitocans consists of agents inhibiting the hexokinase (HK) activity. Hexokinase is an enzyme important not only in glucose metabolism where it converts glucose to glucose-6-phosphate, but it also binds to the voltage-dependent anion channel (VDAC) in the OMM, where it prevents binding of the pro-apoptotic proteins Bax and Bak to VDAC. These proteins together form a pore in the MOM by which cyt c can be mobilized into the cytosol. Thus, inhibitors of HK activity suppress glycolysis, therefore tumour growth, and promote susceptibility of cancer cells to apoptosis. The second class of mitocans includes BH3 mimetics targeting the Bcl-2 family of proteins. Small molecular BH3 mimetics interfere with the interaction of pro- and anti-apoptotic proteins and leave pro-apoptotic proteins Bak and Bax free to form a pore in the OMM. The third class comprises thiol redox inhibitors that act by modifying the reactive thiol groups of VDAC in the OMM and adenine nucleotide transporter (ANT) in the inner mitochondrial membrane (IMM). VDAC and ANT together create the permeability transition pore complex connecting the mitochondrial matrix with the cytosol serving for the transport of small molecules, such as ATP and ADP. This complex is also the target of the fourth class of mitocans, and its deregulation results in apoptosis induction in cancer cells through increased formation of reactive oxygen species (ROS) and ATP depletion. The members of the fifth class act by targeting the components of the electron transport chain ETC, leading to rapid increase of ROS production and apoptosis induction. The sixth class of mitocans includes lipophilic cations targeting the IMM of cancer cells and dissipating mitochondrial inner trans-membrane potential ($\Delta\psi_m$) to cause apoptosis. Class seven of mitocans comprises agents targeting the tricarboxylic acid (TCA) cycle, and the eighth class of mitocans comprises agents interfering with the stability and function of mitochondrial DNA (mtDNA) accompanied by decrease in cancer cell proliferation (Neuzil et al., 2012).

Table 1 Classification of mitocans. Note, that some agents act on mitochondria by several ways.

Class	Type	Member examples
1.	Hexokinase inhibitors	3-Bromopyruvate, 2-deoxyglucose
2.	Compounds targeting Bcl-2 family proteins	Gossypol, antimycin A, α-TOS
3.	Thiol redox inhibitors	Isothiocyanates, arsenic trioxide
4.	VDAC/ANT targeting drugs	Lonidamine, arsenites, steroid analogues like CD437
5.	Electron transport targeting drugs	α-TOS, MitoVES, tamoxifen, adaphostin, 3.bromopyruvate
6.	Lipophilic cations targeting inner membrane	Rhodamine-123, F16, (KLAKKLAK)2 peptide
7.	Drugs targeting the tricarboxylic acid cycle	Dichloroacetate, 3-bromopyruvate
8.	Drugs targeting mtDNA	Vitamin K3, fialuridine, 1-methyl-4-phenyl-pyridinium, MitoVES
9.	Drugs targeting other (unknown) sites	Betulinic acid
		(adapted from Neuzil et al., 2012)

I.3.3. Vitamin E analogue α-tocopheryl succinate and its mitochondrially targeted counterpart as anti-cancer agents from the group of mitocans

The term vitamin E (VE) is often used as a synonymum for α-tocopherol (α-TOH), a lipid-soluble compound with an important biological antioxidant activity, being the most active of the 8 compounds classified as VE forms (Sen et al., 2006). Recently, redox-silent analogues of VE have been found as promising anti cancer agents, and these are represented by α-tocopheryl succinate (α-TOS) and its mitochondrially targeted counterparts, mitochondrially targeted VE succinate (MitoVES). In contrast to α-TOH, α-TOS and MitoVES act in a completely different manner. They lack the antioxidant activity of α-TOH and promote cell death in a wide range of cancer types, while being non-toxic to normal cells and tissues (Neuzil et al., 2001a, 2004; Dong et al., 2011a). α-TOS and MitoVES induce apoptosis in cancer cells by targeting mitochondria, therefore they belong to the group of anti-cancer drugs termed mitocans. α-TOS is classified as ETC targeting and BH3 mimetic-like compound, and MitoVES targets the ETC and mtDNA.

I.3.3.1. Structure-function relationship of α-tocopheryl succinate and mitochondrially targeted vitamin E succinate

The reason for the apoptogenic activity of α-TOS and its exceptional selectivity lies in its unique structure as well as in differences between normal and cancer cells. The molecules of α-TOS and α-TOH can be divided into three major domains: functional, signalling and hydrophobic (Fig. 2). Both compounds share most of the structural features, differing only in the functional domain. While the functional domain is crucial for the apoptogenic activity of α-TOS, all three domains are needed to induce this effect (Birringer et al., 2003). The hydrophobic domain is responsible for association of the agents with biological membranes and circulating lipoproteins (Pussinen et al., 2000). The signalling domain takes part in the regulation of signalling pathways such as those involving protein kinase C by increasing the protein phosphatase 2A (PP2A) activity (Neuzil et al., 2001b). The functional domain of α-TOH makes it redox-active while the succinyl moiety is redox-inactive and necessary for the anti-cancer effect of α-TOS. The investigation of different functional domains reveal that the presence of the free carboxylic group is essential for α-TOS to exert the apoptogenic activity (Birringer et al., 2003).

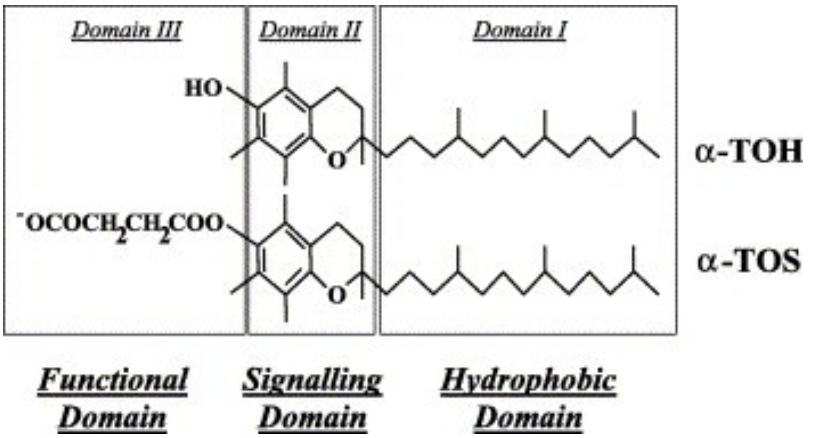

Figure 2. The structures of α-TOH and α-TOS divided in three major domains: functional, signalling and hydrophobic (adapted from Neuzil and Massa, 2005).

In contrast to normal cells, cancer cells utilize high levels of glucose in order to satisfy high energetic demands of proliferating cells. However, more than 90% of this

glucose is processed and converted eventually to lactate, which leads to significant acidification of the tumour microenvironment (DeBerardinis et al., 2007). Further explanation of this phenomenon is in section I.5. To prevent the acidification of the cytosol due to increased lactate production, the activity of the proton-pumping ATPase increased to maintain the cytosolic pH neutral. Therefore the extracellular, interstitial pH is acidified to 6.2-6.6. α-TOS is a weak acid with pK_a of ~5.6 that can exist in two forms, the deprotonated (charged) and protonated (uncharged) form, in which α-TOS can cross the plasma membrane by free diffusion. At neutral pH, 99% of α-TOS is in its deprotonated form, but at pH of 6.2 the proportion of protonated form is increased 25-fold. Thus, the acidic pH of tumour microenvironment favours the selective uptake of α-TOS by cancer cells (Neuzil et al., 2002).

MitoVES was generated by tagging α-TOS with the cationic triphenylphosphonium (TPP^+) group (Fig. 3) that is responsible for delivering the compound directly to mitochondria (Dong et al., 2011a, b). It has been found that cancer cells exhibit higher $\Delta\psi_m$ compared to their normal counterparts due to altered mitochondrial bioenergetics (Rodríguez-Enríquez et al., 2009). This aspect explains the selectivity with which MitoVES accumulates preferably in mitochondria of cancer cells.

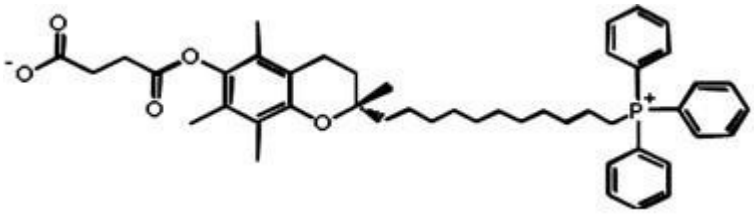

Figure 3. The structure of MitoVES (adapted from Dong et al., 2011b).

Although, the differences between the pH and $\Delta\psi_m$ are the main reasons for α-TOS and MitoVES selectivity, there are other possible mechanisms. Cancer cells seem to lack the level of the esterase activity found in normal cells. Esterases hydrolyze α-TOS and MitoVES into their non-apoptotic counterparts lacking succinnyl moiety that is important for the apoptotic function of α-TOS and MitoVES. Finally, the selectivity of α-TOS and MitoVES may be due to their capacity to generate ROS (Neuzil et al., 2004; Dong et al., 2011a; Rodríguez-Enríquez et al., 2012). Normal cells possess high levels of anti-oxidant enzymes such as superoxide dismutase or catalase that are able to effectively remove ROS. However, these enzymes are expressed at lower levels in cancer cells, and cancer cells

need low, sustained levels of ROS to promote their mitogenic function (Neuzil et al., 2007b).

I.3.3.2. Mechanisms of apoptosis induced by α-tocopheryl succinate and mitochondrially targeted vitamin E succinate

The main mechanism of apoptosis induced by α-TOS and MitoVES is linked to the generation of ROS due to the interference of the agents with the mitochondrial ETC. The target of these compounds is the mitochondrial CII. It has been proposed that ROS generation is a consequence of the interaction of α-TOS and MitoVES with CII (Neuzil et al., 2007b; Dong et al., 2011a). CII is a membrane bound protein complex containing the TCA cycle enzyme, succinate dehydrogenase (SDH). SDH converts succinate to fumarate and the electrons released during this reaction are accepted by ubiquinone (UbQ) of the membrane part of CII (Voet and Voet, 2004). Molecular modelling based on the crystal structure of porcine CII revealed that α-TOS binds to the proximal and distal UbQ binding sites of CII. The binding energy of α-TOS for the UbQ binding sites is comparable or even higher to that of UbQ. Similar results were obtained for MitoVES which was found to bind to the proximal UbQ site. Thus, α-TOS and MitoVES are thought to compete for these binding sites, whereby blocks the transport of electrons to UbQ and further to CIII. Free electrons then recombine with molecular oxygen to give rise to superoxide that, in turn, triggers the apoptotic cascade (Dong et al., 2008, 2011b).

As described earlier, mitochondrially mediated apoptosis induction involves the MOMP formed by Bak and Bax proteins that, upon activation, undergo a conformational change and homo-/hetero-oligomerize in the OMM. Treatment with α-TOS and MitoVES caused conformational change of the Bak protein resulting in its homo-oligomerization in the OMM. In this context, Bak activation is promoted by the pro-apoptotic BH3 only proteins. Recently, it has been elucidated that exposure of several cancer cell lines to α-TOS and MitoVES resulted in the increased expression of the pro-apoptotic BH3 only protein Noxa, whereas the other proteins from Bcl-2 family remained unchanged. Increased expression of pro-apoptotic proteins such as Noxa and the resulting induction of apoptosis are supposed to be promoted by p53. However, in case of α-TOS and MitoVES, this phenomenon was observed also in *P53*-deficient cells. Bak and Bax are normally

inactivated by the interaction with the anti-apoptotic proteins such as Mcl-1 and Bcl-x_L. Noxa was found to interact with Mcl-1. This interaction causes the release of Bak from the Mcl-1/Bak complexes, enabling Bak to form pores in the OMM. This was not observed for Bax. Further, RNAi experiments confirmed the importance of the Noxa-Bak axis in the apoptosis induction in response to α-TOS and MitoVES (Prochazka et al., 2010; Dong et al., 2011a).

While ROS generation is the main pathway in apoptosis induced by α-TOS and MitoVES, it is not the only mechanism for α-TOS. Activation of sphingomyelinase (SMase) and destabilization of lysozomes are other mechanisms leading to the induction of apoptosis by α-TOS (Wang et al., 2006). SMase is an enzyme that converts sphingomyelin to ceramide, which is able to induce anti-proliferative responses involving cell cycle arrest, apoptosis or differentiation. Ceramide mediates these responses by regulating specific protein targets such as protein phosphatases and kinases. For example, activation of PPA2 by ceramide leads to the dephosphorylation and thus inactivation of anti-apoptotic protein Bcl-2, which causes induction of apoptosis (Ogretmen and Hannun, 2004). It was found that lysosomal destabilization is an early event during α-TOS treatment, contributing to apoptosis induction as was showed by experiments using cancer cells deficient in the lysosomal enzyme cathepsin D (Neuzil et al., 2002). Moreover, α-TOS was also documented to act as BH3 mimetic. With this regards, exposure of the prostate cancer cells PC-3 to this agent reduced association of Bak with the anti-apoptotic proteins Bcl-x_L and Bcl-2 resulting in caspase-dependent apoptosis (Shiau et al., 2006). However, MitoVES and, in particular α-TOS, target predominantly mitochondria leading to ROS generation and this pathway has been found to play the major role in apoptosis induction in response to these agent. Other pathways appear to amplify this process as demonstrated using cancer cells deficient in mtDNA (Wang et al., 2005).

I.4. The Hippo signalling pathway

I.4.1. The Hippo signalling pathway – the kinase cascade and its regulation

The Hippo signalling pathway presents a conserved basic mechanism regulating cell proliferation and cell death, ensuring cell contact inhibition and organ size control in all metazoans (Camargo et al., 2007). This can be seen in regenerating liver after partial hepatectomy. Hepatocytes are stimulated to divide and once liver reach the original size, the cells stop dividing to ensure the proper organ size (Fausto et al., 2006).

The Hippo pathway was originally identified in *Drosophila melanogaster* during the genetic screen for tumour suppressor genes, whose inactivation causes tissue overgrowth. The core components of the Hippo signalling pathway in *Drosophila* are the serine/threonine-protein kinase Hippo (Hpo), the scaffold protein Salvador (Sav), the MOB kinase activator-like 1 (Mats) and the serine/threonine-protein kinase Warts (Wts). The target of this pathway is the transcriptional co-activator protein Yorkie (Yki) which is, upon activation of the Hippo pathway, phosphorylated and transported from the nucleus to the cytoplasm, where it is retained by association with the 14-3-3 proteins (Fig. 4, page 31) (Zhao et al., 2008).

Individual components of the Hippo pathway are evolutionarily conserved in mammals, including two Hpo homologues, the serine/threonine-protein kinases mammalian sterile 20-like kinase 1 and 2 (Mst1 and Mst2), one Sav homologous protein, the salvador homolog 1 (Sav1), two Mats homologues, the MOB kinase activator 1A and MOB kinase activator 1B, collectively referred to as Mob1, and two Wts homologues, serine/threonine-protein kinase large tumour suppressor 1 and 2 (Lats1 and Lats2. The target of this pathway in mammals is transcriptional regulator Yki homologue, the Yes-associated protein (Yap) and the transcription co-activator WW domain-containing transcription regulator protein 1 (WWTR1 or Taz) (Fig. 4, page 31) (Pan, 2010).

The core components of the Hippo pathway are regulated by cell contacts and cellular polarity, and this upstream regulation is rather complex. In *Drosophila*, the trans-membrane protein Fat-like cadherin-related tumour suppressor homologue (Fat) was found to have impact on the Hippo pathway. It controls the growth and planar cell polarity by the interaction with another cadherin-like protein Dachsous (Ds), and this interaction is

modulated by the trans-membrane kinase Four-jointed (Fj) (Willecke et al., 2008). Fat signalling involves the unconventional myosin Dachs that negatively regulate the Wts protein level (Cho et al., 2006). Fat and Hippo signalling are linked by an apical protein complex. This complex is composed from WW domain-containing protein Kibra, and the protein Expanded (Ex) and Moesin/ezrin/radixin homologue 2 known as Merlin (Mer) that both contain the 4,1 protein/Ezrin/Radixin/Moesin (FERM) domain responsible for Mer and Ex membrane association. Mer, Ex and Kibra interact with each other, and together they bind to the Hpo-Sav complex bringing it to the plasma membrane for activation (Yu et al., 2010) by phosphorylation and association with the scaffold protein Sav that serves for assembling Hpo with Wts. Activated Hpo phosphorylates Sav and Wts with its associated protein Mats. Wts is activated by Hpo phosphorylation and Mats association (Fig. 4, page 31) (Sudol and Harvey, 2010).

While the regulation of the Hippo pathway in *Drosophila* is well understand, little is known about the upstream regulation of this pathway in mammals. The mammalian genome also contains homologues of the upstream regulators of Hippo pathway reported in *Drosophila*, including two Kibra homologous proteins KIBRA (or the WW domain-containing protein-1 and -2), two Ex homologues, the FERM domain-containing protein 6 and 1 (FRMD6 and FRMD1), and one Mer homologue Neurofibromin (NF2). To date only KIBRA and NF2 are known to play role in the mammalian Hippo pathway. NF2 physically interact with KIBRA and Sav1, and is known to be necessary for Lats1/2 and Yap phosphorylation, suggesting conserved regulation of the Hippo pathway in mammals (Zhang et al., 2010). KIBRA was also found to be involved in Lats1/2 and Yap phosphorylation independent of Mst1/2 (Moleirinho et al., 2013). Activated Mst1/2 phosphorylate the Lats1/2 kinase in a reaction that is stabilized by Sav1. Sav1 interacts with Mst1/2 and promotes its activation, stabilization and nuclear localization, at least in mouse primary embryonic keratinocytes induced by Ca^{2+} to differentiate (Lee et al., 2008). Activated Mst1/2 phosphorylates also Sav1 (Park and Lee, 2011) and Mob1 at Thr12/Thr35. The phosphorylation of Mob1 by Mst1/2 diminished the ability of Mob1 to bind Mst1/2 and increase its affinity for Lats1/2 (Praskova et al., 2008). Mst1/2 phosphorylates Lats1/2 at Thr1079/Thr1041, which is necessary but not sufficient for the activation and binding of Mob1 to Lats1/2, which mediates Lats1/2 autophosphorylation at Ser909/Ser872 and its activation (Fig. 4, page 31) (Avruch et al., 2012).

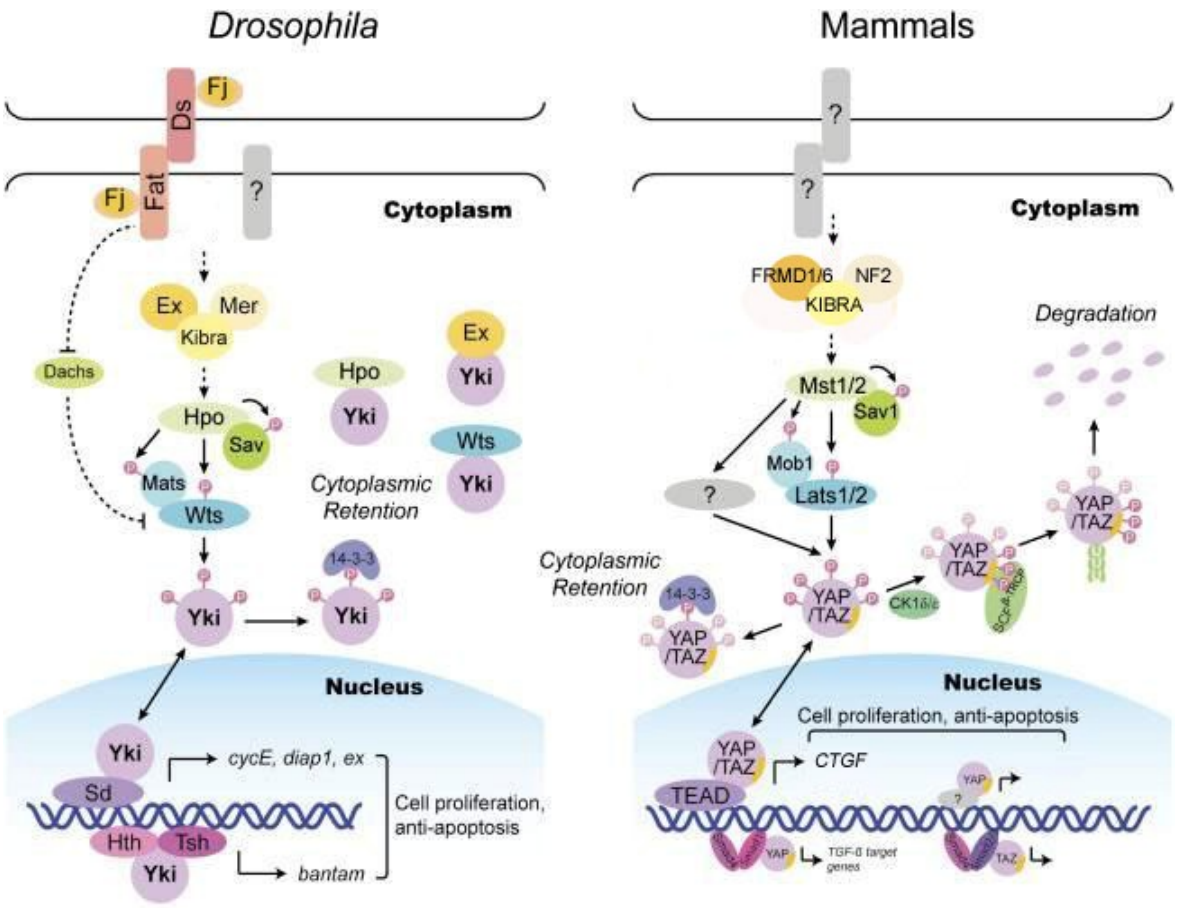

Figure 4. The Hippo signalling pathway in *Drosophila melanogaster* and mammals (adapted from Zhao et al., 2010a).

I.4.2. Targets of Hippo pathway – their regulation and function

The upstream components, no matter how complex they are, all converge at a common downstream component, the transcription co-activators Yki in *Drosophila*, and Yap and Taz in mammals. Yki is directly phosphorylated by Wts on Ser168. This phosphorylation is crucial for its nuclear export and cytoplasmic retention due to the interaction with the phosphoserine- and phosphothreonine-binding proteins of the 14-3-3 family (Fig. 4). Yki can be also regulated by a phosphorylation-independent mechanism via a protein-protein interaction involving its WW domain. The WW domain interacts with the PPXY motifs of Ex, Wts and Hpo, and this interaction results in Yki repression because WW domain is also required for Yki transcriptional activity. Yki does not bind directly to the DNA regulatory sequences, but interacts with transcription factors such as

Scalloped (Sd) from the family of transcriptional enhancer factors (TEF) containing the TEA/ATTS DNA-binding domain (TEAD/TEF). The other known DNA-binding partner for Yki is the Homeobox protein Homothorax (Hth), which regulates cell proliferation and the expression of the microRNA *bantam*. Yki target genes play a role in cell proliferation (microRNA *bantam*), apoptosis inhibition (*Drosophila inhibitor of apoptosis diap1*), or cell cycle regulation (*cyclin E, E1F2*). Yki also regulates genes coding for upstream Hippo pathway proteins (Kibra, Ex, Fj) and genes coding for proteins involved in the cell-cell interaction and cell signalling (E-cadherin, ligand for the Notch receptor protein Serrate, Wingless) (Oh and Irvine, 2010; Pan, 2010). Recently, it was reported that the transcription factor and proto-oncogene diminutive Myc (dMyc) is also a target gene of Yki (Neto-Silva et al., 2010).

Mammalian Yap is phosphorylated by Lats1/2 at five serins in the specific HXRXXS motif from which Ser127 and Ser381 are the crucial phophorylation sites to suppress the Yap activity. The phosphorylation of Ser127 by Lats1/2 results in Yap nuclear export and cytoplasmic retention by 14-3-3 proteins. Lats1/2 also phosphorylates Ser381 that is required for further phosphorylation of Ser384 by casein kinase 1 δ/ε (CK1δ/ε) and recruiting of SCF (SKP1-CUL1-F-box protein) E3 ubiquitin ligase with the substrate recognition component F-box/WD repeat-containing protein 1A β-TRCP ($SCF^{\beta\text{-}TRCP}$) which leads to the protein degradation (Zhao et al., 2010b). Taz is regulated by a similar mechanism as Yap. It contains four specific HXRXXS Lats1/2 phosphorylation motifs, from which phosphorylation of Ser89 by Lats1/2 mediates its interaction with 14-3-3 proteins and phosphorylation of Ser311 by Lats1/2 primes further phosphorylation of Ser314 by CK1δ/ε and recruitment of the $SCF^{\beta\text{-}TRCP}$ E3 ubiquitin ligase (Liu et al., 2010). Phosphorylation-independent regulation of Yap and Taz has not been identified yet. However, Yap seems to be regulated also by the Hippo pathway in a Lats1/2- or Mst1/2-independent mechanism. It has been shown that in mouse liver, the Yap protein is regulated by Mst1/2 via an unknown intermediary kinase other than Lats1/2. Upon achieving confluence, mouse embryonic fibroblasts exhibit activation of Lats1/2, Yap phosphorylation and its export from the nucleus even in the case of Mst1/2 deletion. Therefore, it seems that the Hippo signalling pathway in mammals is more complex and tissue-dependent (Zhou et al., 2009). Like Yorkie, Yap and Taz promote gene expression in interaction with other transcription factors such as the Runt family member RUNX2 and the TEAD/TEF family of transcription factors that are main mediators of Hippo signalling

in mammals. Yap also interacts with the tumour protein p73, and Taz interacts with the thyroid transcription factor-1, peroxisome proliferator-activated receptor-γ or the SMAD1-4 proteins. Importantly, the Hippo signalling pathway is known to regulate the expression of genes coding for growth-promoting proteins such as the transcription factors c-Myc, Sox4 and α-fetoprotein, cytokines such as connective tissue growth factor and fibroblast growth factor-1, as well as genes coding for anti-apoptotic proteins such as IAP, baculoviral IAP repeat-containing protein-5 (BIRC5)/survivin and Mcl-1 (Dong et al., 2007; Zhao et al., 2010a).

I.4.3. Activation of Mammalian sterile 20-like kinase 1

Activation of Mst1 and thus the Hippo pathway seems to play an important role in tumour suppression and apoptosis activation. It has been shown that overexpression of Mst1 causes morphological changes characteristics for apoptosis (Graves et al., 1998). While the exact mechanism of Mst1 activation remains elusive, it is known that this process is accompanied by Mst1 phosphorylation and cleavage.

Caspase-dependent Mst1 cleavage presents the best known mechanism of Mst1 activation. The Mst1 molecule contains two functional nuclear export signals in the C-terminal domain causing nuclear export of the full length Mst1 (Ura et al., 2001). In response to apoptotic stimuli, caspases cleave the C-terminal domain of Mst1, generating approximately 36 kDa N-terminal fragment of the protein with 10-fold higher kinase activity than full-length Mst1. The cleaved N-terminal part of Mst1 accumulates in the nucleus where it phosphorylates histone H2AX at Ser139 and histone H2B at Ser14, leading to chromatin condensation and apoptosis induction (Cheung et al., 2003; Wen et al., 2010). Mst1 homodimerizes via the C-terminal coiled coil domain known as the SARAH domain, and Mst1 homodimerization is necessary for Mst1 activation by intermolecular auto-phosphorylation of Thr183 within the activation loop (Praskova et al., 2004).

Mst1 has also been reported to be required for apoptosis induction in response to several anti-tumour drugs including the mitocans α-TOS and MitoVES (Watabe et al., 1999; Dong et al., 2011a; Valis et al., 2011). It has been shown that Mst1 is auto-phosphorylated at Thr183 and induces cell death in cancer cells in response to hydrogen

peroxide treatment (Lehtinen et al., 2006; Morinaka et al., 2011). α-TOS and MitoVES are known to produce ROS, it is believed that the generated superoxide anion radicals are converted into highly diffusible hydrogen peroxide that is responsible for Mst1 activation (Dong et al., 2011a; Valis et al., 2011).

I.4.4. Apoptosis induced by α-tocopheryl succinate and mitochondrialy targeted vitamin E succinate requires Mammalian sterile 20-like kinase 1

As discussed earlier, exposure of cancer cells to α-TOS and MitoVES causes up-regulation of Noxa resulting in Bak-mediated MOMP and apoptosis induction. The *NOXA* gene is known to be transcriptionally regulated by p53, but *NOXA* up-regulation in response to α-TOS and MitoVES treatment occurred also in *P53*-deficient cells (Prochazka et al., 2010; Dong et al., 2011a). Analysis of the *NOXA* promoter revealed a conserved DAF-16-binding element, the TTGTTTAC consensus sequence that is recognized by the forkhead box O (FoxO) transcription factors (Valis et al., 2011). Four members of this group FoxO1, FoxO3, FoxO4 and FoxO6 have been identified in mammals (Fu and Tindall, 2008). They are known to regulate genes participating in the regulation of cell cycle, differentiation, metabolism, ROS detoxification and important genes involved in apoptosis induction such as *BIM*, *TRAIL*, *FASL*, *PUMA* (Zhang et al., 2011) and *NOXA* (Valis et al., 2011).

The *NOXA* gene expression has been previously showed to be regulated by FoxO3 (Czymai et al., 2010), but in response to α-TOS and MitoVES treatment *NOXA* is regulated by FoxO1. It is also known that Mst1 is activated by oxidative stress-induces apoptosis through phosphorylation of the FoxO transcription factors (Lehtinen et al., 2006; Yuan et al., 2009). These transcription factors are sequestered in the cytoplasm by interaction with 14-3-3 proteins. Treatment with α-TOS and MitoVES causes phosphorylation of FoxO1 at Ser212 by Mst1, which disrupt its interaction with 14-3-3 proteins and results in FoxO1 nuclear translocation. In the nucleus, FoxO1 induces *NOXA* expression and thus apoptosis. Involvement of Mst1 and FoxO1 in this process was also documented by silencing of *MST1* and *FOXO1* gene expression using specific siRNAs. Jurkat cells with silenced *MST1* expression were more resistant to α-TOS and MitoVES treatment. This points to the Mst1-

FoxO1 pathway being responsible for apoptosis induction in cancer cells treated by α-TOS and MitoVES (Valis et al., 2011).

I.5. The metabolic requirements of cancer cells

Uncontrolled cell proliferation represents not only changes involved in the deregulated control of cell growth but also changes in the cellular energy metabolism. Altered cellular metabolism is one of the hallmarks of cancer (Hanahan and Weinberg, 2011). Cancer cells have high energetic demands as they grow and proliferate rapidly. Each passage through the cell cycle requires doubling of all intracellular components such as proteins, lipids and nucleic acids, and these processes need high level of nutrients, energy and biosynthetic activity. Although the metabolic alterations in cancer cells are similar to those in normal proliferative cells, cancer cell alterations are driven by specific molecular events such as the activation of oncogenes, inactivation of tumour suppressor genes, and by specific tumour microenvironment, which also plays an important role in tumour progression (Li et al., 2007). Apart from normal cells that proliferate in response to growth factors and nutrients, cancer cells proliferate independently of growth factors and have developed mechanisms, which allow them a limitless replication and thus immortality. Among the main attributes of cancer cell metabolism are the glucose and glutamine dependence.

I.5.1. Aerobic glycolysis

In the presence of oxygen, normal differentiated cells metabolize glucose by means of aerobic respiration. It is a highly effective process converting glucose via glycolysis to pyruvate, which is then metabolized to carbon dioxide in the TCA cycle to generate high amounts of ATP through the process of oxidative phosphorylation. This process generates about 38 molecules of ATP per one glucose molecule. Only under anaerobic conditions, the normal differentiated cells convert pyruvate to lactate in order to oxidize reduced equivalents generated during glycolysis in a process that is much less effective: it generates only 2 molecules of ATP per one glucose molecule (Voet and Voet, 2004).

The first discovery that cancer cells exhibit altered metabolism was made by Otto Warburg almost a century ago. He recognized that cancer cells exhibit high glucose uptake and metabolism compared to cells in normal differentiated tissues (Warburg et al., 1927). Warburg observed that cancer cells generate ATP by converting glucose to lactate, even in the presence of sufficient amounts of oxygen, by a process referred to as "anaerobic glycolysis" (Fig. 5). This process has been referred to as the "Warburg effect". Warburg thought that alterations in the metabolism of cancer cells is due to a defect in mitochondria respiration, so that cancer cells utilize high amounts of glucose in the process of anaerobic glycolysis to compensate for the more effective aerobic respiration and to sustain high intracellular ATP levels (Warburg, 1956).

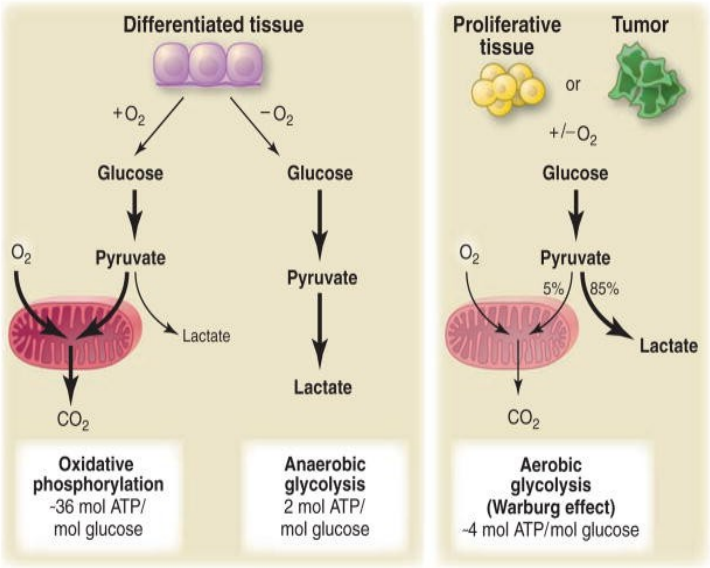

Figure 5. Scheme of glucose metabolism in differentiated and proliferative tissues under aerobic and anaerobic conditions (adapted from Vander Heiden et al., 2009).

Normal proliferating cells also exhibit aerobic glycolysis (Fig. 5) (Wang et al., 1976; Brand and Hermfisse, 1997), but in this case this process is most likely linked to cell growth rather than to malignancy. Nowadays, it has also been recognized that mitochondrial respiration of most cancer cells is not severely impaired (Fantin et al., 2006), still being the main source of ATP. Moreover, the dysfunction in mitochondrial oxidative phosphorylation probably leads to the decrease in cancer cell proliferation (Fogal et al., 2010). Importantly, it has been widely documented that cancer cells are sensitive to anti-cancer drugs targeting mitochondria, pointing to these organelles as a relevant target in cancer cells (Neuzil et al., 2007a). Since most tumours exhibit higher lever of aerobic

glycolysis, but normal differentiated cells from which they arise do not, the high proliferative potential of the tumour requires a shift of tumour metabolism to aerobic glycolysis, which seems advantageous for proliferating cells even though this process is much less effective for ATP generation.

I.5.2. Glucose requirement and utilization in cell proliferation

It has become clear that the main purpose for proliferating cells to utilize aerobic glycolysis is not only to produce high amount of ATP but also to enable higher biosynthetic activity, as well as maintaining the proper redox potential. The enhanced glucose metabolism allows higher flux of glucose carbons in the form of macromolecular precursors into the biosynthetic pathways such as the pentose phosphate pathway for nucleotide biosynthesis and biosynthetic pathways of amino acids and lipids (Locasale and Cantley, 2011). Detailed description of glucose utilization in biosynthetic processes is shown in (Fig. 6, page 39).

The crucial point in this process is probably the expression of the M2 form of pyruvate kinase, which is regulated by tyrosine kinases to be less active. Its lower activity is necessary for aerobic glycolysis in proliferative cells as it probably enables glucose metabolites to be used for anabolic processes (Christofk et al., 2008). The carbons for nucleotide synthesis come from glucose-6-phosphate, fructose-6-phosphate and glyceraldehyde-3-phosphate which are shunted in pentose phosphate pathway to produce ribose-5-phosphate, activated by phosphoribosyl-pyrosphosphate synthetase to form 5-phosphoribosyl-α-pyrosphosphate, thus forming the precursors for the synthesis of purines and pyrimidines. The glycine carbons may also come from the glucose metabolite, 3-phosphoglycerate. Carbons carried by N10-formyl-tetrahydrofolates are then mainly derived from glycine. Glucose-6-phosphate metabolized through oxidative reactions in the pentose phosphate pathway is also the source of the reduced form of NADPH which is important for amino acid, lipid and nucleotide biosynthesis (Voet and Voet, 2004; Vander Heiden et al., 2009).

The carbons for amino acid synthesis are derived from glucose metabolites such as pyruvate (for alanine synthesis) and 3-phosphoglycerate (for serine and further glycine and cysteine synthesis). The carbons from glucose metabolites also give rise to lipid production

as the glyceraldehyde-3-phosphate turns in dihydroxyacetone phosphate, the glycerol-3-phosphate precursor, which is necessary for the synthesis of phospholipids and triacylglycerol. The 3-phosphoglycerate, converted to serine, is then utilized for the biosynthesis of sphingosine (Voet and Voet, 2004).

Fatty acids are synthesized *de novo* and their formation depends on acetyl-coenzyme A (CoA), which is derived from glucose by means of oxidative decarboxylation of pyruvate in mitochondria. Acetyl-CoA is not used for fatty acids synthesis directly, instead it enters the TCA cycle to form citrate. Citrate is then transported via the tricarboxylate transporter in the cytosol, where it is cleaved by ATP citrate lyase to produce the cytosolic acetyl-CoA and oxaloacetic acid (OAA). Acetyl-CoA serves as a precursor for fatty acyl chain components of various lipid classes as well as for mevalonate that is further utilised for the synthesis of cholesterol and similar molecules (Voet and Voet, 2004). The enzymes of the lipogenic pathway such as ATP citrate lyase, fatty acid synthase and acetyl CoA carboxylase have been found up-regulated in numerous tumour types, and their activity is crucial in cancer cell proliferation as the inhibition or knock-down of these enzymes can block or reverse tumour progression (Abramson, 2011).

Although glucose is presented here as an important carbon source, its vast majority is excreted in the form of lactate and only less than 10 % of total glucose is used for biosynthetic pathways (DeBerardinis et al., 2007). Lactate generation has an important role in maintenance of redox balance because NADH is regenerated into its oxidized form NAD^+ during conversion of pyruvate to lactate in a reaction catalyzed by the enzyme lactate dehydrogenase (LDH). It is necessary to maintain a certain NAD^+/NADH ratio in cells, as NAD^+ is obligatory for the conversion of glyceraldehyde-3-phosphate to 1,3-bisphosphoglycerate and thus for continuing the glycolysis. NAD+ is also important for amino acid and nucleotide biosynthesis. NADH can be oxidized in the mitochondrial ETC, but it requires removal of the NADH electrons into the mitochondria matrix by other metabolites involved in the cytoplasmic shuttle system such as the malate-aspartate shuttle. This process includes a series of reactions which are kinetically slower than NADH regeneration by LDH, and thus lactate production may allow for faster glucose flux through glycolysis (Lunt and Vander Heiden, 2011). It seems to be favourable for proliferating cells, as inhibition of LDH activity impairs the proliferation (Fantin et al., 2006).

As glucose has an important role in cell proliferation, it is not the only necessary molecule involved in this process. Glutamine is the second molecule which is catabolized together with glucose in appreciable quantities.

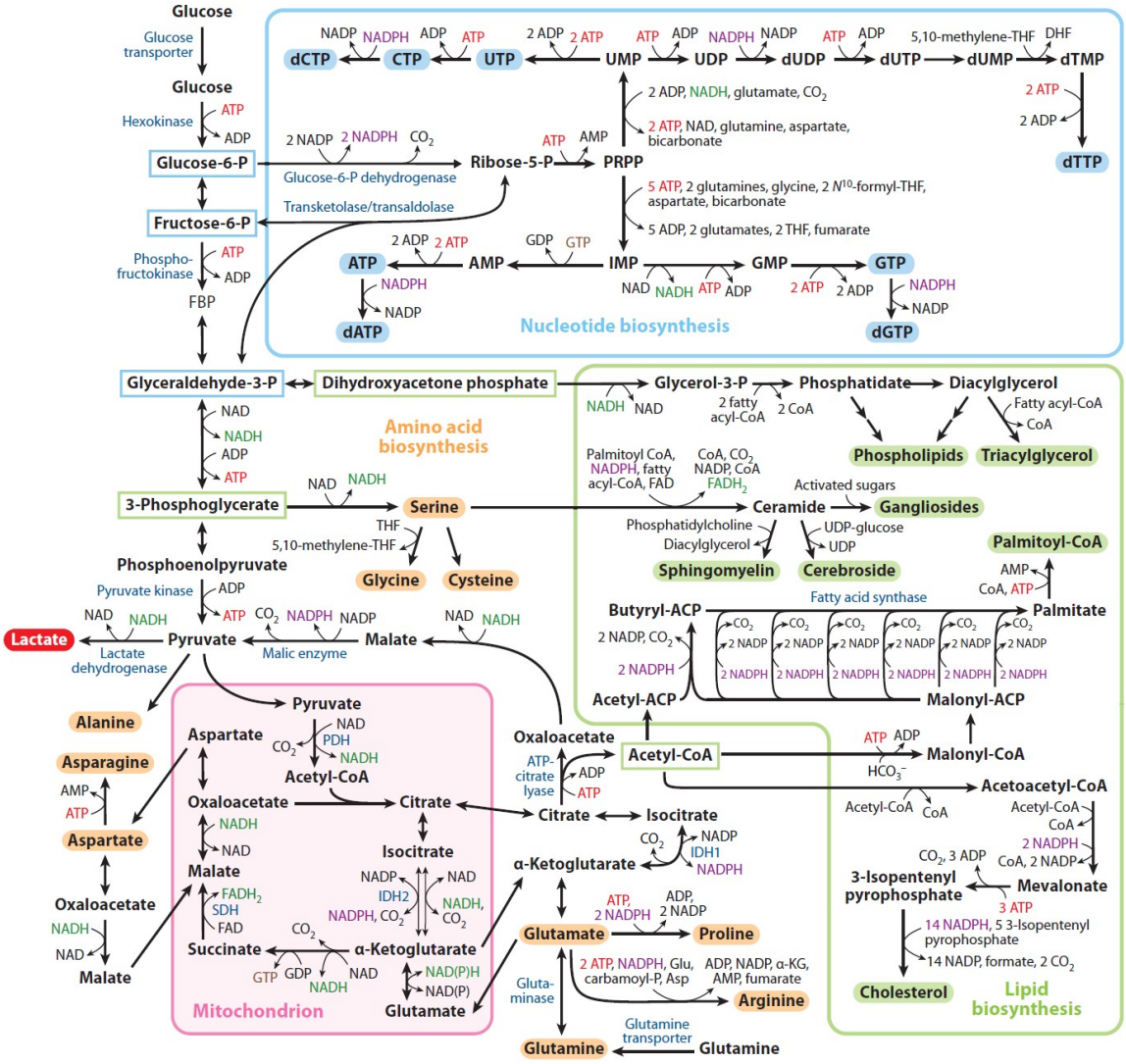

Figure 6. Glucose and glutamine utilization in biosynthetic pathways. For abbreviations meaning check the original article (adapted from Lunt and Vander Heiden, 2011)

I.5.3. The glutamine requirement and utilization during cell proliferation

Although glucose metabolised by means of aerobic glycolysis has great impact on proliferation, it cannot supply all needs of fast growing cancer cells. The non-essential

amino acid glutamine, the most abundant amino acid in human plasma (Stein and Moore, 1954), was found to be consumed by cancer cells 10 times more than any other amino acid (Eagle, 1955). Glutamine essentially contributes to most metabolic processes during cancer cell proliferation. It complements glycolysis as it also serves as carbon and nitrogen donor for nucleotide, lipid and amino acid biosynthesis. The metabolism of glutamine referred to as glutaminolysis has an important function in anaplerosis (replenishing TCA cycle intermediates that have been used for biosynthesis), as well as in NADPH and ATP production (Fig. 6, page 39) (DeBerardinis and Cheng, 2010).

During the synthesis of nucleotides, glutamine is converted to glutamate, and the nitrogen group is incorporated into the purine and pyrimidine ring (Voet and Voet, 2004). Aspartate for pyrimidine synthesis is also derived from glutamine, which is discussed later in the text. Conversion of glutamine to glutamate produces nitrogen for non-essential amino acid synthesis through transamination reactions, and glutamine nitrogen is also used by glutamine:fructose-6-phosphate amido transferase, which catalyzes the formation of glucosamine-6-phosphate, the precursor for N-linked and O-linked glycosylation reaction, from fructose-6-phosphate and glutamine (Fig. 6, page 39) (Donadio et al. 2008).

Glutaminolysis starts with the conversion of glutamine to glutamate by enzyme glutaminase (GLS). This enzyme has an important role in rapidly dividing cells, and its activity correlates with tumorigencity; inhibition of GLS expression leads to a decrease in cancer cells growth and revert the malignant phenotype (Lobo et al. 2000). Glutamate is then converted to α-ketoglutarate (α-KG) by the enzyme glutamate dehydrogenase and enters the TCA cycle where serves as a crucial anaplerotic source of OAA because α-KG and OAA are used to generate non-essential amino acids such as aspartate and asparagine, and citrate is used for lipid production as mentioned earlier. Glutamate itself serves as a carbon source for proline and arginine biosynthesis. After glucose, glutamine provides the second source of carbon for fatty acid synthesis. Similar to glucose, glutamine is degraded to lactate but also to alanine, and 60% of glutamine is excreted in form of these two compounds (DeBerardinis et al. 2007). This pathway of glutamine catabolism involves the malic enzyme, which oxidatively decarboxylates malic acid, producing carbon dioxide, pyruvate and NADPH, and has an important role in the production of NADPH (Fig. 6, page 39) (Wise and Thompson, 2011).

However, the glutamine anaplerotic flux can be also important for the generation of the reduced forms of NADH and flavin adenine dinucleotide, which are important to

maintain the $\Delta\psi_m$ and ATP generation (Voet and Voet, 2004). It was also shown that a portion of the glutamine pool is rapidly exported through the bidirectional amino acid transporter SLC7A5/SLC3A2, which regulates cellular efflux of glutamine and transport of essential amino acids into cells. This glutamine flux was suggested to activate the mammalian target of rapamycin mTOR kinase, which regulates protein translation, cell growth and autophagy (Nicklin et al., 2009).

This short overview of glucose and glutamine utilization in main biosynthetic pathways points to glucose and glutamine as important attributes of cell proliferation.

I.6. The c-Myc proto-oncogenic protein as a regulator of cancer cell metabolism

The *C-MYC* gene is the most prominent human oncogene coding for the c-Myc proto-oncogene protein. c-Myc functions as a transcription factor with the helix-loop-helix motif and the leucine zipper domain, and dimerizes with its obligate partner Myc-associated factor X (Max). Together they regulate the expression of many genes involved in the cell cycle, growth, metabolism, apoptosis and differentiation. Deregulated *C-MYC* expression contributes to malignant transformation by promoting cell growth and increasing the genomic instability, and its increased level was found in a broad range of cancers including breast, ovarian, prostate, colon and bladder cancer (Albihn et al., 2010). *C-MYC* is also one of the four genes that could collectively re-programme differentiated cells back to a pluripotent stem cells (Takahashi and Yamanaka, 2006). c-Myc promotes cell growth and metabolic re-programming of cancer cells via the regulation of ribosomal and mitochondrial biogenesis, protein and nucleic acid synthesis and increased glycolysis and glutaminolysis (Dang et al., 2009). Many genes involved in glucose metabolism were found to be direct targets of c-Myc. Among them are the glucose transporter type 1 (*GLUT1*), hexokinase 2 (*HK2*), phosphofructokinase, *LDH A* and enolase 1 (*ENO1*) (Osthus et al., 2000; Kim et al., 2004). It seems that by the regulation of glycolysis, c-Myc could contribute to the Warburg effect. In addition to glycolysis, c-Myc also regulates the metabolism of glutamine. It directly activates the gene expression of glutamine transporters sodium-coupled neutral amino acid transporter 5 (*SLC38A5*) and the neutral amino acid transporter B(0) (*SLC1A5*) (Wise et al., 2008). It also activates the expression of *GLS* via

the inhibition of the expression of microRNAs miR-23a and miR-25b that target *GLS* mRNA. This links c-Myc with the catabolism of glutamine to glutamate and thus provides cells with a large pool of carbons for anaplerosis and NADPH production (Gao et al., 2009).

I.6.1. Regulation of the c-Myc protein level

In normal cells, *C-MYC* expression is tightly regulated by transcriptional, post-transcriptional, translational and posttranslational mechanisms. It responds to many growth-promoting signal transduction pathways and its levels increase rapidly in cells after serum stimulation. The *C-MYC* mRNA and the c-Myc protein feature short half-lives of approximately 20 min. c-Myc is post-transcriptionally regulated by phosphorylation. Phopshorylation on Ser62 in response to proliferative signals stabilizes and promote c-Myc activation, but also allows for phosphorylation at Thr58 by glycogen synthase kinase-3β, resulting in its ubiquitination and proteasomal degradation. On the transcriptional level, *C-MYC* is under downstream regulation of many receptor signalling pathways including Wnt, Notch, Sonic Hedgehog, transforming frowth factor β and tyrosine kinase signalling pathways (Albihn et al., 2010).

Recently it was found in *Drosophila melanogaster* that expression of dMyc is under the control of Yki, the component of the Hippo pathway, and that dMyc functions as an important cellular growth effector of this pathway (Neto-Silva et al., 2010; Ziosi et al., 2010). Furthermore, a negative feedback regulation of Yki by dMyc as a function of the dMyc cellular level was suggested (Neto-Silva et al., 2010). This pathway seems to be conserved in mammals as well. The treatment of Jurkat cells with α-TOS causes activation of the Mst1 kinase that seems to result in the decrease in c-Myc mRNA and protein levels within 6 h of treatment. The involvement of Mst1 activation in c-Myc regulation was examined by *MST1* gene expression silencing using specific siRNA. Examination of c-Myc regulated gene *GLUT1* showed a decrease in its expression as well (Valis et al., unpublished data). This data suggest that treatment of Jurkat cells with α-TOS causes not only apoptosis through the Mst1-FoxO1-Noxa pathway but could also result in the cessation of energy metabolism in cancer cells. It was documented that c-Myc depletion in cancer cells reduces cell proliferation and induces apoptosis in some cases (Wang et al.,

2008). Elucidation of Hippo signalling pathway involvement in the regulation of *C-MYC* gene and influence of downregulated *C-MYC* expression on genes involved in glucose and glutamine metabolism of cancer cells is the goal of this thesis.

II. AIMS OF THE STUDY

The aim of this thesis was the elucidation of the role of the Hippo signalling pathway in the regulation of *C-MYC* gene expression and the influence of altered c-Myc expression on the expression c-Myc target genes that are involved in the metabolism of glucose and glutamine. For this purpose Jurkat cells were exposed to α-TOS, MitoVES and hydrogen peroxide which are known to activate Mst1, the central component of the Hippo signalling pathway.

The objectives of this thesis can be summarized in the following points:

1) The study of mechanisms leading to Mst1 activation by α-TOS, MitoVES and hydrogen peroxide.
2) Determination of Mst1 activation and Yap phosphorylation on Ser127 and their cellular localization.
3) Evaluation of *C-MYC, HK2*, *SLC38A3*, *ENO1* and *GLUT1* mRNA expression.
4) Estimation of c-Myc and Glut1 protein expression.
5) Functional studies related to glucose utilization (glucose uptake and lactate production).

III. MATERIALS AND METHODS

III.1. Materials and devices

III.1.1. Used materials

Abcam

Primary antibody against Glut1

Active Motif

Phosphatase inhibitors (20x), phosphate buffered saline (PBS) (10x), Nuclear Extract Kit

Amersham Biosciences

Ammonium persulphate (APS), glycerol

Becton Dickinson Biosciences

Annexin V-binding buffer (10x), Fluorescein isothiocyanate (FITC) labelled Anexin V

BioRad

Acrylamide/N,N-methylen-bis-akrylamid (BIS) solution, elution solution from the Aurum total RNA mini kit, precision plus protein all blue standards, Fast Eva Green supermix

Cell Signaling Technology

Primary antibodies against: phospho-Mst1 (Thr183)/Mst2 (Thr180), Mst1, cleaved Caspase-3 (Asp175), c-Myc, phospho-Yap (Ser127), Yap

Fermentas

RevertAid First Strand cDNA Synthesis Kit

Fluka

Sodium deoxycholate, nonidet P 40 (NP40), hydrochloric acid, 2-mercaptoethanol, N,N,N´,N´-tetramethylethylendiamin (TEMED)

Illumina

Special optic foil and 48 wells plate for qPCR

LachNer

Ethyl alcohol

Linde

Carbon dioxide

Live Technologies

2-(N-(7-Nitrobenz-2-oxa-1,3-diazol-4-yl)Amino)-2-Deoxyglucose (2-NDBG)

Lonza

Medium RPMI 1640 with L-glutamine

Molecular Research Center

RNAzol, 4-bromoanisole (phase separation reagent)

Penta

Methyl alcohol

Santa Cruz Biotechnology

Primary antibodies against: Lamin B, Actin

Serva

Glycin

Sigma-Aldrich

α-TOS, 4-(2-Hydroxyethyl)piperazine-1-ethanesulfonic acid (HEPES), tris(hydroxymethyl)aminomethan (TRIS), sodium chloride, sodium dodecyl sulphate (SDS), triton X 100, bromophenol blue, Tween 20, nonfat – dried milk bovine, bovine serum albumin (BSA), fetal bovine serum (FBS), antibiotic (ATB) antimycotic solution (100×) stabilized, L-glutamine, protease inhibitor mix (100x), hydrogen peroxide solution, linear polyacrylamide (LPA), propidium iodide (PI), 2′,7′-dichlorodihydrofluorescein diacetate (DCF-DA), tetramethylrhodamine methyl ester perchlorate (TMRM), secondary antibodies: anti-rabbit immunoglobulin type G (IgG) conjugated with peroxidase (antibody produced in goat), anti-goat IgG conjugated with peroxidase (antibody produced in rabbit)

Thermo Scientific

Pierce's BCA protein assay kit, BSA standard solution, super signal west femto maximum sensitivity substrate, super signal west pico maximum sensitivity substrate

Trinity Biotech

Lactate Reagent, Lactate Standard Solution

Whatman

Protran nitrocellulose membrane

MitoVES was synthesized by Jan Štursa from the Institute of Organic Chemistry and Biochemistry, Academy of Sciences, Czech Republic

III.1.2. Used devices

Centrifuges	Mini spin plus centrifuge (Eppendorf)
	5415 R (Eppendorf)
	5702 R (Eppendorf)
	5804 R (Eppendorf)
Balance	PL 403-IC (METTLER TOLEDO)

Cell counter and analyzer	CASY Model TT (Roche)
Cycler	Mastercycler epgradient S (Eppendorf)
Equipment for electrophoresis	Mini-PROTEAN 3 Electrophoresis Cell (BioRad)
Equipment for western blotting	Mini Trans-Blot Cell (BioRad)
Flow cytometer	BD FACSCalibur (Becton Dickinson Biosciences)
Fume hood	Filtair 834 (Erlab)
Incubator	MCO-20AIC (SANYO)
Laminar box	CA/RE 6 (Clean Air) Steril-VBH Compact (Angelantoni Industrie)
Magnetic stirrers	RCT basic safety control (IKA)
Microplate absorbance reader	Sunrise (TECAN)
Microscope	NIB-100 Inverted Biological Microscope (Novel Optics)
Mini rocker	MR 1 (BioSan)
Multifunctional microplate reader	Infinite M200 (TECAN)
Multipurpose CCD camera system	ImageQuant LAS 4000 (GE Healthcare)
Orbital multi-shaker	PSU 20 (BioSan)
Orbital shaker	OS-10 (BioSan)
pH meter	S20 SevenEasy (METTLER TOLEDO)
Pipettes	Automatic pipettes (Eppendorf) Easypet 4420 (Eppendorf)
Power supply	PowerPac™ HC High-Current (BioRad) PowerPac 200 (BioRad)
Real-time PCR system	Eco (ILLUMINA)
Thermomixer	Comfort (Eppendorf)
Vortex	TK 3S (TechnoKartell)
Water bath	Julabo TW20 (Biotech)

III.2. Methods

III.2.1. Cell culture

In the following experiments, the human Jurkat T lymphocyte cell line was used. It is a suspension cell line established in the late 1970s from the peripheral blood of a 14 year old boy with T cell leukemia (Schneider et al., 1977). Jurkat cells were grown in the RPMI 1640 medium with L-glutamine supplemented with 1 % ATB, 1 mM HEPES (pH 7.2), 3 % L-glutamine (w/v) and 10 % FBS (v/v) at 37°C and 5 % CO_2, and passaged three times per week.

III.2.2. Whole cell lysate preparation

The lysis radio-immunoprecipitation assay (RIPA) buffer: 50 mM TRIS, 150 mM NaCl, 0.1% SDS (w/v), 0.5% sodium deoxycholate (w/v), 1% NP40 (v/v), 1 x concentrated protease inhibitors

10 ml of Jurkat cell suspension at $5x10^5$ cells per ml were placed in T75 flasks (bottom surface 75 cm^2) and cultivated under normal culture conditions as mentioned in section III.2.1. Next day, 10 ml of fresh medium was added together with α-TOS (final concentration of 50 μM) or MitoVES (final concentration of 2.5 μM) or hydrogen peroxide (final concentration of 50 μM). After 2, 4, 6, 8 and 10 h of exposure to α-TOS, MitoVES or hydrogen peroxide, about $8.5x10^6$ of treated and control Jurkat cells were taken for the whole cell protein analysis and about 1.5 $x10^6$ cells were used for total RNA isolation (section III.2.6). Cells were transferred into Falcon tubes and spinned down (9 min, 200 x g, 4°C). Medium was removed, and the pellet re-suspended in 900 μl of 1 x concentrated PBS with 1 x concentrated phosphatase inhibitors and transferred to a cold Eppendorf tube. The cells were then spinned down (9 min, 200 x g, 4°C), the supernatant discarded and the pellet re-suspended in 100 μl of the lysis RIPA buffer. Cell lysates were placed on ice and on the shaker for 30 min, vortexed for several times and spinned down (5 min, 14,000 x g, 4°C). The supernatant was placed in a cold Eppendorf tube and stored at 80°C.

III.2.3. Isolation of nuclear and cytosolic fractions

Nuclear and cytosolic fractions were isolated using the Nuclear Extraction Kit. 25 ml of Jurkat cell suspension at $5x10^5$ cells per ml were placed in T150 flasks (bottom surface 150 cm^2) and cultivated under normal culture conditions as mentioned in section III.2.1. Next day, 25 ml of fresh medium was added together with α-TOS (final concentration in cell suspension 50 μM) or MitoVES (final concentration in cell suspension 2.5 μM) or hydrogen peroxide (final concentration in cell suspension 50 μM). After 0.25, 0.5, 1, 2, 4, and 8 h of exposure to α-TOS, MitoVES or hydrogen peroxide, about $2.5x10^7$ of treated and control Jurkat cells were transferred into Falcon tubes and spinned down (9 min., 200 x g, 4°C). The medium was removed, and the pellet re-suspended in 1 ml of 1 x concentrated PBS with 1 x concentrated phosphatase inhibitors and transferred to a cold Eppendorf tube. The nuclear and cytosolic fractions were isolated according to the manufacture protocol, but instead of 500 μl of 1 x concentrated hypotonic buffer, 250 μl of 1 x concentrated hypotonic buffer with 1 x concetrated protease inhibitors was used. The purity of individual fractions was assessed by western blotting using antibody against lamin B for the cytosolic fraction and actin for the nuclear fraction.

III.2.4. Protein concentration assessment

Protein concentration was assessed using Pierce BCA Protein Assay Kit with BSA (Thermo Scientific) as the protein standard. This method combines the reduction of Cu^{2+} to Cu^{1+} by peptide bonds resulting in the with colorimetric detection of the Cu^{1+} cation reacting with bicinchoninic acid (BCA) (Wiechelman et al., 1988). The purple-coloured product of this reaction is formed by chelation of two BCA molecules with one Cu^{1+} cation and exhibits absorbance at 562 nm. Albumin standards were prepared by diluting one BSA standard ampule at the concentration 2 mg/ml into several Eppendorf tubes, using water as the diluent. The final BSA standard concentrations were: 2,000, 1,500, 1,000, 750, 500, 250, 125 and 25 μg/ml. 1.25 μl of whole cell lysate or nuclear or cytosolic fraction and 23.75 μl of water were pippeted into the well of the 96 wells plate. 25 μl of each BSA

standard at different concentration was pipetted into the wells of the plate. 200 µl of the reagent, which was prepared by mixing 50 parts of BCA Reagent A with one part of BCA reagent B, was added to each well. The plate was shaked for 30 sec and incubated at 37°C for 30 min. It was then cooled down to room temperature (RT) and the absorbance was assessed at 570 nm using a plate absorbance reader (Sunrise). 1.25 µl of the lysis buffers used during protein isolation diluted with 23.75 µl of water were used as a blanks.

III.2.5. Western blotting

4 x concentrated sample loading buffer: 8% SDS (w/v), 40% glycerol (v/v), 20% 2-mercaptoethanol (v/v), 0.04% bromphenol blue (w/v), 0.25 M TRIS.HCl, pH 6.8
Separating gel: 375 mM TRIS.HCl, pH 8.8, 0.1% SDS (w/v), 10% acrylamide/BIS (v/v), 0.1% TEMED (v/v), 0.05% APS (w/v)
Stacking gel: 125 mM TRIS HCl, pH 6.8, 0.1% SDS (w/v), 4% acrylamide/BIS (v/v), 0.1% TEMED (v/v), 0.05% APS (w/v)
Running buffer: 25 mM TRIS, 192 mM glycin, 5% SDS (w/v)
Transfer buffer: 25 mM TRIS, 192 mM glycine, 200ml MetOH, H_2O to 1 l
TBS (TRIS buffered saline) buffer: 10 mM TRIS, 165 mM NaCl, 0.05 % Tween 20 (v/v)

80 µg of the whole cell lysate, 80 µg of the cytosolic fraction or 30 µg of the nuclear fraction were adjusted to the same volume with water. 4 x concentrated sample-loading buffer was added so that its final concentration was 1 x. Samples were heated for 5 min at 99°C. The separating gel was poured between two glass plates approximately 2 cm under the top of the glass and overlaid with ethanol. When the separating gel polymerized, the stacking gel was poured onto the wetted separating gel and a comb was inserted. After polymerization, the comb was removed and the glass plates with the gel were placed in the electrophoresis chamber. The electrophoresis chamber was placed in a tank and filled up with the running buffer. The gel was loaded with samples and 5 µl of the standard was used. Electrophoresis ran at 0.04A till the samples were approximately 5 mm above the bottom of the glass plates.

After electrophoresis, a “sandwich” for western blotting to transfer proteins onto nitrocellulose membrane was made and fixed in the blotting chamber, which was then

placed in a tank that was filled up with the transfer buffer. The blot ran at 0.30 A and 4°C for 2 h. After blotting, the membrane was washed with the TBS buffer and blocked for 1 h in 5% milk (w/v) dissolved in the TBS buffer. The primary antibody was diluted according to the manufacturer's protocol in 5% BSA (w/v) dissolved in the TBS buffer with 0.1 % Tween 20. The membrane was incubated with the primary antibody overnight at 4°C on a rocking platform. In the morning, the membrane was washed 3 x for 10 min with the TBS buffer, incubated for 45 min with the secondary antibody, which was diluted according to the manufacturer's manual in 5% milk (w/v) dissolved in the TBS buffer with 0.1 % Tween 20, and then washed 3 x for 5 min with the TBS buffer. The chemiluminescent substrates (Super Signal West Femto maximum sensitivity substrate and Super Signal West Pico maximum sensitivity substrate) were mixed 1:1, and 600 µl of this solution was applied on the membrane. The signal was detected using the Multipurpose CCD camera system (ImageQuant LAS 4000). The Super Signal West Pico maximum sensitivity substrate was used to detect actin and lamin. Other proteins in this thesis were detected by using of the Super Signal West Femto maximum sensitivity substrate.

III.2.6. Total RNA isolation

Total RNA isolation was performed using RNAzol. Cells were treated as described in the section III.2.2. About 1.5 x 10^6 cells were transferred into Falcon tubes and spinned down (9 min, 200 x g, 4°C). The medium was removed and the pellet re-suspended in 500 µl of RNAzol. 2 µl of LPA to get a visible pellet in the subsequent steps and 200 µl of water were added. The lysate was vortexed for 15 s, incubated for 10 min at RT and spinned down (15 min, 12,500 x g, RT). 600 µl of the supernatant was transferred into new Eppendorf tube and 3 µl of 4-bromoanisole was added. The lysate was vortexed for 15 s, incubated for 5 min at RT and spun down (10 min, 12,500 x g, RT). The supernatant was transferred into a fresh Eppendorf tube and equal volume of cold (-20°C) isopropanol was added. The mixture was mixed by inverting the tube several times and placed at -20°C for 60 min. It was then spun down (15 min, 14,000 x g, 4°C), washed twice with 800 µl ice-cold 80 % EtOH, and spun down (2 min, 10,000 x g, 4°C). After each spin, all supernatants was aspirated. An open tube with the pellet was placed on a heated block set to 55°C. After

1-2 min, 30 µl of elution solution TE was added and the pellet was solubilized for 10 min. Isolated total RNA was stored at -80°C.

III.2.7. Total RNA concentration assessment

Concentration of total RNA was assessed by using the multifunctional microplate reader (Infinite M200). 2 µl of total RNA were pipetted on the special NanoQuant plate. Absorption of total RNA was assessed at 260 nm. 2 µl of the elution solution were used as blank. The ratio of absorbance at 260nm and 280nm should be 2.

III.2.8. Reverse transcription

Reverse transcription was performed using the RevertAid First Strand cDNA Synthesis Kit. Total RNA (2.5 µg) was used as a template and oligo $(dT)_{18}$ as primers. Reverse transcription was performed according to the manufacturer's protocol. cDNA was stored at -20°C.

III.2.9. Quantitative PCR (qPCR)

qPCR was performed by using the Real time PCR system Eco and the ssoFast Eva Green supermix. Mastermix was prepared as follows: 3,94 µl of 2x Eva Green supermix, 0.197 µl of 10 µM forward and reverse specific primers and 1.116 µl of water. 5 µl of Mastermix were pipetted into each well of a 48 wellsplate and spun down (10 s, 2,250 x g, RT). cDNA was diluted so that 2.5 µl corresponded to 10 ng total RNA. 2.5 µl of the diluted cDNA was pipetted into the wells of the plate, and the plate was sealed with a special adhesive foil. The plate was centrifuged 2250 x g for 10 s, then mixed by flipping up and down and centrifuged again at 2,250 x g for 2 min. The plate was incubated in the cycler as follows: 98°C for 30 s (polymerase activation, 37 cycles: 98°C for 5 s (denaturation), 60°C for 15 s (annealing), 72°C for 20 s (extension). To verify the product identity, we analysed the melting curves. Human ribosomal protein large *P0* (*RPLP0)* was

used as the “house-keeping” gene for comparison of expression levels between samples. Data were evaluated using the ΔΔCt method. The values were assessed for statistical significance using the t-test.

III.2.10. Primer design

Sequences of the tested genes were obtained from NCBI (National Center for Biotechnology Information, www.**ncbi**.nlm.nih.gov). All primers were designed using the Primer-BLAST (http://www.ncbi.nlm.nih.gov/tools/primer-blast/). The length of the primers was between 18 and 23 nucleotides, the GC content was between 50% and 60%, and all primers were tested for the secondary structure presence to avoid interfering structures. The following primers were used for PCR analysis:

C-MYC	Forward	5′-TCG GAT TCT CTG CTC TCC TC-3′
	Reverse	5′-TCG GTT GTT GCT GAT CTG TC-3′
GLUT1	Forvard	5′-CTG ACG TGA CCC ATG ACC TG-3′
	Reverse	5′-GTG TTG ACG ATA CCG GAG CC-3′
ENO1	Forward	5′-CTT CCA GGT GTC TCA AAG GCT-3′
	Reverse	5′-CTT CTC AAC GGC ACC AGC TT-3′
HK2	Forward	5′-GTG GCA CCC AGC TGT TTG AC-3′
	Reverse	5′-CCT TCC GGA TCA GAG CCA CA-3′
SCL38A3	Forward	5′-TCA TCA AGT CTG AGC TGC CAC-3′
	Reverse	5′-TTC CCG TTC ATG TAC CAG TCC-3′
RPLP0	Forward	5′-TCG ACA ATG GCA GCA TCT AC-3′
	Reverse	5′-ATC CGT CTC CAC AGA CAA GG-3′

III.2.11. Detection of cell death

Annexin V detection reaction mix: 1 µl of annexin V-FITC, 10 µl of 10 x concentrated annexin V-binding buffer, 89 µl of 1 x concentrated PBS.

The level of cell death was assessed by flow cytometry using the annexin V/PI method. Annexin V is a Ca^{2+} dependent phospholipid-binding protein with high affinity for phosphatidyl serine (PS) that becomes exposed at the external surface of the cell during the early phases of apoptosis. PI stains cells that loose plasma membrane integrity, which occurs during necrosis (Vermes et al., 1995). To characterise the extent and the nature of cell death, the 'dual' staining method with FITC-labelled Anexin V (green fluorescence) and PI (red fluorescence) was performed. 1 ml of Jurkat cell suspension containing 10^5 cells was pipetted into 12-well plates and cultivated under normal culture conditions as mentioned in section III.2.1. Next day, the cells were exposed to 50 µM α-TOS or 2.5 µM MitoVES or 50 µM hydrogen peroxide for 8 h. After the drug treatment, the cells were transferred into special tubes for flow cytometry, spun down (9 min., 200 x g, RT), and washed with 800 µl of PBS. The supernatant was removed and the pellet re-suspended in 100 µl the annexin V detection reaction mix. The samples were incubated for 20 min at 4°C in the dark, followed by the addition of PI to a final concentration of 1.5 µM, and incubated for additional 10 min. Cell death was assessed by flow cytometry, using the BD FACS Calibur flow cytometer. The FITC fluorescence was measured on channel FL1 (emissions wavelength 515-545 nm) and PI fluorescence on channel FL3 (emissions wavelength >650 nm). The acquired data were analysed using the FlowJo 9.6.2. software. The percentage of apoptotic cell death was calculated by sum of quadrants indicating percentage of PI-positive cells, FITC-labelled annexin V-positive cells and FITC-labelled annexin V/PI-positive cells. The values were graphed and assessed for statistical significance using the t-test.

III.2.12. Assessment of cellular level of reactive oxygen species

To estimate the cellular level of ROS, the cell permeable probe DCF-DA was used. Upon entering the cell, DCF-DA is deacetylated by cellular esterases to a non-fluorescent

membrane-impermeable 2,7-dichlorodihydrofluorescein, which is then oxidised by ROS to a green fluorescent 2,7-dichlorofluorescein (Gomes et al., 2005). 1 ml of Jurkat cell suspension containing 10^5 cells was pippeted into 12-well plates and cultivated under normal culture conditions as mentioned in section III.2.1. Next day, the cells were exposed to 50 μM α-TOS or 2.5 μM MitoVES or 50 μM hydrogen peroxide for 7.5, 15, 30, 60, 120 and 180 min. 20 min before the end of the drug exposure, DCF-DA was added into each well to a final concentration of 2.5 μM, and cells were incubated in the dark at 37°C. The cells were then transferred into the flow cytometry tubes, spun down (9 min., 200 x g, RT) and washed with 800 μl of PBS. The supernatant was removed and the pellet re-suspended in 100 μl of PBS. The level of cellular ROS during the drug treatment was assessed by flow cytometry, using the BD FACS Calibur flow cytometer. The 2,7-dichlorofluorescein fluorescence was evaluated on channel FL1 (emissions wavelength 515-545 nm). The acquired data were analysed using the FlowJo 9.6.2. software. The level of cellular ROS was evaluated as geometric mean of DCF-DA fluorescence. The values were graphed and assessed for statistical significance using the t-test. DCF-DA was used in combination with TMRM (see bellow).

III.2.13. Assessment of mitochondrial inner trans-membrane potential ($\Delta\psi_m$)

$\Delta\psi_m$ is usually evaluated using cationic lipophilic dyes that are sequestered by mitochondria in amounts proportional to their membrane potential. TMRM, a cationic red-orange fluorescent dye, was used to assess the changes in $\Delta\psi_m$ during the drug treatment. 1 ml of Jurkat cell suspension containing 10^5 cells was pipetted into 12-well plates and cultivated under normal culture conditions as mentioned in section III.2.1. Next day, the cells were exposed to 50 μM α-TOS or 2.5 μM MitoVES or 50 μM hydrogen peroxide for 7.5, 15, 30, 60, 120 and 180 min. 20 min before the end of the drug exposure, TMRM was added into each well to a final concentration of 50 nM and cells were incubated in the dark at 37°C. The cells were then transferred into the flow cytometry tubes, spun down (9 min., 200 x g, RT) and washed with 800 μl of PBS. The supernatant was removed and the pellet re-suspended in the 100 μl of PBS. The changes in $\Delta\psi_m$ during the drug treatment were assessed by flow cytometry using the BD FACS Calibur flow cytometer. The TMRM

fluorescence was evaluated on channel FL2 (emissions wavelength 564-606 nm). The acquired data were analysed using the FlowJo 9.6.2. software. The changes in $\Delta\psi_m$ were evaluated as geometric mean of TMRM fluorescence. The values were graphed and assessed for statistical significance using the t-test.

III.2.14. Assesment of glucose uptake

To monitor glucose uptake in live cells, a fluorescent glucose analogue 2-NBDG was used. Dual staining with PI was used for the exclusion of dead cells. 1 ml of Jurkat cell suspension containing 10^5 cells was pipetted into 12-well plates and cultivated under normal culture conditions as mentioned in section III.2.1. Next day, the cells were exposed to 50 μM α-TOS or 2.5 μM MitoVES or 50 μM hydrogen peroxide for 2, 4, 6, 8 and 10 h. 20 min before the end of the drug exposure, 2-NBDG was added into each well to a final concentration of 50 μM and cells were incubated in the dark at 37°C. The cells were then transferred into flow cytometry tubes, spun down (9 min., 200 x g, RT) and washed with 800 μl of PBS. The supernatant was removed and the pellet re-suspended in 100 μl of PBS. Then PI was added to a final concentration of 1.5 μM and samples incubated for additional 10 min. Glucose uptake during the drug treatment was assessed by flow cytometry using the BD FACS Calibur flow cytometer. PI-positive cells, evaluated on channel FL3 (emissions wavelength >650 nm), were 'gated out' to assess only live cells. 2-NBDG fluorescence was evaluated on channel FL1 (emissions wavelength 515-545 nm). The acquired data were analysed using the FlowJo 9.6.2. software. Glucose uptake was evaluated as geometric mean of 2-NBDG fluorescence. The values were graphed and assessed for statistical significance using the t-test.

III.2.15. Assessment of lactate production

Lactate production was assessed on the bases of an enzymatic reaction when lactic acid is converted to pyruvate and hydrogen peroxide by lactate oxidase. In the presence of the generated hydrogen peroxide, a peroxidase catalyzes the oxidation of the chromogen precursors to produce a dye with an absorption maximum at 540 nm. The increase in the

absorbance at 540 nm is proportional to the lactate concentration in the sample. 1 ml of Jurkat cell suspension containing 10^5 cells were pipetted into 12-well plates and cultivated under normal culture conditions as mentioned in section III.2.1. Next day, the cells were exposed to 2.5 µM MitoVES for 8 h. The cells were then transferred into Eppendorf tubes and their number assessed using the CASY Model TT cell counter. The cells were spun down (9 min, 200 x g, RT). 100 µl of the lactate reagent were pipetted into a 96 well plate together with 1 µl of the medium taken from treated cells. 1 µl of fresh medium was used as a blank.

IV. RESULTS

IV.1. Vitamin E analogues induce apoptosis in cancer cells

It was shown in several reports, that VE analogues MitoVES and α-TOS induce apoptosis in cancer cells. Since the concentrations of these agents used in this thesis were selected based on previous work (Dong et al., 2011a), the assessment of apoptotic cell death was performed to check if their efficacy to kill cancer cells is comparable. Hydrogen peroxide in this thesis was used as a control for other experiments, therefore its efficacy in apoptosis induction was also studied. Detection of apoptotic cell death induced by MitoVES, α-TOS and hydrogen peroxide was assessed by flow cytometry using annexin V labelled FITC/PI assay. Jurkat cells were treated and stained as described in the section III.2.11. The drugs used at concentrations of 2.5 μM (MitoVES), 50 μM (α-TOS) and 50 μM (hydrogen peroxide) elicit similar efficacy in apoptosis induction. About 30 % of apoptotic cells were detected within 8 h of treatment (Fig.7).

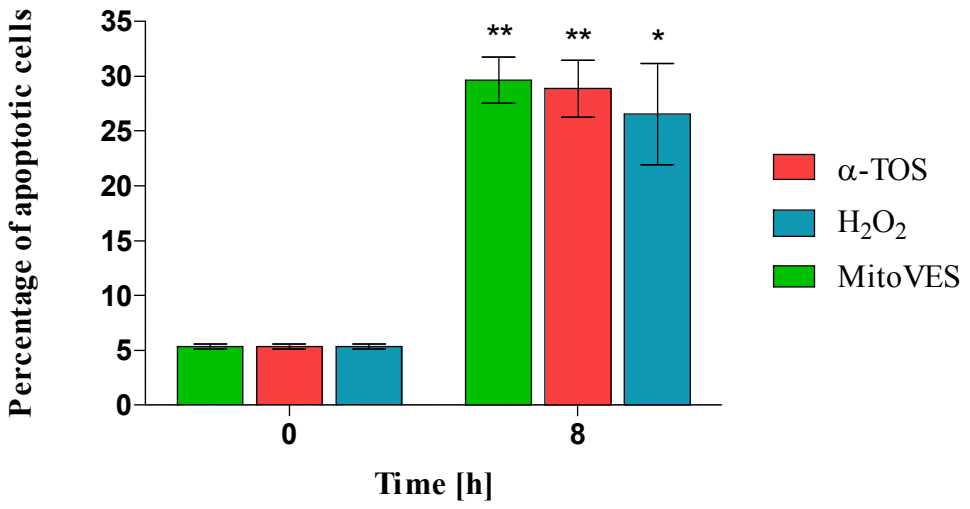

Figure 7. Percentage of apoptotic Jurkat cells exposed to 2.5 μM MitoVES, 50 μM α-TOS and 50 μM H_2O_2 measured by flow cytometry with FITC-labelled annexin V and propidium iodide. Results are represented as mean values ± S.E.M. (n=3). Statistical significance was calculated using the t-test, where the values obtained from the treated cells were compared to the control values; * $p < 0.05$, ** $p < 0.01$.

IV.2. Vitamin E analogues induce generation of ROS and dissipation of mitochondrial inner transmembrane membrane potential

Generation of mitochondrial ROS has emerged as an important mechanism by which vitamine E analogues induce cell death (Dong et al., 2011a). Flow cytometry using DCF-DA as a probe was utilized to investigate the levels and time when ROS is produced in response to α-TOS and MitoVES. Jurkat cells were treated as described in section III.2.12. MitoVES at 2.5 μM promoted 4-fold increased in the ROS level within 7.5 min, the level of ROS further increased to achieve the maximum at 30 min when a 5-fold increase in the ROS level related to the control was observed. The effect of 50 μM α-TOS on ROS production was very low during the early time, but it increased to about 2-fold in 2 h and to 3-fold in 3 h. Since 50 μM hydrogen peroxide was used as a control for other experiments, the cellular level of ROS in response to this agent was also probed. 2.5 fold increased levels of ROS were observed within 7.5 min, then the ROS level stagnated and increased again after 1 h when it reached the maximum (Fig.8, page 61).

It was documented that high levels of ROS have an impact on the function of mitochondrial enzymes and on the leakage of proteins from the mitochondrial inter-membrane space into the mitochondrial matrix, leading to dissipation of $\Delta\psi_m$ (Mailloux and Harper, 2012). To assess the effect of MitoVES and α-TOS on $\Delta\psi_m$ in Jurkat cells, flow cytometry using TMRM was used. The cells were treated as described in section III.2.13. Fig. 9, page 61 displays a massive decrease in $\Delta\psi_m$ within 7.5 min of exposure of the cells to 2.5 μM MitoVES. 50 μM α-TOS had no effect on $\Delta\psi_m$ at least for the times indicated in this experiment, and 50 μM hydrogen peroxide showed 2-fold decrease in $\Delta\psi_m$ in 2 h, which continued further.

These results indicate that the mitochondrially targeted VE analogue MitoVES is significantly more efficient in ROS generation than its parental compound α-TOS. Moreover, MitoVES and hydrogen peroxide dissipate $\Delta\psi_m$.

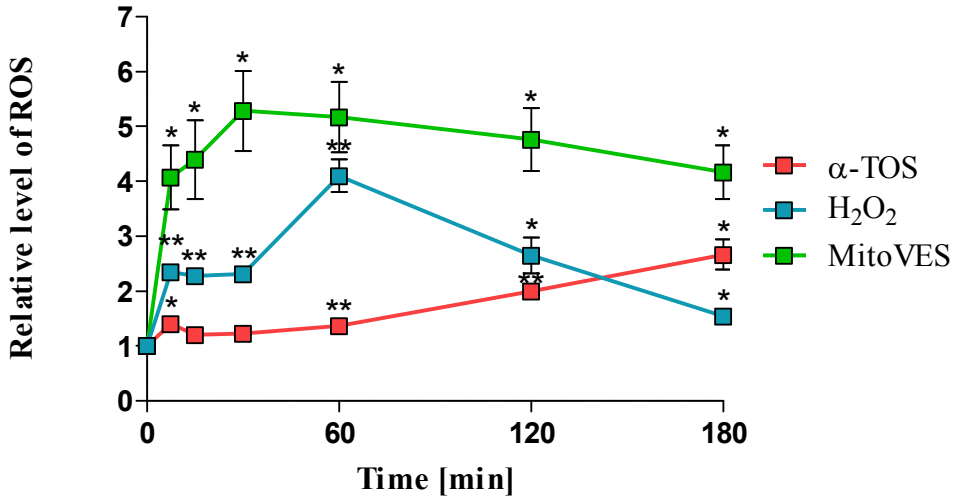

Figure 8. Relative level of ROS during treatment of Jurkat cells with 2.5 µM MitoVES, 50 µM α-TOS and 50 µM H_2O_2 assessed by flow cytometry using DCF-DA as a probe. Results are represented as mean values ± S.E.M (n=3). Statistical significance was calculated using the t-test, where values obtained from the treated cells were compared to the control values at time 0; * $p < 0.05$, ** $p < 0.01$.

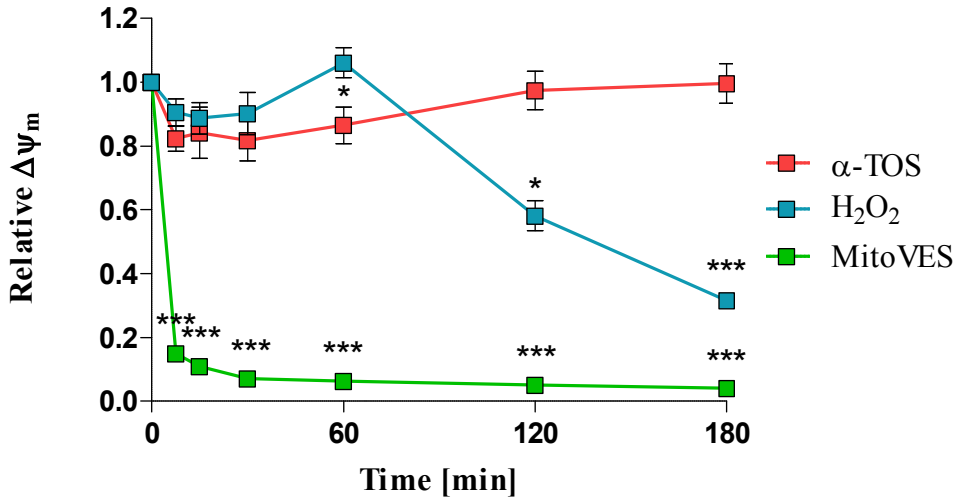

Figure 9. Relative $\Delta\psi_m$ during treatment of Jurkat cells with 2.5 µM MitoVES, 50 µM α-TOS and 50 µM H_2O_2 measured by flow cytometry using TMRM as a probe. Results are represented as mean values ± S.E.M. (n=3). Statistical significance was calculated using the t-test, where the values obtained from the treated cells were compared to the control values at time 0; * $p < 0.05$, *** $p < 0.001$

IV.3. Vitamin E analogues promotes phosphorylation of Mammalian sterile 20-like kinase 1

Mitochondrially generated superoxid anion radicals, in response to MitoVES and α-TOS treatment, are believed to be converted into highly diffusible hydrogen peroxide that is responsible for Mst1 activation by its autophosphorylation on Thr183 (Lehtinen et al., 2006; Morinaka et al., 2011). This was probed by western blotting (section III.2.5) with antibody against Mst1 phosphorylated on Thr183. Hydrogen peroxide was used as a control compound. Cytosolic and nuclear protein fractions were prepared from Jurkat cells treated with 2.5 μM MitoVES, 50 μM α-TOS and 50 μM hydrogen peroxide as described in the sections III.2.3.

Activation of Mst1 was detected in cytosolic fractions within 15 min following incubation with MitoVES, α-TOS and hydrogen peroxide (Fig. 10-12, pages 63-65). The level of phosphorylated Mst1 was also slightly higher in the nuclear fractions of the treated samples. We also observed the appearance of a 36 kDa Mst1 fragment in the cytosolic fractions within 4 h following incubation with MitoVES (Fig. 10, page 63) and hydrogen peroxide (Fig. 12, page 65) and within 8 h following incubation with α-TOS (Fig.11, page 64). Almost no 36 kDa Mst1 fragment was observed in the nuclei of treated cells (Fig. 10-12, pages 63-65). Activated caspase-3 was documented earlier to cleave Mst1 (Cheung et al., 2003; Wen et al., 2010). The occurrence of the 36 kDa Mst1 fragment correlated with the appearance of cleaved caspase-3 in the cytosolic fractions of the exposed cells (Fig. 10-12, pages 63-65).

Collectively, these data document that MitoVES, α-TOS and hydrogen peroxide promote the activation of Mst1 and its caspase-3 dependent cleavage.

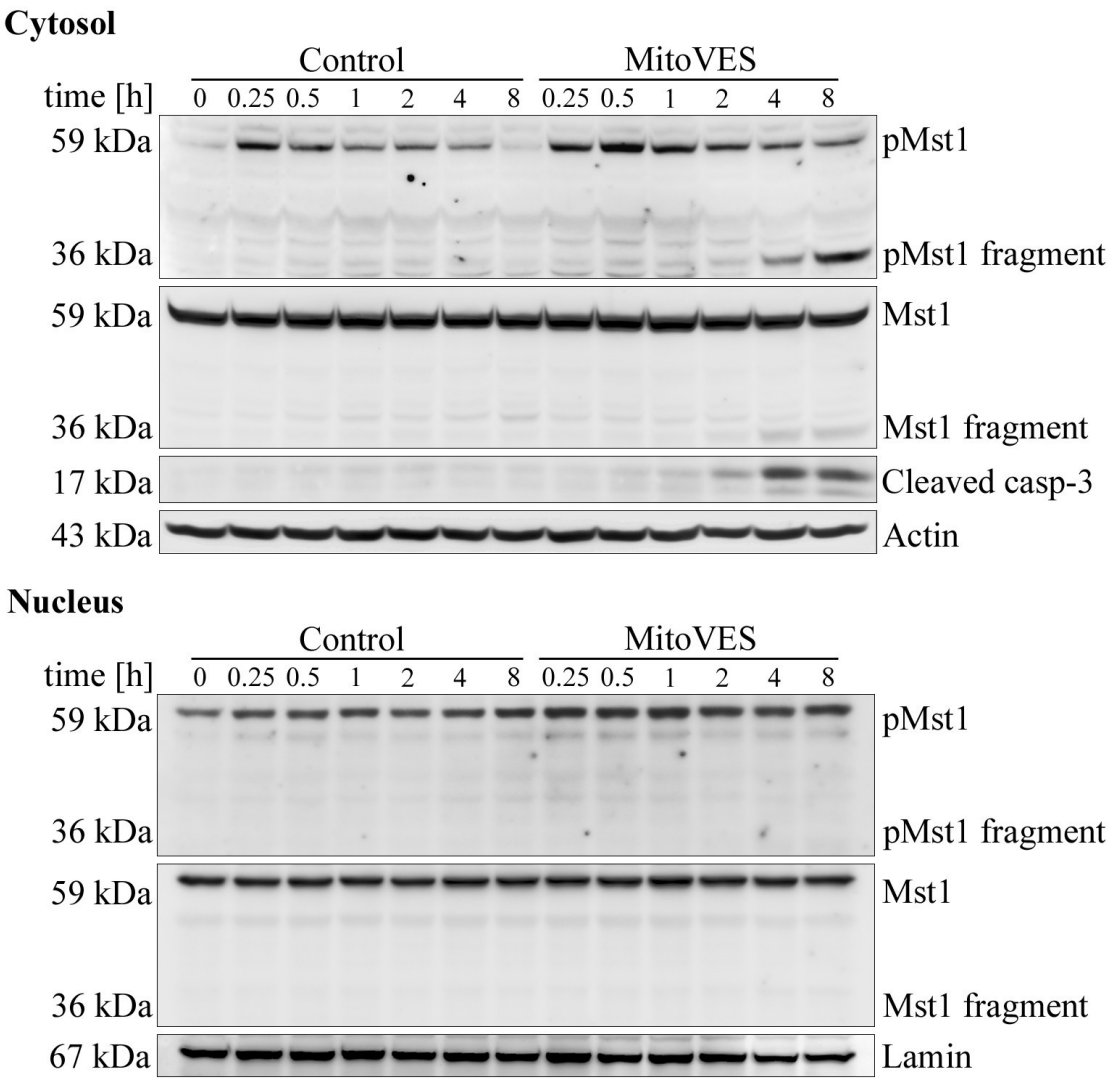

Figure 10. Western blot showing Mst1, its form phosphorylated on threonine 183 (pMst1) and cleaved caspase-3 (cleaved casp-3) in cytosolic and nuclear fractions obtained from Jurkat cells treated with 2.5 μM MitoVES. Actin and lamin were used as loading controls. The images shown are representative of 3 independent experiments.

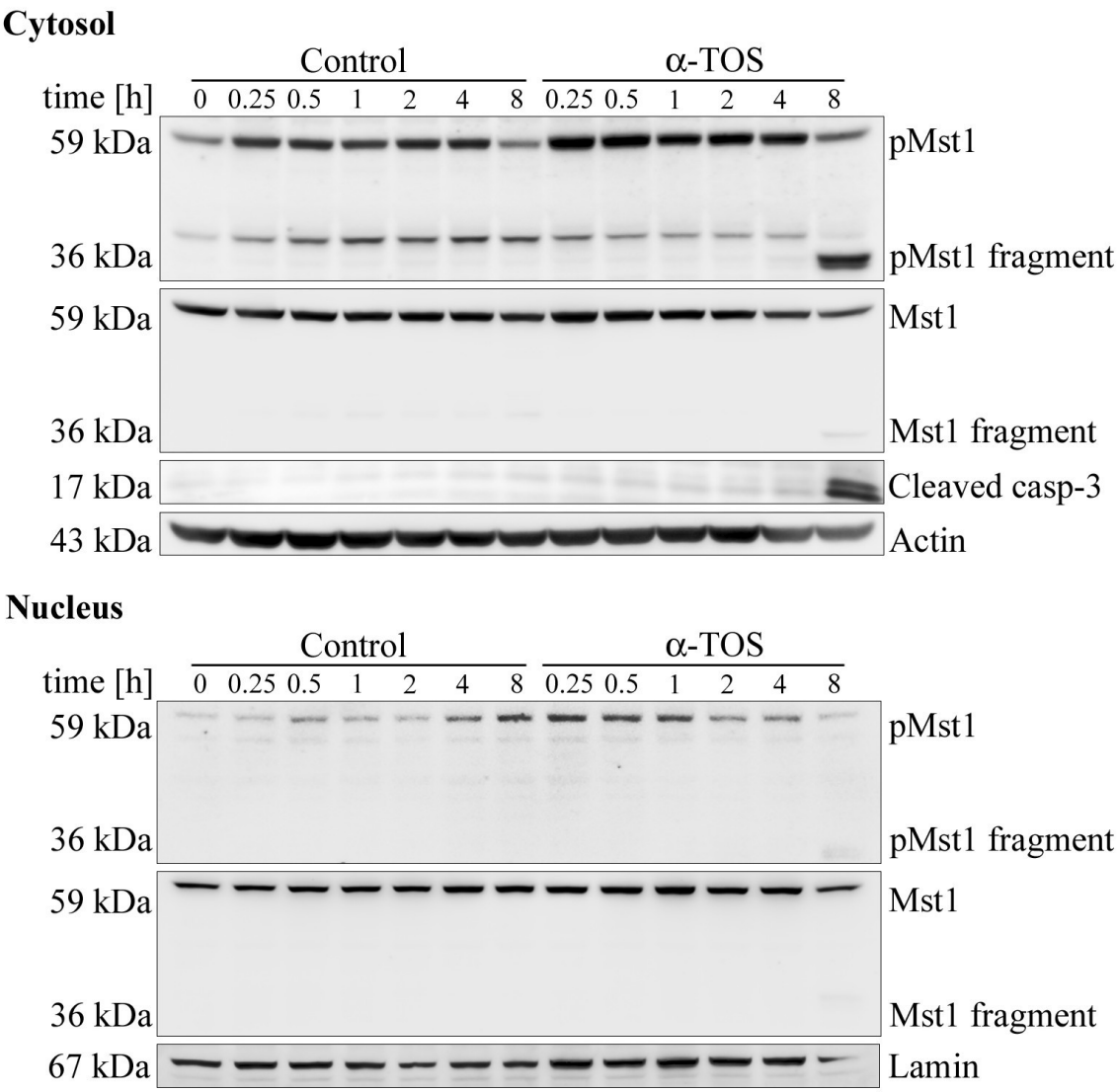

Figure 11. Western blot showing Mst1, its form phosphorylated on threonine 183 (pMst1) and cleaved caspase-3 (cleaved casp-3) in cytosolic and nuclear fractions obtained from Jurkat cells treated with 50 μM α-TOS. Actin and lamin were used as loading controls. The images shown are representative of 3 independent experiments.

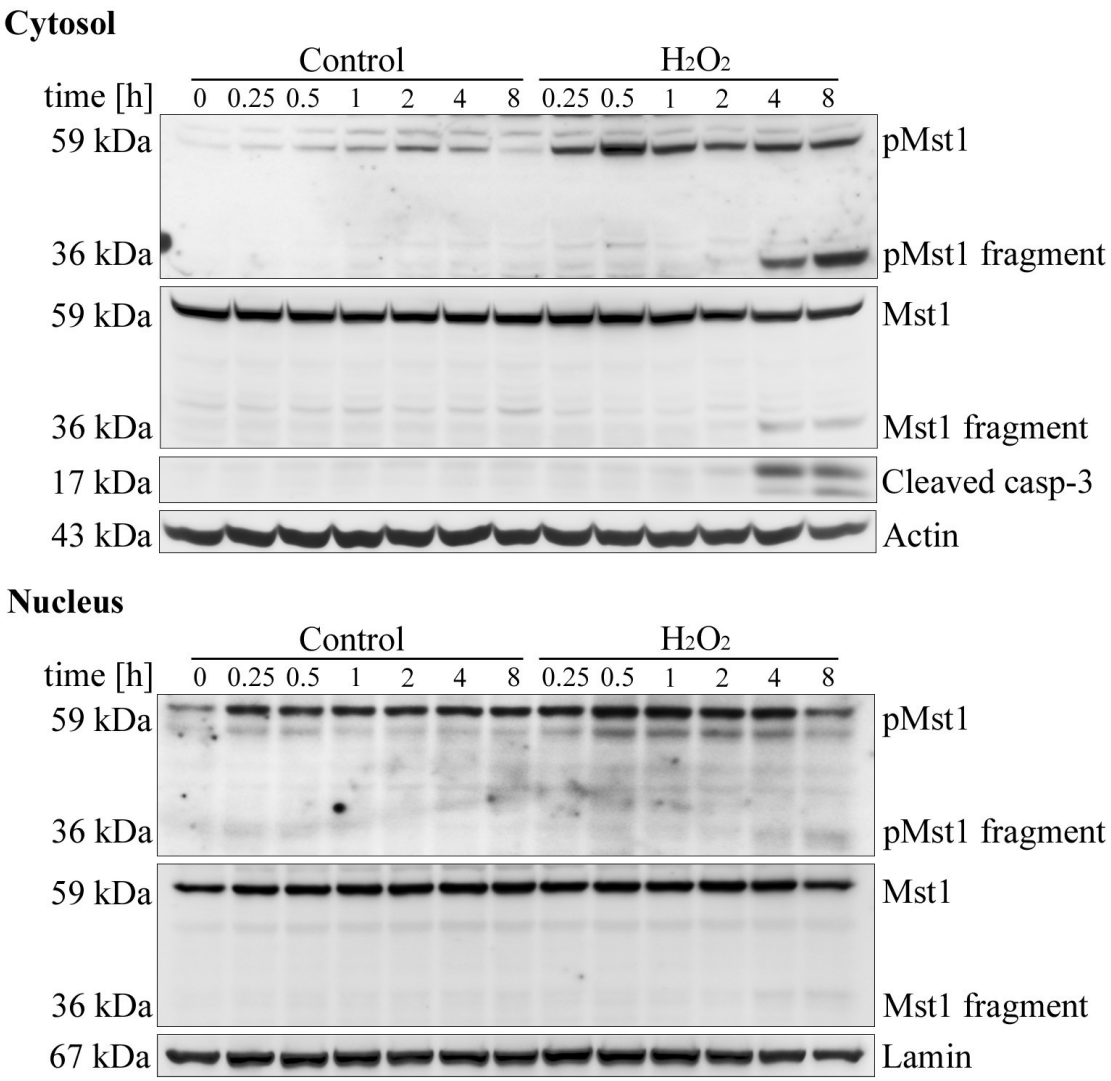

Figure 12. Western blot showing Mst1, its form phosphorylated on threonine 183 (pMst1) and cleaved caspase-3 (cleaved casp-3) in the cytosolic and nuclear fractions obtained from Jurkat cells treated with 50 μM H_2O_2. Actin and lamin were used as loading controls. The images shown are representative of 3 independent experiments.

IV.4. Vitamin E analogues promotes phosphorylation of Yes-associated protein and its transport from nucleus to cytosol

The activation of Mst1, the central part of the Hippo signalling pathway, results in Yap phosphorylation on Ser127 and its cytoplasmic retention by 14-3-3 proteins (Pan,

2010). Phosphorylation of Yap on Ser127 and its translocation from the nucleus to the cytoplasm in response to MitoVES, α-TOS and hydrogen peroxide was assessed by analysing cytosolic and nuclear fractions by western blotting (section III.2.5) with antibodies against Yap and its form phosphorylated on Ser127 (pYap). Cytosolic and nuclear protein fractions were prepared from Jurkat cells treated with 2.5 μM MitoVES, 50 μM α-TOS and 50 μM hydrogen peroxide as described in the sections III.2.3.

pYap was observed in the cytosolic fractions of cells treated with MitoVES, α-TOS and hydrogen peroxide within 15 min, after which the level of pYap was relatively unchanged until 1 h in cells treated with MitoVES (Fig. 13, page 67) and until 2 h in cells treated with α-TOS (Fig. 14, page 67) and hydrogen peroxide (Fig. 15, page 68), then it decreased. The increase in pYap was also observed in the nuclear fractions of cells treated with MitoVES, α-TOS and hydrogen peroxide (Fig. 13-15, pages 67-68). The level of pYap in the cytosolic fractions of the treated cells relatively correlated with the total Yap level in the same fractions. Massive increase of Yap in the cytosolic fractions was observed within a 15 min exposure of cells to MitoVES, α-TOS and hydrogen peroxide, then its level was unchanged till 1 h in cells treated with MitoVES (Fig. 13, page 67) and hydrogen peroxide (Fig. 15, page 68), and till 30 min in cells treated with α-TOS (Fig. 14, page 67), since when diminished. The level of Yap in the nuclear fractions reduced gradually during the treatment with MitoVES (Fig. 13, page 67) and hydrogen peroxide (Fig. 15, page 68). The nuclear Yap level in α-TOS exposed cells seems to increase slightly at early times and then went down, but about 2 h later then with MitoVES and hydrogen peroxide (Fig. 14, page 67).

Taken together, these data suggest that exposure of Jurkat cells to MitoVES, α-TOS and hydrogen peroxide lead to phosphorylation of Yap on Ser127 and its transport from the nucleus to the cytoplasm, where it is degraded.

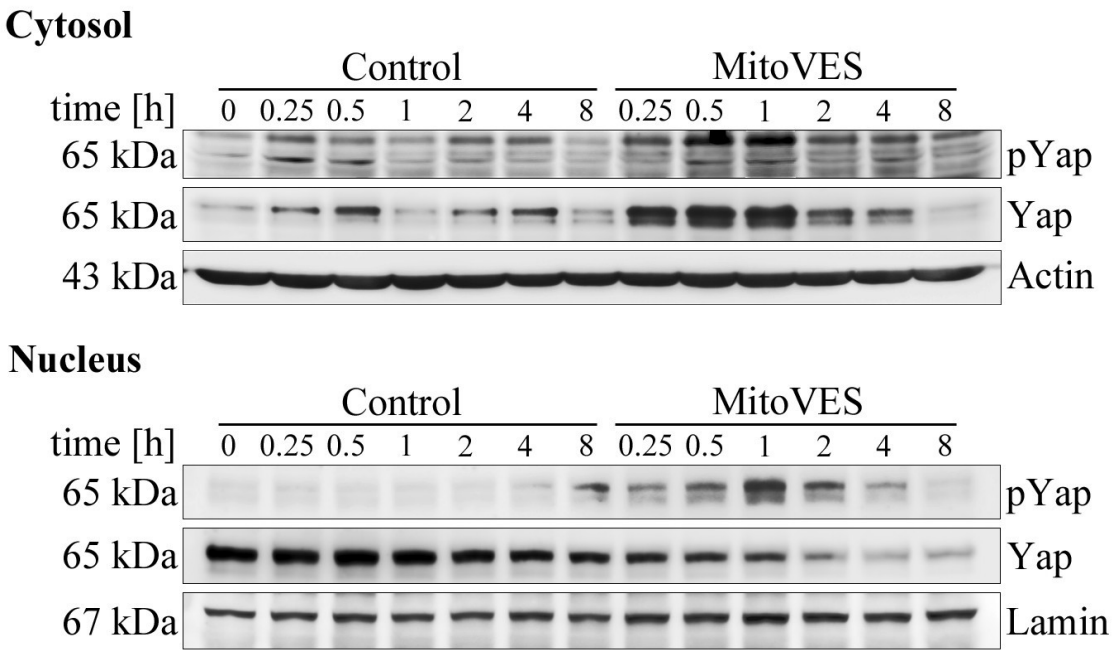

Figure 13. Western blot showing Yap and its form phosphorylated form on serin 127 (pYap) in the cytosolic and nuclear fractions obtained from Jurkat cells treated with 2.5 μM MitoVES. Actin and lamin were used as loading controls. The images shown are representative of 3 independent experiments.

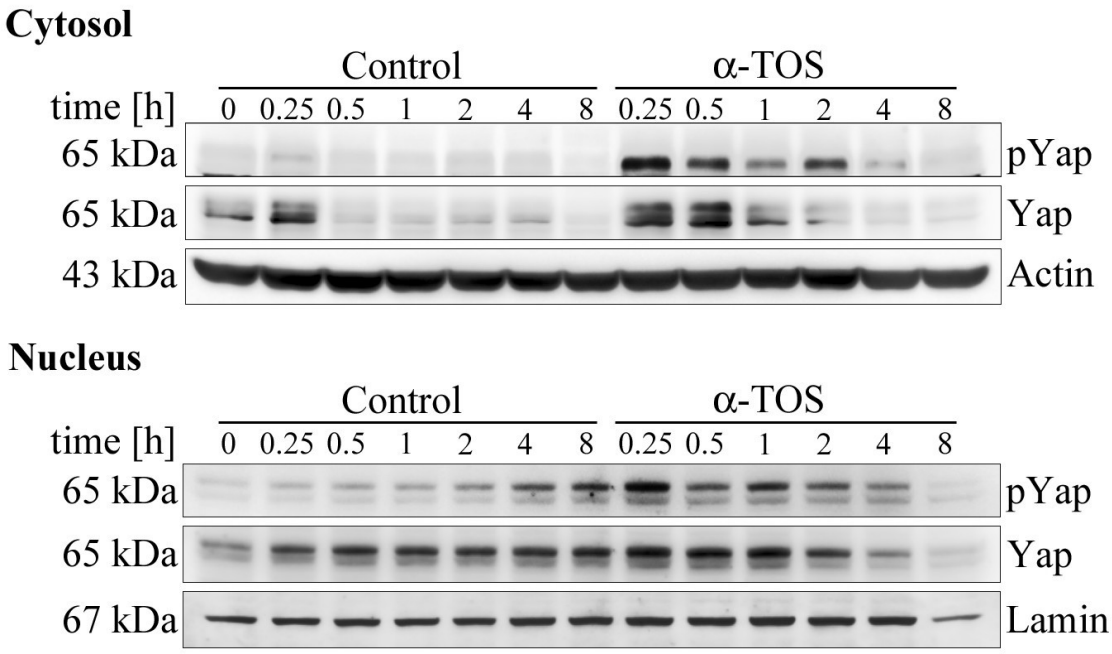

Figure 14. Western blot showing Yap and its form phosphorylated on serin 127 (pYap) in the cytosolic and nuclear fractions obtained from Jurkat cells treated with 50 μM α-TOS. Actin and lamin were used as loading controls. The images shown are representative of 3 independent experiments.

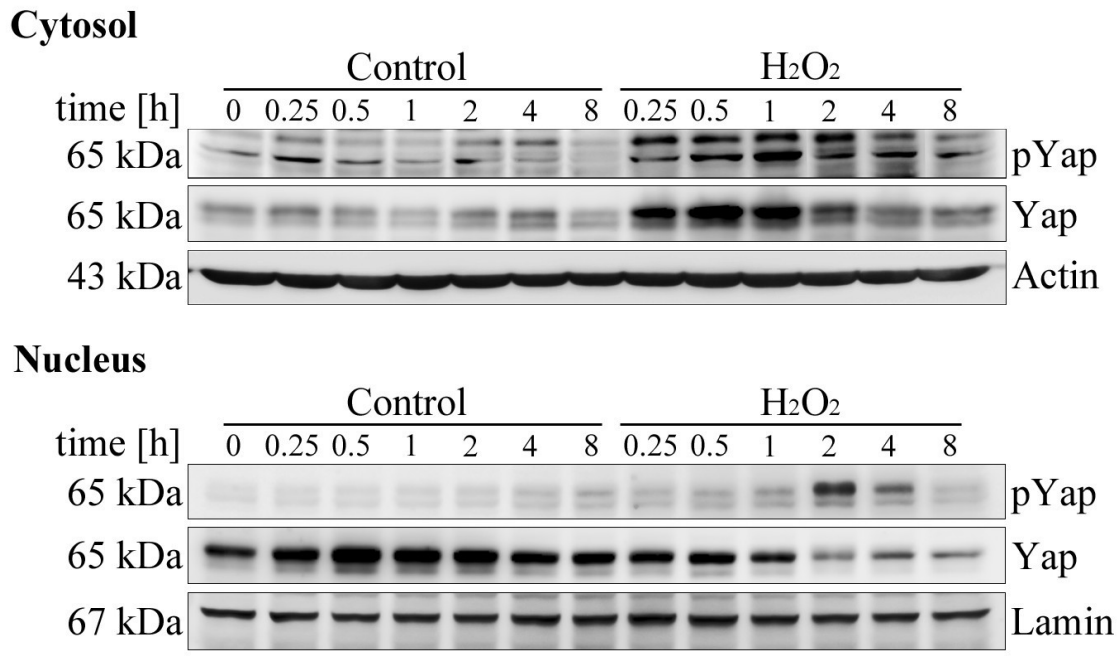

Figure 15. Western blot showing Yap and its form phosphorylated on serin 127 (pYap) in cytosolic and nuclear fractions obtained from Jurkat cells treated with 50 μM H_2O_2. Actin and lamin were used as loading controls. The images shown are representative of 3 independent experiments.

IV.5. Vitamin E analogues cause a decrease in c-Myc

Since it is known that the Hippo pathway regulates the *C-MYC* gene expression, the effect of MitoVES, α-TOS and hydrogen peroxide on *C-MYC* mRNA was studied using qPCR (section II.2.9). Jurkat cells were treated with 2.5 μM MitoVES, 50 μM α-TOS and 50 μM hydrogen peroxide and total RNA was isolated and transcribed into cDNA as described in the sections III.2.6 and II.2.8.

The effect of MitoVES and hydrogen peroxide on the *C-MYC* gene expression was evident within 2 h of exposure, when 2-fold down-regulation of the *C-MYC* gene expression was caused by MitoVES and 4-fold down-regulation by hydrogen peroxide (Fig. 16, page 70). The down-regulation of *C-MYC* gene expression evoked by MitoVES and hydrogen peroxide continued during the course treatment, and at 8 h 4-fold down-regulation was observed with MitoVES and almost 19-fold down-regulation with hydrogen peroxide. The impact of α-TOS on the *C-MYC* mRNA expression was not that apparent as with MitoVES and hydrogen peroxide but we also observed a decrease in the *C-MYC* mRNA expression, which was almost 2-fold at 8 h (Fig. 16, page 70).

To estimate, whether the down-regulation of the *C-MYC* gene expression also results in down-regulation of the c-Myc protein, we isolated the whole cell lysate from Jurkat cells treated with 2.5 μM MitoVES, 50 μM α-TOS and 50 μM hydrogen peroxide as described in the sections III.2.3. and analyzed it by western blotting (section III.2.5). Very low levels of the c-Myc protein were detected in cells treated with MitoVES already at 2 h and remained unchanged during the whole course of the treatment. The c-Myc protein gradually decreased during the treatment with hydrogen peroxide, where its sharp fall occurred at 6 h. In cells treated with α-TOS, the c-Myc protein also declined gradually but slower than with hydrogen peroxide (Fig. 17, page 71).

These data reveal that MitoVES, α-TOS and hydrogen peroxide cause down-regulation of the *C-MYC* gene and the c-Myc protein expression.

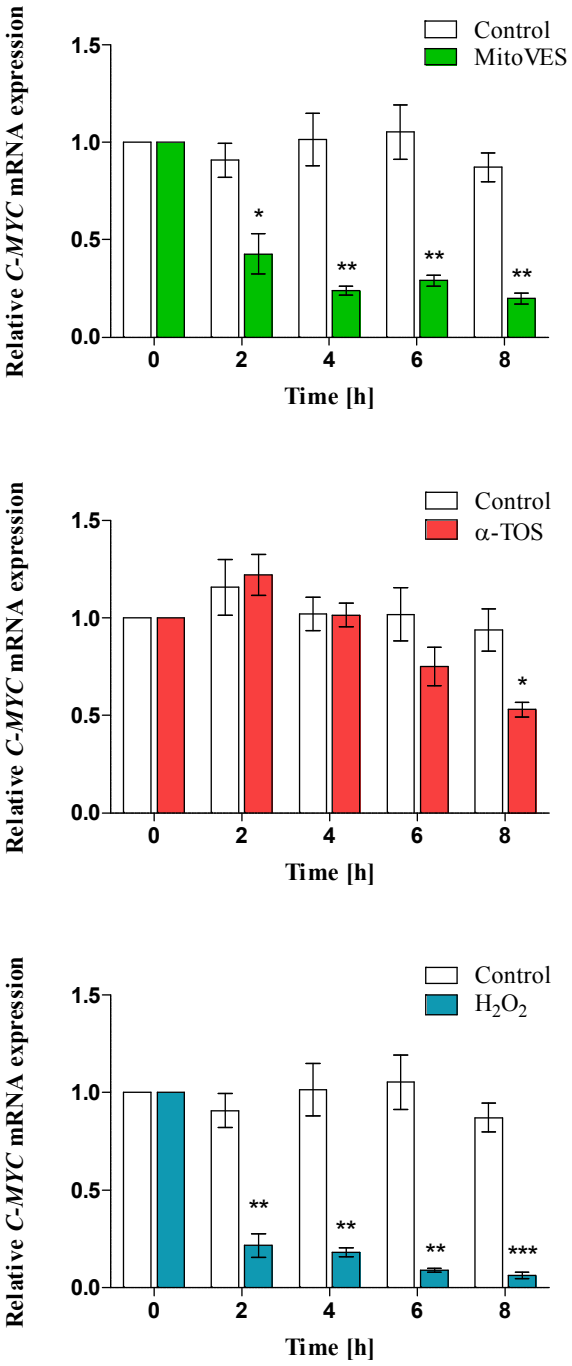

Figure 16. Relative expression of the *C-MYC* mRNA during treatment of Jurkat cells with 2.5 μM MitoVES, 50 μM α-TOS and 50 μM H_2O_2 assessed by qPCR. Data are expressed relative to the control at time 0. Results are represented as mean values ± S.E.M. (n=3). Statistical significance was calculated using the t-test, where values obtained from the treated cells were compared to the control values at each time point; * $p < 0.05$, ** $p < 0.01$, *** $p < 0.001$.

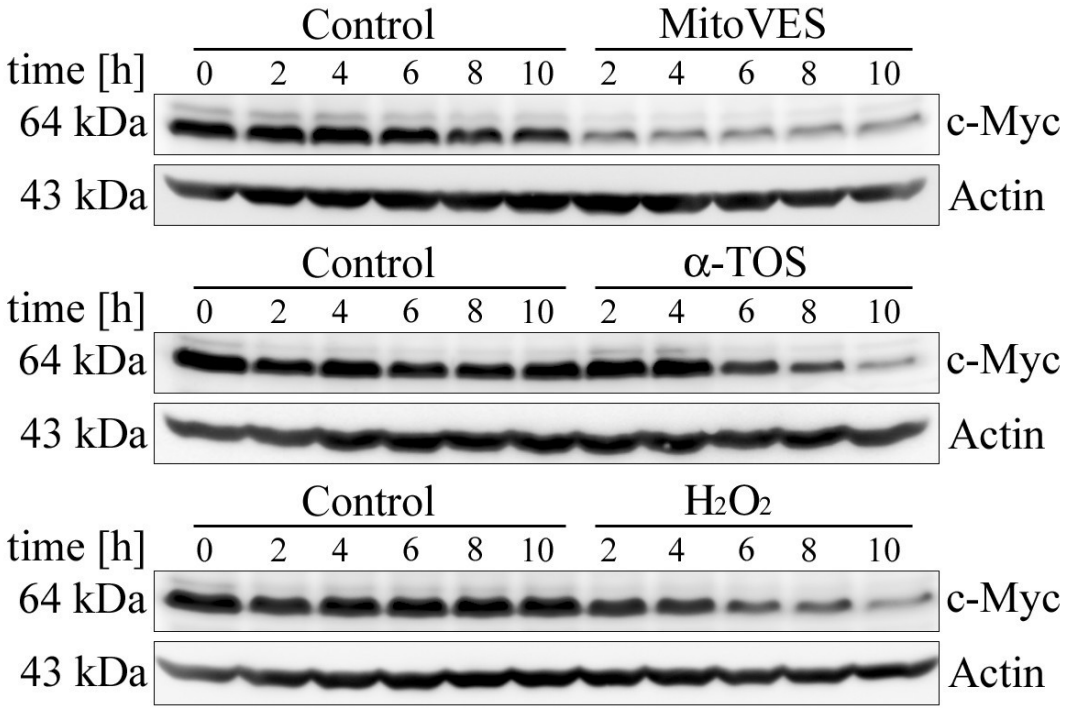

Figure 17. Western blot showing c-Myc protein in whole cell lysate obtained from Jurkat cells treated with 2.5 μM MitoVES, 50 μM α-TOS and 50 μM H_2O_2. Actin was used as the loading control. The images shown are representative of 3 independent experiments.

IV.6. Vitamin E analogues cause differential expression of genes regulated by c-Myc protein

The observation that treatment with VE analogues causes down-regulation of the *C-MYC* mRNA and the c-Myc protein led to further studies. Here we focused on the expression of genes involved in metabolism of glucose and glutamine. The influence of MitoVES, α-TOS and hydrogen peroxide on expression of *GLUT1*, *SLC38A3*, *ENO1* and *HK2* genes was evaluated by qPCR (section III.2.9). Jurkat cells were treated with 2.5 μM MitoVES, 50 μM α-TOS and 50 μM hydrogen peroxide, and total RNA was isolated and transcribed into cDNA as described in the sections III.2.6 and III.2.8.

Although the following data are not significant in some cases, some differences in gene expression can be observed. The expression of the *SLC38A3* gene was slightly increased by MitoVES: almost 1.5-fold up-regulation was detected at 6 and 8 h, but no change was caused by α-TOS and hydrogen peroxide (Fig. 18, page 73). Exppression of

the *ENO1* gene was marginally upregulated at 2 and 6 h by MitoVES. A trend of down-regulation of the *ENO1* gene was observed with α-TOS while no effect was evoked by hydrogen peroxide (Fig. 19, page 74). A significant down-regulation was observed in the *HK2* mRNA level in response to MitoVES in all time points, at 2 h in response to hydrogen peroxide and at 8 h in response to α-TOS (Fig. 20, page 75). Expression of the *GLUT1* mRNA was slightly down-regulated in all time points during the treatment with MitoVES. Treatment with α-TOS lowered *GLUT1* mRNA about 1.7-fold at 8 h, and no change in *GLUT1* mRNA level was caused by hydrogen peroxide (Fig. 21, page 76).

The effect of MitoVES, α-TOS and hydrogen peroxide on the Glut1 protein was also tested by western blotting (sections III.2.3). The whole cell protein lysate from Jurkat cells treated with 2.5 μM MitoVES, 50 μM α-TOS and 50 μM hydrogen peroxide was isolated as described in the sections III.2.3. α-TOS and hydrogen peroxide caused down-regulation of the Glut1 protein compared to MitoVES, that induced its up-regulation (Fig. 22, page 77). A relationship between the Glut1 mRNA and protein levels was seen only for α-TOS (Fig. 21, 22, pages 76-77).

Taken together, these data do not show significant influence of MitoVES, α-TOS and hydrogen peroxide on the gene expression of *SLC38A3* and *ENO1*. Minor down-regulation was observed for the mRNA of the *GLUT1* and *HK2* genes, and the Glut1 protein was down-regulated by treatment with α-TOS and hydrogen peroxide and up-regulated in cells exposed to MitoVES.

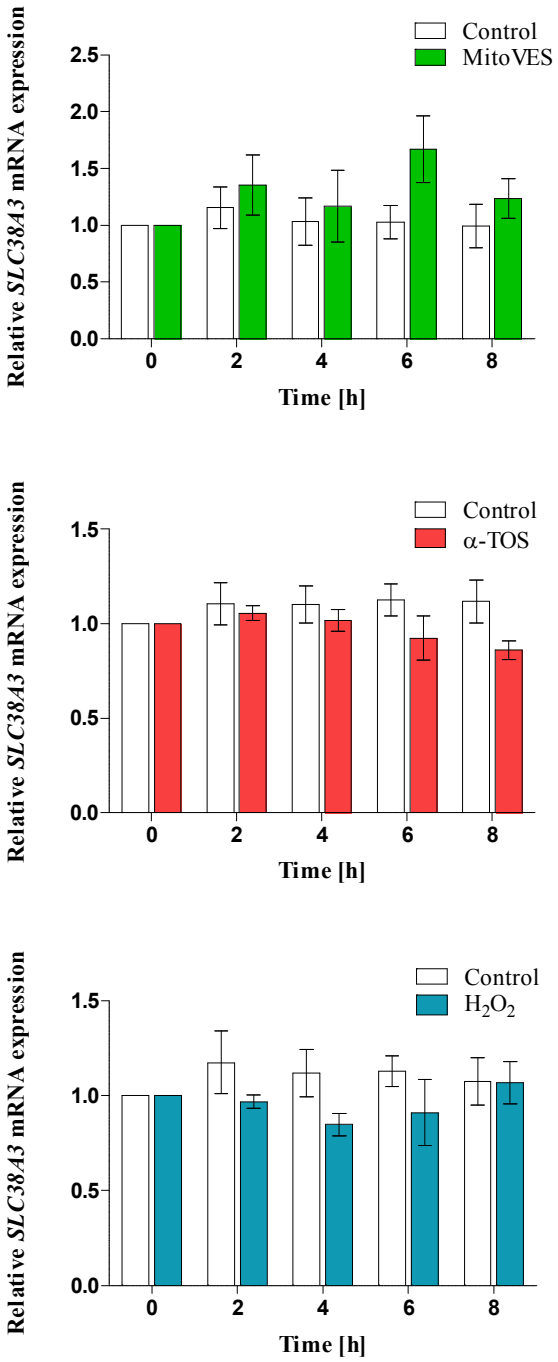

Figure 18. Relative expression of the *SLC38A3* mRNA during treatment of Jurkat cells with 2.5 µM MitoVES, 50 µM α-TOS and 50 µM H_2O_2 assessed by qPCR. Results are represented as mean values ± S.E.M. (n=3). Statistical significance was calculated using the t-test, where values obtained from the treated cells were compared to the control values at each time point.

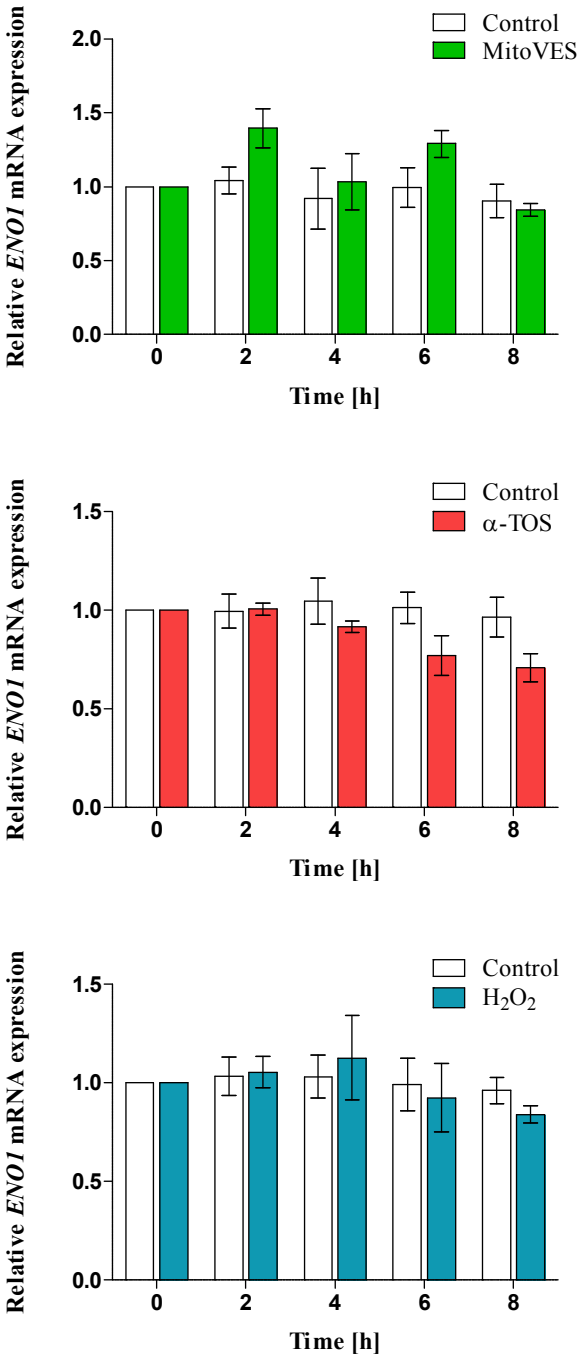

Figure 19. Relative expression of the *ENO1* mRNA during treatment of Jurkat cells with 2.5 μM MitoVES, 50 μM α-TOS and 50 μM H_2O_2 assessed by qPCR. Results are represented as mean values ± S.E.M. (n=3). Statistical significance was calculated using the t-test, where values obtained from the treated cells were compared to the control values at each time point.

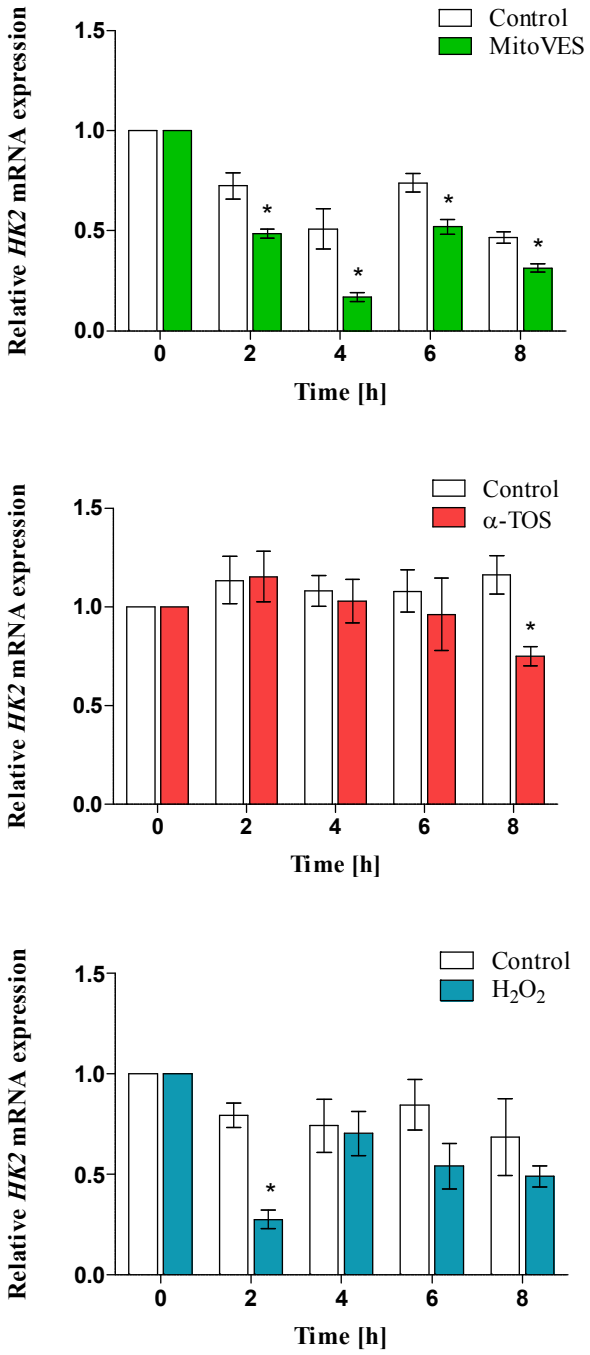

Figure 20. Relative expression of the *HK2* mRNA during treatment of Jurkat cells with 2.5 µM MitoVES, 50 µM α-TOS and 50 µM H_2O_2 assessed by qPCR. Results are represented as mean values ± S.E.M. (n=3). Statistical significance was calculated using the t-test, where values obtained from the treated cells were compared to the control values at each time point; * $p < 0.05$.

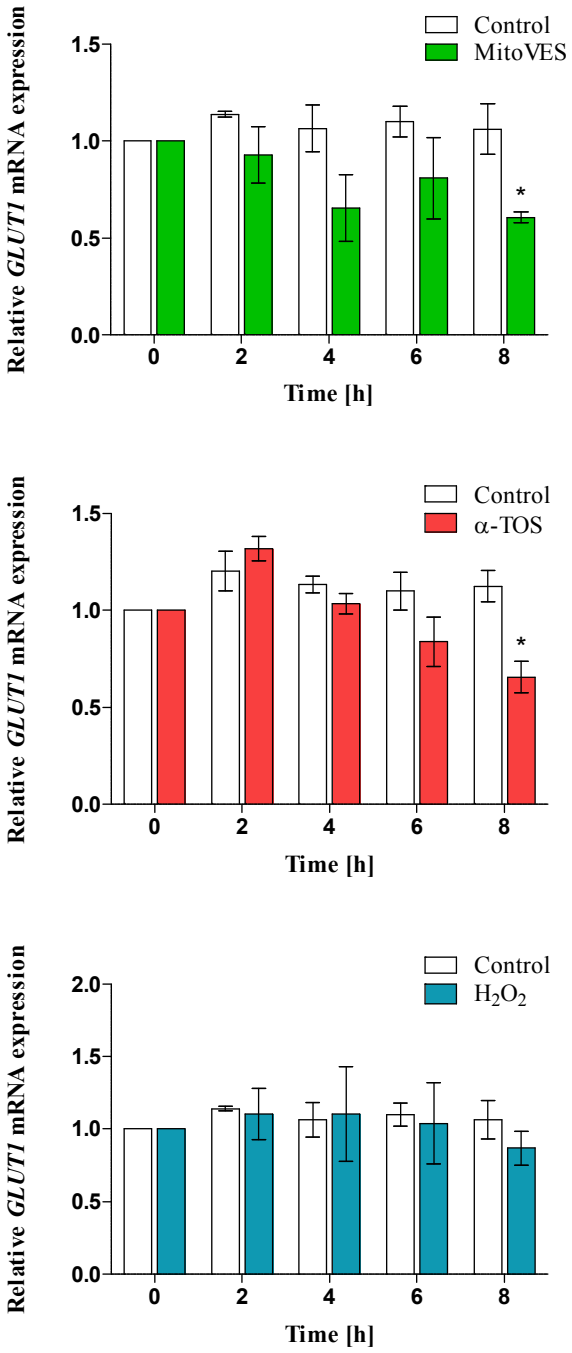

Figure 21. Relative expression of the *GLUT1* mRNA during treatment of Jurkat cells with 2.5 μM MitoVES, 50 μM α-TOS and 50 μM H_2O_2 assessed by qPCR. Results are represented as mean values ± S.E.M. (n=3). Statistical significance was calculated using the t-test, where values obtained from the treated cells were compared to the control values at each time point; * $p < 0.05$.

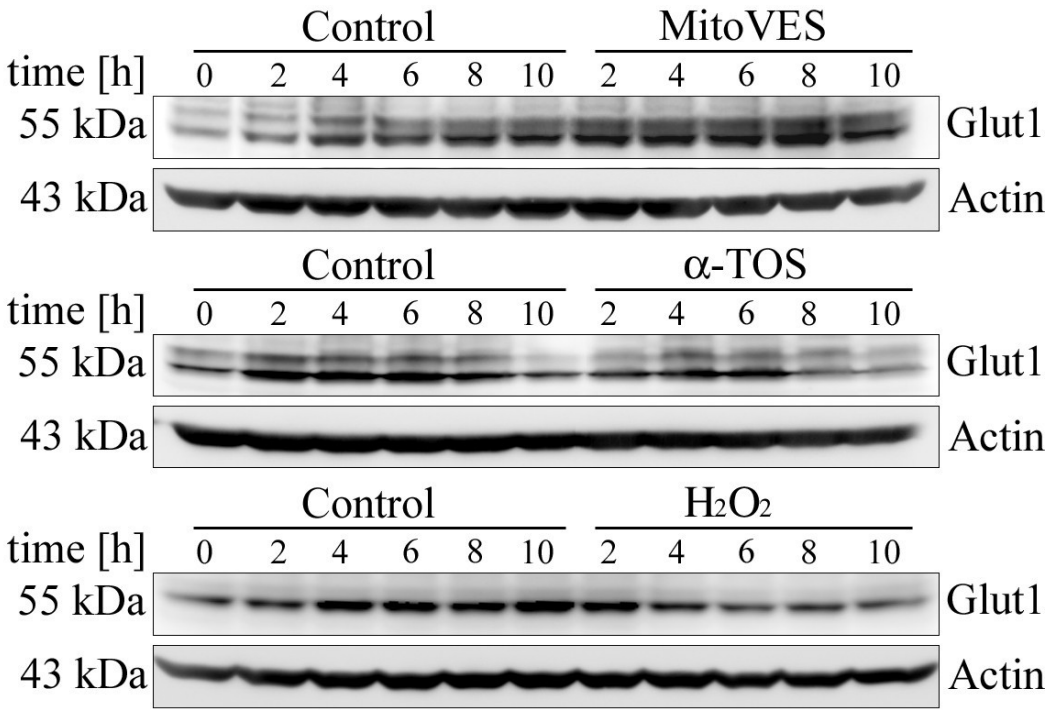

Figure 22. Western blot of the Glut1 protein in whole cell lysate obtained from Jurkat cells treated with 2.5 μM MitoVES, 50 μM α-TOS and 50 μM H_2O_2. Actin was used as the loading control. The images shown are representative of 3 independent experiments.

IV.7. Treatment of Jurkat cells with vitamin E analogues results in modulation of glucose uptake

It was reported that VE analogues α-TOS and MitoVES target the mitochondrial CII and inhibit the transfer of electrons from oxidation of succinate to CIII (Neuzil et al., 2007b; Dong et al., 2011a). Moreover MitoVES causes rapid dissipation of $\Delta\psi_m$ (Fig. 9, page 61). The effect of impaired mitochondrial function with the possibility of a glycolytic switch was evaluated by testing the uptake of glucose. The fluorescently labelled glucose analogue 2-NBDG was used and its uptake by Jurkat cells treated with 2.5 μM MitoVES, 50 μM α-TOS and 50 μM hydrogen peroxide assessed by flow cytometry (section III.2.14). α-TOS and hydrogen peroxide did not show any effect on glucose uptake compared to MitoVES which caused its 1.5-fold increase (Fig. 23, page 78). The treatment with MitoVES also caused 1.5-fold higher lactate production (Fig. 24,page 78). Lactate levels were detected enzymatically in the medium taken form cells treated with 2.5 μM MitoVES for 8 h (section III.2.15.)

This observation suggests that treatment of Jurkat cells with MitoVES causes an increase in the glucose uptake that correlates with the production of lactate.

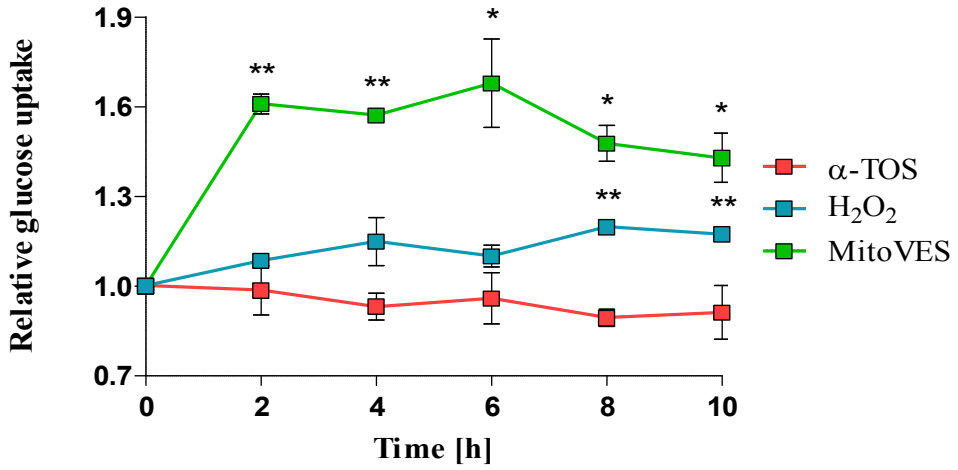

Figure 23. Relative glucose uptake during treatment of Jurkat cells with 2.5 μM MitoVES, 50 μM α-TOS and 50 μM H_2O_2 measured by flow cytometry using 2-NBDG. Results are represented as mean values ± S.E.M. (n=3). Statistical significance was calculated using the t-test, where values obtained from the treated cells were compared to the control values at time 0; * $p < 0.05$, ** $p < 0.01$

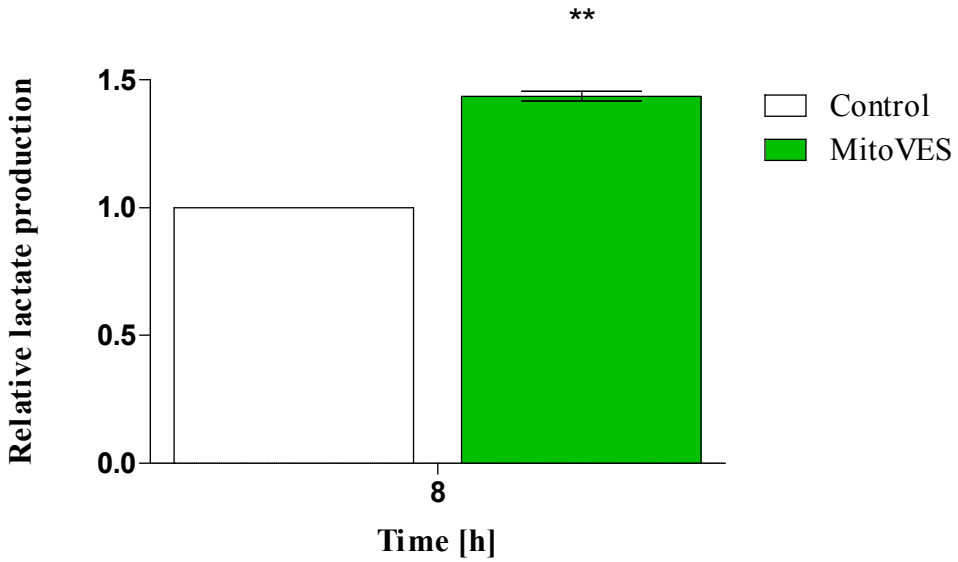

Figure 24. Relative lactate production per cell during treatment of Jurkat cells with 2.5 μM MitoVES. Lactate was measured by absorbance of the probe at 540 nm formed during enzymatic reaction proportional to lactate production. Results are represented as mean values ± S.E.M. (n=3). Statistical significance was calculated using the t-test, where values obtained from the treated cells were compared to the control values; ** $p < 0.01$.

V. DISCUSSION

VE analogues are chemical substances that induce apoptosis in cancer cells while being largely non-toxic to normal cells and tissues. Since cancer represents a term for broad range of diseases evolving from a distinct alterations in the genome, finding an 'Achilles heel' common to these pathologies is of a paramount clinical importance. The regulation of cellular processes is usually rather abundant and thus it seems to be unlikely to cure cancer by targeting a single signalling pathway. VE analogues target mitochondria, the essential cell organelles which present a promising target of anti-cancer drugs. Targeting mitochondria leads to activation of signalling pathways inducing apoptosis. Mst1-FoxO1 axis was found to be such a molecular pathway leading to upregulation of pro-apoptotic protein Noxa followed by apoptosis induction in response to α-TOS and MitoVES treatment. Mst1 is a central component of Hippo signalling pathway whose inactivation is often seen in cancer. Thus, activation of Mst1 and so Hippo pathway can contribute to apoptosis induction also through other mechanisms. One of these mechanisms can be activation of Hippo signalling pathway leading to Yap inactivation and downregulation of *C-MYC* gene expression which is studied in this thesis.

VE analogues α-TOS and MitoVES are documented to induce apoptosis in cancer cells by targeting mitochondria, which leads to the generation of ROS (Dong et al., 2008, 2011a). α-TOS and MitoVES in concentrations used in this study induced apoptosis in Jurkat cells approximately to the same degree (Fig. 7, page 59). However, MitoVES caused generation of ROS within 7.5 min exposure of Jurkat cells, α-TOS significantly increased the ROS level after 2 h (Fig. 8, page 61). This result can be explained by mitochondrial targeting of MitoVES. The cationic TPP^+ group of MitoVES is responsible for its practically exclusive accumulation in mitochondria as documented using fluorescently labelled MitoVES, whereas α-TOS was detected in non-mitochondrial compartments and partially in mitochondria (Kovarova et al., submitted for publication). It may take longer time for α-TOS to accumulate in mitochondria at levels sufficient to promote ROS generation.

It has been shown that the Mst1 kinase is activated by auto-phosphorylation at Thr183 in response to hydrogen peroxide treatment (Lehtinen et al., 2006; Morinaka et al., 2011). Mst1 activation has also been reported for α-TOS and MitoVES in Jurkat cells with

assumption that it is caused by ROS generation, particularly also by hydrogen peroxide that is believed to be formed by the conversion of superoxide anion radicals produced by the cells in response to the VE analogues (Dong et al., 2011a; Valis et al., 2011). The activation of Mst1 correlates with ROS production in case of MitoVES and hydrogen peroxide but not with α-TOS (Fig. 8, 10, 11, 12, pages 61, 63-65). Hydrogen peroxide was used as a positive control for oxidative stress-induced mechanisms. Moreover, activation of Mst1 caused by MitoVES and hydrogen peoxide seems to have very similar kinetics; higher levels of pMst1 were observed after 30 min and then it decreased, possibly due to a feedback regulation.

Mst1 is a kinase activated by several stress stimuli (Radu and Chernoff, 2009). α-TOS-induced generation of ROS is not the only mechanism by which this agent induces apoptosis in cancer cells. The hydrophobic character of α-TOS allows it to associate with hydrophobic structures in cells such as various membranous structures but also with hydrophobic parts of proteins. This is supported again by results with fluorescently labelled α-TOS. Thus, it is plausible to assume that α-TOS acts by several mechanisms to induce apoptosis. For example, the sphingomyelinase activation and lysosomal destabilisation were observed as early events during Jurkat cell treatment, leading to apoptosis induction (Neuzil et al., 2002; Wang et al., 2006). These facts support a possibility that α-TOS activates Mst1 by thus far unknown, ROS-independent mechanisms at early times; this activation is rather enhanced by ROS generation at later times. It is in line with the observation that the level of pMst is relatively unchanged during the time of treatment with the agent (Fig. 10, page 63). ROS-dependent Mst1 activation should be father validated by other experiments, for example using antioxidants such as N-acetylcysteine.

Caspase-3-mediated cleavage of Mst1 is documented to produce fragments of about 10-fold higher catalytic efficacy than the full length Mst1, which translocate to the nucleus to induce chromatin condensation through phosphorylation of histones H2AX and H2B (Ura et al., 2001; Cheung et al., 2003; Wen et al., 2010). Previous work with α-TOS showed appearance of ~36 kDa Mst1 fragments in the nucleus of Jurkat cells within 2 h of exposure suggesting some degree of caspase-independent Mst1 cleavage, since caspases are activated by the agent at later times (Valis et al., 2011). This hypothesis was also tested in this work. The 36 kDa Mst1 fragments were observed in the cytosol and their appearance coincided with the presence of cleaved caspase-3 (Fig. 10, 11, 12, pages 63-

64). These results does not support the theory for caspase-independent cleavage Mst1. However, this possibility needs to be confirmed in additional experiments using caspase inhibitors. Surprisingly, almost no Mst1 fragments were observed in the nucleus, where only very low amounts of the cleaved Mst1 can be seen in the cells treated with α-TOS and hydrogen peroxide with much higher amounts of the fragments in the cytosol. Therefore, our experiments do not support the notion of Mst1 fragments accumulating in the nucleus (Fig. 11, 12, pages 64-65). Further, our results contradict those of Valis et al. (2011) and therefore, more experiments will be needed to test the translocation of Mst1 fragments into the nucleus in response to α-TOS and MitoVES, plus their effect on histones phosphorylation, which has not been examined thus far. We need to resolve whether the reason for the detection of low amounts of the fragments of Mst1 was not due to technical problems when running the western blots, such as the use of low amounts of protein, etc.

The activation of Mst1 as the central part of Hippo signalling cascade has been documented to result in the phosphorylation of Yap at Ser127 and its translocation into the cytosol where is sequestered by the 14-3-3 proteins (Zhou et al., 2009). Yap phosphorylation is mediated by the Lats1/2 kinase. This has been reported to phosphorylate Yap on Ser127 but also on Ser381, which is required for further phosphorylation of Ser384 by CK1δ/ε and thus recruiting an E3 ubiquitin ligase, leading to protein degradation (Zhao et al., 2010b). It seems that this mechanism is initiated in Jurkat cells by α-TOS, MitoVES and hydrogen peroxide (Fig. 13, 14, 15, pages 67-68). The Yap phosphorylation on Ser127 and its translocation was observed, followed by highly reduced level of the Yap protein in the nucleus as well as in the cytosol. To implement Yap phosphorylation, Lats1/2 must be first activated by its phosphorylation by activated Mst1. The observed Mst1 activation by α-TOS, MitoVES and hydrogen peroxide supports this assumption but needs to be verified: the assessment of Lats1/2 activity and Yap phosphorylation on Ser384 are subject of further work.

The observation that α-TOS and MitoVES cause activation of Mst1 and inactivation of Yap may have an important clinical outcome, since deregulation of the Hippo pathway may contribute to a wide range of neoplastic pathologies. Yap has been as a candidate oncogene that was found to be frequently overexpressed in non-small cell lung, ovarian, hepatocelullar, prostate and colorectal carcinomas. Its high nuclear expression is associated with poor prognosis and short overall survival (Dong et al., 2007; Steinhardt et al., 2008). It also promotes the growth of glioblastomas (Orr et al., 2011); Yap expression is also an

independent prognostic marker for hepatocellular and colorectal cancinomas (Xu et al., 2009; Wang et al., 2013). Increased Yap activity has also been shown to be pro-metastatic in breast cancer and melanomas via the activation of the TEAD transcription factors (Lamar et al., 2012). Thus, the activation of mechanisms that leads to Yap inactivation and degradation could be considered as anti-tumourigenic.

In the next part of this work the effect of VE analogues on c-Myc mRNA and protein expression and its influence on the c-Myc target genes were assessed. It was found that α-TOS decreases the c-Myc mRNA and protein level at later times, while MitoVES and hydrogen peroxide showed much more profound effect as a decrease in c-Myc mRNA and protein levels was detected already within 2 h of the exposure (Fig. 16, 17, pages 70-71). This observation could have an important clinical connotation since c-Myc is the most prominent oncogene and is upregulated in a broad range of cancers including breast, ovarian, prostate, colon and bladder cancer (Albihn et al., 2010). Its increased expression is estimated to contributes to at least 40% of all human cancers (Dang et al., 2009).

The impact of c-Myc protein downregulation caused by α-TOS, MitoVES and hydrogen peroxide on the expression of known c-Myc target genes involved in glucose and glutamine metabolism, inluding *HK2*, *SCL38A3*, *ENO1* and *GLUT1* was assessed in further experiments. α-TOS seems to have a potential effect on expression of these genes. *GLUT1* mRNA and protein expression was slightly downregulated after 8 h of treatment; other genes also showed a decreasing pattern of expression, however this was not statictically significant. Although the expression of c-Myc mRNA and protein was decreased after 6 h of treatment, it probably takes more time to affect the expression of the c-Myc targets genes. At 8 h, 30 % of apoptotic cells were detected, thus it would be advisable to try lower concentrations of α-TOS and treat the cells for longer times to analyse the effect of c-Myc downregulation on its target genes. Surprisingly, both MitoVES and hydrogen peroxide, which caused massive decrease of the c-Myc protein expression, had no significant effect on the c-Myc target genes. Of these, only the *HK2* gene showed a decline in its expression followed later by its increase (Fig. 20, page 75). Taken together, it seems that c-Myc downregulation had no statistically significant effect on the expression of the *HK2*, *SCL38A3*, *ENO1* and *GLUT1* genes. The *GLUT1* mRNA expression does not correlate with the protein expression in case of MitoVES and hydrogen peroxide, suggesting that some post-transcriptional modification and regulation takes place (Fig. 22, page 77). In additional experiments, other targets of c-Myc should be

tested. We should also check whether downregulation of c-Myc by RNA interference will cause a decrease in the known c-Myc target genes.

It is also possible that high levels of cellular ROS evoked by MitoVES and hydrogen peroxide create a "pseudohypoxic" environment that stabilizes the hypoxia-inducible factor-1α (HIF-1α). Prolyl hydroxylase target constitutively expressed HIF-1α for subsequent degradation under normal oxygen tension, and ROS are known to inactivate them (Pan et al., 2007). HIF-1α is reported to regulate the expression of the *HK2*, *ENO1* and *GLUT1* genes as well (Gordan et al., 2007). It is therefore possible that HIF-1α compensates for the effect of c-Myc downregulation during high cellular ROS levels. Stabilization of HIF-1α has been documented for human colon cancer cells treated with MitoVES for 12 h (Dong et al., 2011b). Thus, we should test potential HIF-1α stabilization also in Jurkat cells, in response to the VE analogues and hydrogen peroxide.

The assessment of $\Delta\psi_m$ during the treatment of Jurkat cells with α-TOS, MitoVES and hydrogen peroxide showed that MitoVES causes sharp dissipation of $\Delta\psi_m$ within 7.5 min in contrast to α-TOS that had hardly any effect on $\Delta\psi_m$ at least during the time of treatment as well as to hydrogen peroxide that caused a 2-fold decreased of $\Delta\psi_m$ at 2 h (Fig. 9, page 61). The immense effect of MitoVES on $\Delta\psi_m$ is probably due to fast accumulation of the cationic molecules at the interphase of the mitochondrial inner membrane and the mitochondrial matrix. Thus, MitoVES causes a collapse of the H^+ electrochemical gradient across the inner membrane probably leading to the inhibition of oxidative phosphorylation. Hydrogen peroxide also seems to affect the mitochondrial function as well, but at later times. The experiments with the fluorescent glucose analogue 2-NBDG showed that Jurkat cells revealed 1.5-fold higher glucose uptake during MitoVES treatment, and this uptake was only slightly increased in the case of hydrogen peroxide while α-TOS showed no significant effect (Fig. 23, page 78). The Glut1 protein level was also increased by MitoVES, but not by hydrogen peroxide or α-TOS, in which cases it decreased. This suggests that the impairment of oxidative phosphorylation by MitoVES is at least partially compensated by generation of ATP by the conversion glucose to lactate in the process of glycolysis. This observation is further confirmed by the evaluation of lactate production, which was increase by 1.5-fold in Jurkat cells treated with MitoVES (Fig. 24, page 78). This result corresponds to the previously reported one, where MitoVES at low concentrations was shown to evoke a collapse of $\Delta\psi_m$ leading to the inhibition of oxidative phosphorylation while the ATP levels were affected only slightly (Rodríguez-Enríquez et

al., 2012). It is also possible that the metabolic adaptation of the MitoVES-treated cells can overcome the effect of c-Myc on the downregulation of the *HK2*, *SCL38A3*, *ENO1* and *GLUT1* genes. These results again demonstrate the different action of MitoVES and α-TOS in apoptosis induction, pointing to mitochondria as an exclusive target of MitoVES.

c-Myc is known to promote cell growth by orchestrating a variety of changes in cell metabolism necessary for cell cycle entry through regulation not only of glycolysis and glutaminolysis, but also through ribosomal and mitochondrial biogenesis and protein and nucleic acid synthesis (Dang et al., 2009). Thus, c-Myc downregulation can affect also other processes, and it would be desirable to assess the expression of other known c-Myc target genes and activity of the relevant processes.

Recently, it has been found in *Drosophila melanogaster* that expression of dMyc is under the control of Yki, a component of the Hippo pathway, and that dMyc functions as an important cellular growth effector of this pathway (Neto-Silva et al., 2010; Ziosi et al., 2010). Elucidation, whether this pathway is also conserved in mammals, has been the main aim of this study. The decreased expression of the *C-MYC* gene partially correlates with the decreased presence of Yap in the nuclei of Jurkat cells treated with MitoVES, α-TOS and hydrogen peroxide (Fig. 13, 14, 15, 16, pages 67-68, 70). This indicates that some conserved mechanism exists but other experiments are necessary to validate it. The decline in *C-MYC* mRNA level does not corresponded to its protein level (Fig. 16, 17, pages 70-71) suggesting that some post-translational mechanism might regulate c-Myc protein degradation. FoxO3-dependent regulation of c-Myc expression has been recently described. It has been shown that FoxO3 inhibits c-Myc expression by increasing the expression of microRNA that perturbs the translation of the *C-MYC* mRNA and by reducing the c-Myc protein stability (Ferber et al., 2012). FoxO3 has been shown to be phosphorylated by active Mst1 kinase upon oxidative stress insult, resulting in its transport to the nucleus (Lehtinen et al., 2006). Increasing nuclear level of FoxO3 was also observed during Jurkat cell treatment with α-TOS (Valis et al., 2011) suggesting that Mst1-FoxO3 can represent an alternative in c-Myc regulation besides the Mst1-Lats-Yap pathway.

Altogether, the results presented in this thesis suggest that exposure of Jurkat cells to the VE analogues α-TOS and MitoVES leads to the activation of Mst1, which results in the activation of FoxO1-*NOXA* pathway and probably also in inactivation of Yap. Moreover, both analogues induce downregulation of the c-Myc gene expression but have no statistically significant effect on the expression of the *HK2*, *SCL38A3*, *ENO1* and *GLUT1*

genes. The results also show that MitoVES acts exclusively through mitochondria while induction of apoptosis by α-TOS includes also other mechanisms. The role of α-TOS and MitoVES in apoptosis induction is shown in the Fig. 25. Unfortunately the precise mechanisms explaining the role of the Hippo signalling pathway in c-Myc down-regulation and cancer cell metabolism has not been elucidated due to the complexity of these mechanisms, which require further experimental work.

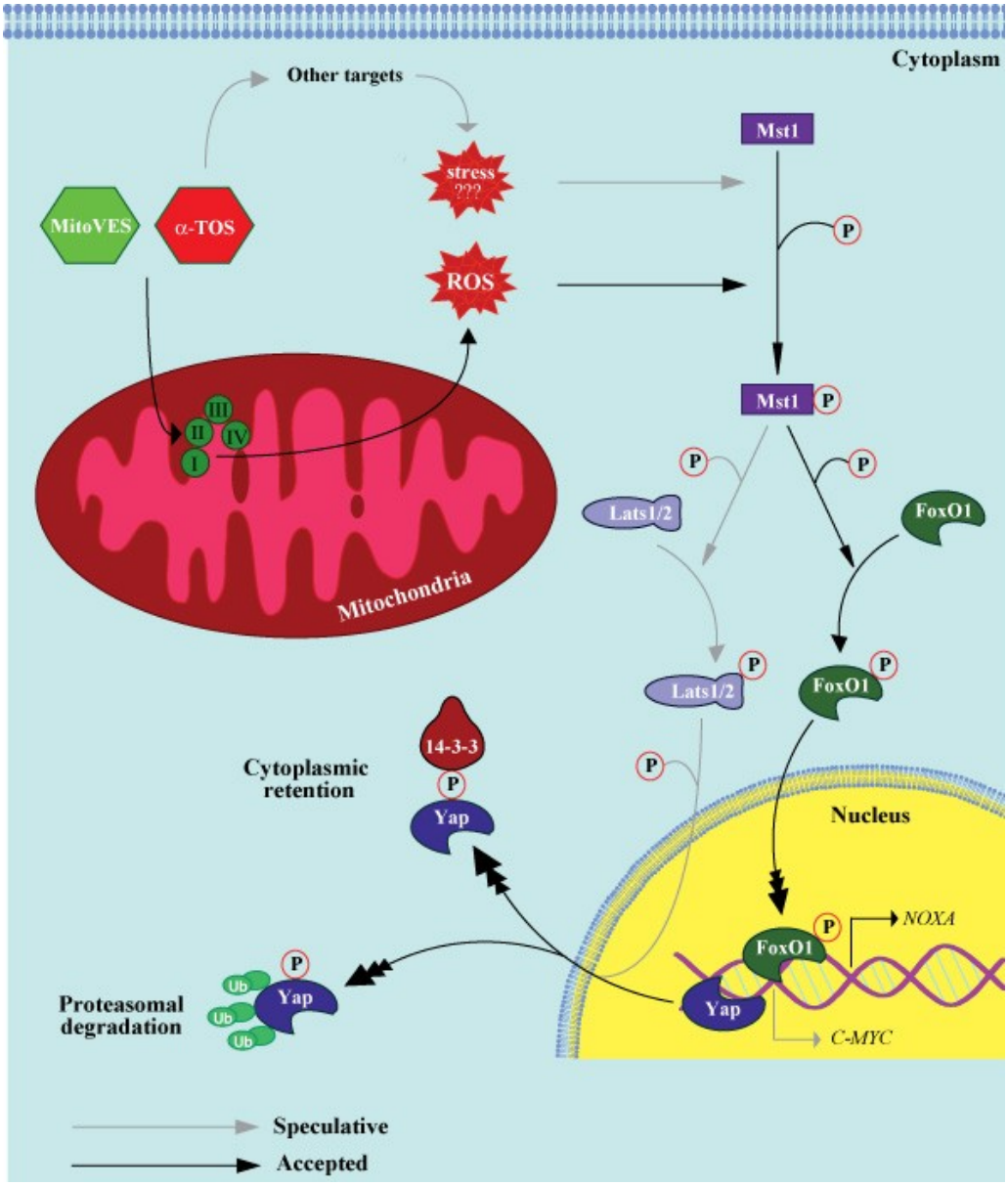

Figure 25. Scheme of actions of MitoVES and α-TOS that lead to apoptosis induction. Both compounds activate Mst1 that results in phosphorylation of FoxO1 and its transport into nucleus where induce transcription of pro-apoptotic gene *NOXA*. Moreover, Mst1 activation is followed by phosphorylation and inactivation of Yap transcription co-activator, probably through Lats1/2 kinase, and downregulation of *C-MYC* gene expression.

VI. SUMMARY

This thesis focused on study of action of anticancer drugs, vitamin E analogues α-TOS and MitoVES, on activation of Hippo signalling pathway and its influence on cancer cell metabolism. For these purposes, the Jurkat cell line was used and hydrogen peroxide was used as a control of oxidative stress-induced mechanisms.

The most important findings identified in this thesis can be summarized as follows:

- MitoVES causes fast generation of ROS after application whereas α-TOS stimulates the ROS generation at later times. Moreover, MitoVES evokes massive dissipation of $\Delta\psi_m$ and also increase Glut1 protein expression, glucose uptake and lactate production indicating for some compensatory mechanism following mitochondria impairment.
- MitoVES, α-TOS and hydrogen peroxide promote the activation of Mst1 and its caspase-3 dependent cleavage. The activation of Mst1 corresponds to ROS generation in case of MitoVES and hydrogen peroxide but not in α-TOS suggesting for some ROS-independent mechanism of Mst1 activation.
- MitoVES, α-TOS and hydrogen peroxide induce phosphorylation of Yap, the target of Hippo signalling pathway, resulting in its nuclear export and degradation in cytoplasm.
- All three compounds cause downregulation of *C-MYC* gene and c-Myc protein expression but MitoVES and hydrogen peroxide have much faster and profound effect.
- The downregulation of c-Myc protein has no pronounced effect on expression of its target genes *SCL38A3* and *ENO1* under conditions and times studied in this thesis, only *HK2* and *GLUT1* showed a slight decrease.

Taken together, since Yap and c-Myc increased activity contributes to wide range of human cancers, inactivation of Yap and downregulation of c-Myc expression may present an another mechanism of α-TOS and MitoVES antitumourigenic action, but the precise mechanism linking c-Myc to Hippo signalling pathway require further experimental research.

VII. REFERENCES

Abramson, H.N. The lipogenesis pathway as a cancer target. J. Med. Chem. 54, 5615–5638 (2011)

Albihn, A., Johnsen, J.I., Henriksson, M.A. MYC in oncogenesis and as a target for cancer therapies. Adv. Cancer Res. 107, 163–224 (2010)

Ashe, P.C., Berry, M.D. Apoptotic signaling cascades. Prog. Neuropsychopharmacol. Biol. Psychiatry 27, 199–214 (2003)

Avruch, J., Zhou, D., Fitamant, J., Bardeesy, N., Mou, F., Barrufet, L.R. Protein kinases of the Hippo pathway: regulation and substrates. Semin. Cell Dev. Biol. 23, 770–784 (2012)

Birringer, M., EyTina, J.H., Salvatore, B.A., Neuzil, J. Vitamin E analogues as inducers of apoptosis: structure-function relation. Br. J. Cancer 88, 1948–1955 (2003)

Brand, K.A., Hermfisse, U. Aerobic glycolysis by proliferating cells: a protective strategy against reactive oxygen species. FASEB J. 11, 388–395 (1997)

Budd, R.C., Yeh, W.-C., Tschopp, J. cFLIP regulation of lymphocyte activation and development. Nat. Rev. Immunol. 6, 196–204 (2006)

Camargo, F.D., Gokhale, S., Johnnidis, J.B., Fu, D., Bell, G.W., Jaenisch, R., Brummelkamp, T.R. YAP1 increases organ size and expands undifferentiated progenitor cells. Curr. Biol. 17, 2054–2060 (2007)

Croce, C.M. Oncogenes and cancer. N. Engl. J. Med. 358, 502–511 (2008)

Czymai, T., Viemann, D., Sticht, C., Molema, G., Goebeler, M., Schmidt, M. FOXO3 modulates endothelial gene expression and function by classical and alternative mechanisms. J. Biol. Chem. 285, 10163–10178 (2010)

Dang, C.V., Le, A., Gao, P. MYC-induced cancer cell energy metabolism and therapeutic opportunities. Clin. Cancer Res.15, 6479–6483 (2009)

DeBerardinis, R.J., Cheng, T. Q's next: the diverse functions of glutamine in metabolism, cell biology and cancer. Oncogene 29, 313–324 (2010)

DeBerardinis, R.J., Mancuso, A., Daikhin, E., Nissim, I., Yudkoff, M., Wehrli, S., Thompson, C.B. Beyond aerobic glycolysis: transformed cells can engage in glutamine metabolism that exceeds the requirement for protein and nucleotide synthesis. Proc. Natl. Acad. Sci. USA 104, 19345–19350 (2007)

Deveraux, Q.L., Takahashi, R., Salvesen, G.S., Reed, J.C. X-linked IAP is a direct inhibitor of cell-death proteases. Nature 388, 300–304 (1997)

Dong, J., Feldmann, G., Huang, J., Wu, S., Zhang, N., Comerford, S.A., Gayyed, M.F., Anders, R.A., Maitra, A., Pan, D. Elucidation of a Universal Size-Control Mechanism in Drosophila and Mammals. Cell 130, 1120–1133 (2007)

Dong, L.F., Jameson, V.J., Tilly, D., Prochazka, L., Rohlena, J., Valis, K., Truksa, J., Zobalova, R., Mahdavian, E.,Kluckova, K., Stantic, M., Stursa, J., Freeman, R., Witting, P.K., Norberg, E., Goodwin, J., Salvatore, B.A., Novotna, J.,Turanek, J., Ledvina, M., Hozak, P., Zhivotovsky, B., Coster, M.J., Ralph, S.J., Smith, R.A., Neuzil, J. Mitochondrial targeting of α-tocopheryl succinate enhances its pro-apoptotic efficacy: a new paradigm for effective cancer therapy. Free Radic. Biol. Med. 50, 1546–1555 (2011a)

Dong, L.F., Jameson, V.J., Tilly, D., Cerny, J., Mahdavian, E., Marín-Hernández, A., Hernández-Esquivel, L.,Rodríguez-Enríquez, S., Stursa, J., Witting, P.K., Stantic, B., Rohlena, J., Truksa, J., Kluckova, K., Dyason, J.C.,Ledvina, M., Salvatore, B.A., Moreno-Sánchez, R., Coster, M.J., Ralph, S.J., Smith, R.A., Neuzil, J. Mitochondrial targeting of vitamin E succinate enhances its pro-apoptotic and anti-cancer activity via mitochondrial complex II. J. Biol. Chem. 286, 3717–3728 (2011b)

Dong, L.F., Low, P., Dyason, J.C., Wang, X.F., Prochazka, L., Witting, P.K., Freeman, R., Swettenham, E., Valis, K., Liu, J., Zobalova, R., Turanek, J., Spitz, D.R., Domann, F.E., Scheffler, I.E., Ralph, S.J., Neuzil, J. Alpha-tocopheryl succinate induces apoptosis by targeting ubiquinone-binding sites in mitochondrial respiratory complex II. Oncogene 27, 4324–4335 (2008)

Eagle, H. Nutrition needs of mammalian cells in tissue culture. Science 122, 501–504 (1955)

Elmore, S. Apoptosis: a review of programmed cell death. Toxicol. Pathol. 35, 495–516 (2007)

Fantin, V.R., St-Pierre, J., Leder, P. Attenuation of LDH-A expression uncovers a link between glycolysis, mitochondrial physiology, and tumor maintenance. Cancer Cell 9, 425–434 (2006)

Fausto, N., Campbell, J.S., Riehle, K.J. Liver regeneration. Hepatology 43, 45–53 (2006)

Ferber, E.C., Peck, B., Delpuech, O., Bell, G.P., East, P., Schulze, A. FOXO3a regulates reactive oxygen metabolism by inhibiting mitochondrial gene expression. Cell Death Differ. 19, 968–979 (2012)

Fogal, V., Richardson, A.D., Karmali, P.P., Scheffler, I.E., Smith, J.W., Ruoslahti, E. Mitochondrial p32 protein is a critical regulator of tumor metabolism via maintenance of oxidative phosphorylation. Mol. Cell. Biol. 30, 1303–1318 (2010)

Fu, Z., Tindall, D.J. FOXOs, cancer and regulation of apoptosis. Oncogene 27, 2312–2319 (2008)

Galluzzi, L., Morselli, E., Kepp, O., Vitale, I., Rigoni, A., Vacchelli, E., Michaud, M., Zischka, H., Castedo, M., Kroemer, G. Mitochondrial gateways to cancer. Mol. Aspects Med. 31, 1–20 (2010)

Gao, P., Tchernyshyov, I., Chang, T.C., Lee, Y.S., Kita, K., Ochi, T., Zeller, K.I., De Marzo, A.M., Van Eyk, J.E., Mendell, J.T., Dang, C.V. c-Myc suppression of miR-23a/b enhances mitochondrial glutaminase expression and glutamine metabolism. Nature 458, 762–765 (2009)

Garrido, C., Galluzzi, L., Brunet, M., Puig, P.E., Didelot, C., Kroemer, G. Mechanisms of cytochrome c release from mitochondria. Cell Death Differ. 13, 1423–1433 (2006)

Gerlinger, M., Rowan, A.J., Horswell, S., Larkin, J., Endesfelder, D., Gronroos, E., Martinez, P., Matthews, N.,Stewart, A., Tarpey, P., Varela, I., Phillimore, B., Begum, S., McDonald, N.Q., Butler, A., Jones, D., Raine, K., Latimer, C., Santos, C.R., Nohadani, M., Eklund, A.C., Spencer-Dene, B., Clark, G., Pickering, L., Stamp, G,. Gore, M.,Szallasi, Z., Downward, J., Futreal, P.A., Swanton, C. Intratumor heterogeneity and branched evolution revealed by multiregion sequencing. New Engl. J. Med. 366, 883–892 (2012)

Gomes, A., Fernandes, E., Lima, J.L.F.C. Fluorescence probes used for detection of reactive oxygen species. J. Biochem. Biophys. Methods 65, 45–80 (2005)

Gordan, J.D., Thompson, C.B., Simon, M.C. HIF and c-Myc: sibling rivals for control of cancer cell metabolism and proliferation. Cancer Cell 12, 108–113 (2007)

Graves, J.D., Gotoh, Y., Draves, K.E., Ambrose, D., Han, D.K., Wright, M., Chernoff, J., Clark, E.A., Krebs, E.G. Caspase-mediated activation and induction of apoptosis by the mammalian Ste20-like kinase Mst1. EMBO J. 17, 2224–2234 (1998)

Green, D.R., Kroemer, G. The pathophysiology of mitochondrial cell death. Science 305, 626–629 (2004)

Hanahan, D., Weinberg, R.A. The hallmarks of cancer. Cell 100, 57–70 (2000)

Hanahan, D., Weinberg, R.A. Hallmarks of cancer: the next generation. Cell 144, 646–674 (2011)

Cheung, W.L., Ajiro, K., Samejima, K., Kloc, M., Cheung, P., Mizzen, C.A., Beeser, A., Etkin, L.D., Chernoff, J., Earnshaw, W.C., Allis, C.D. Apoptotic phosphorylation of histone H2B is mediated by mammalian sterile twenty kinase. Cell 113, 507–517 (2003)

Chipuk, J.E., Moldoveanu, T., Llambi, F., Parsons, M.J., Green, D.R. The BCL-2 family reunion. Mol. Cell 37, 299–310 (2010)

Cho, E., Feng, Y., Rauskolb, C., Maitra, S., Fehon, R., Irvine, K.D. Delineation of a Fat tumor suppressor pathway. Nat. Genet. 38, 1142–1150 (2006)

Christofk, H.R., Vander Heiden, M.G., Wu, N., Asara, J.M., Cantley, L.C. Pyruvate kinase M2 is a phosphotyrosine-binding protein. Nature 452, 181–186 (2008)

Jemal, A., Bray, F., Ferlay, J. Global Cancer Statistics. CA: Cancer J. Clinic. 61, 69–90 (2011)

Jones, D.T. et al. Dissecting the genomic complexity underlying medulloblastoma. Nature 488, 100–105 (2012)

Kim, J., Zeller, K.I., Wang, Y., Jegga, A.G., Aronow, B.J., O'Donnell, K.A., Dang, C.V. Evaluation of myc E-box phylogenetic footprints in glycolytic genes by chromatin immunoprecipitation assays. Mol. Cell. Biol. 24, 5923–5936 (2004)

Lamar, J.M., Stern, P., Liu, H., Schindler, J.W., Jiang, Z.G., Hynes, R.O. The Hippo pathway target, YAP, promotes metastasis through its TEAD-interaction domain. Proc. Natl. Acad. Sci. USA 109, 2441–2450 (2012)

Lavrik, I.N. Systems biology of apoptosis signaling networks. Curr. Opin. Biotechnol 21, 551–555 (2010)

Lee, J.H., Kim, T.S., Yang, T.H., Koo, B.K., Oh, S.P., Lee, K.P., Oh, H.J., Lee, S.H., Kong, Y.Y., Kim, J.M., Lim, D.S. A crucial role of WW45 in developing epithelial tissues in the mouse. EMBO J. 27, 1231–1242 (2008)

Lehtinen, M.K., Yuan, Z., Boag, P.R., Yang, Y., Villén, J., Becker, E.B.E., DiBacco, S., de la Iglesia, N., Gygi, S., Blackwell, T.K., Bonni, A. A conserved MST-FOXO signaling pathway mediates oxidative-stress responses and extends life span. Cell 125, 987–1001 (2006)

Li, H., Fan, X., Houghton, J. Tumor microenvironment: the role of the tumor stroma in cancer. J. Cell. Biochem. 101, 805–815 (2007)

Liu, C.Y., Zha, Z.Y., Zhou, X., Zhang, H., Huang, W., Zhao, D., Li, T., Chan, S.W., Lim, C.J., Hong, W., Zhao, S., Xiong, Y., Lei, Q.Y., Guan, K.L. The hippo tumor pathway promotes TAZ degradation by phosphorylating a phosphodegron and recruiting the SCF{beta}-TrCP E3 ligase. J. Biol. Chem. 285, 37159–37169 (2010)

Locasale, J.W., Cantley, L.C. Metabolic flux and the regulation of mammalian cell growth. Cell Metab. 14, 443–451 (2011)

Lovell, J.F., Billen, L.P., Bindner, S., Shamas-Din, A., Fradin, C., Leber, B., Andrews, D.W. Membrane binding by tBid initiates an ordered series of events culminating in membrane permeabilization by Bax. Cell 135, 1074–1084 (2008)

Lunt, S.Y., Vander Heiden, M.G. Aerobic glycolysis: meeting the metabolic requirements of cell proliferation. Annu. Rev. Cell Dev. Biol. 27, 441–464 (2011)

Mailloux, R.J., Harper, M.E. Mitochondrial proticity and ROS signaling: lessons from the uncoupling proteins. Trends Endocrinol. Metab. 23, 451–458 (2012)

Moleirinho, S., Chang, N., Sims, A.H., Tilston-Lünel, A.M., Angus, L., Steele, A., Boswell, V., Barnett, S.C., Ormandy, C., Faratian, D., Gunn-Moore, F.J., Reynolds, P.A. KIBRA exhibits MST-independent functional regulation of the Hippo signaling pathway in mammals. Oncogene 32, 1821–1830 (2013)

Morinaka, A., Funato, Y., Uesugi, K., Miki, H. Oligomeric peroxiredoxin-I is an essential intermediate for p53 to activate MST1 kinase and apoptosis. Oncogene 30, 4208–4218 (2011)

Neto-Silva, R.M., de Beco, S., Johnston, L.A. Evidence for a growth-stabilizing regulatory feedback mechanism between Myc and Yorkie, the Drosophila homolog of Yap. Dev. Cell 19, 507–520 (2010)

Neuzil, J., Dong, L.F., Ramanathapuram, L., Hahn, T., Chladova, M., Wang, X.F., Zobalova, R., Prochazka, L., Gold, M., Freeman, R., Turanek, J., Akporiaye, E.T., Dyason, J.C., Ralph, S.J. Vitamin E analogues as a novel group of mitocans: anti-cancer agents that act by targeting mitochondria. Mol. Aspects Med. 28, 607–645 (2007a)

Neuzil, J., Dong, L.F., Rohlena, J., Truksa, J., Ralph, S.J. Classification of mitocans, anti-cancer drugs acting on mitochondria. Mitochondrion 13, 199-208 (2012)

Neuzil, J., Dyason, J.C., Freeman, R., Dong, L.F., Prochazka, L., Wang, X.F., Scheffler, I., Ralph, S.J. Mitocans as anti-cancer agents targeting mitochondria: lessons from studies with vitamin E analogues, inhibitors of complex II. J. Bioenerg. Biomembr. 39, 65–72 (2007b)

Neuzil, J., Massa, H. Hepatic processing determines dual activity of alpha-tocopheryl succinate: a novel paradigm for a shift in biological activity due to pro-vitamin-to-vitamin conversion. Biochem. Biophys. Res. Comm. 327, 1024–1027 (2005)

Neuzil, J., Tomasetti, M., Mellick, A.S., Alleva, R., Salvatore, B.A., Birringer, M., Fariss, M.W. Vitamin E analogues: a new class of inducers of apoptosis with selective anti-cancer effects. Curr. Cancer Drug Targets 4, 355–372 (2004)

Neuzil, J., Weber, T., Gellert, N., Weber, C. Selective cancer cell killing by alpha-tocopheryl succinate. Br. J. Cancer 84, 87–89 (2001a)

Neuzil, J., Weber, T., Schröder, A., Lu, M., Ostermann, G., Gellert, N., Mayne, G.C., Olejnicka, B., Nègre-Salvayre, A., Stícha, M., Coffey, R.J., Weber, C. Induction of cancer cell apoptosis by alpha-tocopheryl succinate: molecular pathways and structural requirements. FASEB J. 15, 403–415 (2001b)

Neuzil, J., Zhao, M., Ostermann, G., Sticha, M., Gellert, N., Weber, C., Eaton, J.W., Brunk, U.T. Alpha-tocopheryl succinate, an agent with in vivo anti-tumour activity, induces apoptosis by causing lysosomal instability. Biochem. J. 362, 709–715 (2002)

Nicklin, P., Bergman, P., Zhang, B., Triantafellow, E., Wang, H., Nyfeler, B., Yang, H., Hild, M., Kung, C., Wilson, C., Myer, V.E., MacKeigan, J.P., Porter, J.A., Wang,

Y.K., Cantley, L.C., Finan, P.M., Murphy, L.O. Bidirectional transport of amino acids regulates mTOR and autophagy. Cell 136, 521–534 (2009)

Ogretmen, B., Hannun, Y.A. Biologically active sphingolipids in cancer pathogenesis and treatment. Nat. Rev. Cancer 4, 604–616 (2004)

Oh, H., Irvine, K.D. Yorkie: the final destination of Hippo signaling. Trends Cell Biol. 20, 410–417 (2010)

Orr, B.A., Bai, H., Odia, Y., Jain, D., Anders, R.A., Eberhart, C.G. Yes-associated protein 1 is widely expressed in human brain tumors and promotes glioblastoma growth. J. Neuropathol. Exp. Neurol. 70, 568–577 (2011)

Osthus, R.C., Shim, H., Kim, S., Li, Q., Reddy, R., Mukherjee, M., Xu, Y., Wonsey, D., Lee, L.A., Dang, C.V. Deregulation of glucose transporter 1 and glycolytic gene expression by c-Myc. J. Biol. Chem. 275, 21797–21800 (2000)

Pan, D. The hippo signaling pathway in development and cancer. Dev. Cell 19, 491–505 (2010)

Pan, Y., Mansfield, K.D., Bertozzi, C.C., Rudenko, V., Chan, D.A., Giaccia, A.J., Simon, M.C. Multiple factors affecting cellular redox status and energy metabolism modulate hypoxia-inducible factor prolyl hydroxylase activity in vivo and in vitro. Mol. Cell. Biol. 27, 912–925 (2007)

Park, B.H., Lee, Y.H. Phosphorylation of SAV1 by mammalian ste20-like kinase promotes cell death. BMB reports 44, 584–589 (2011)

Parsons, D.W. et al. An integrated genomic analysis of human glioblastoma multiforme. Science 321, 1807–1812 (2008)

Pop, C., Salvesen, G.S. Human caspases: activation, specificity, and regulation. J. Biol. Chem. 284, 21777–21781 (2009)

Praskova, M., Khoklatchev, A., Ortiz-Vega, S., Avruch, J. Regulation of the MST1 kinase by autophosphorylation, by the growth inhibitory proteins, RASSF1 and NORE1, and by Ras. Biochem. J. 381, 453–462 (2004)

Praskova, M., Xia, F., Avruch, J. MOBKL1A/MOBKL1B phosphorylation by MST1 and MST2 inhibits cell proliferation. Curr. Biol. 18, 311–321 (2008)

Prochazka, L., Dong, L.F., Valis, K., Freeman, R., Ralph, S.J., Turanek, J., Neuzil, J. alpha-Tocopheryl succinate causes mitochondrial permeabilization by preferential formation of Bak channels. Apoptosis 15, 782–794 (2010)

Pussinen, P.J., Lindner, H., Glatter, O., Reicher, H., Kostner, G.M., Wintersperger, A., Malle, E., Sattler, W. Lipoprotein-associated alpha-tocopheryl-succinate inhibits cell growth and induces apoptosis in human MCF-7 and HBL-100 breast cancer cells. Biochim. Biophys. Acta 1485, 129–144 (2000)

Radu, M., Chernoff, J. The DeMSTification of mammalian Ste20 kinases. Curr. Biol. 19, 421–425 (2009)

Rodríguez-Enríquez, S., Hernández-Esquivel, L., Marín-Hernández, A., Dong, L.F., Akporiaye, E.T., Neuzil, J., Ralph, S.J., Moreno-Sánchez, R. Molecular mechanism for the selective impairment of cancer mitochondrial function by a mitochondrially targeted vitamin E analogue. Biochim. Biophys. Acta 1817, 1597–1607 (2012)

Rodríguez-Enríquez, S., Marín-Hernández, A., Gallardo-Pérez, J.C., Carreño-Fuentes, L., Moreno-Sánchez, R. Targeting of cancer energy metabolism. Mol. Nutr. Food Res. 53, 29–48 (2009)

Sen, C.K., Khanna, S., Roy, S. Tocotrienols: Vitamin E beyond tocopherols. Life Sci. 78, 2088–2098 (2006)

Sherr, C.J. Principles of Tumor Suppression. Cell 116, 235–246 (2004)

Shiau, C.W., Huang, J.W., Wang, D.S., Weng, J.R., Yang, C.C., Lin, C.H., Li, C., Chen, C.S. alpha-Tocopheryl succinate induces apoptosis in prostate cancer cells in part through inhibition of Bcl-xL/Bcl-2 function. J. Biol. Chem. 281, 11819–11825 (2006)

Schneider, U., Schwenk, H.U., Bornkamm, G. Characterization of EBV-genome negative "null" and "T" cell lines derived from children with acute lymphoblastic leukemia and leukemic transformed non-Hodgkin lymphoma. Inter. J. Cancer 19, 621–626 (1977)

Siegel, R., Naishadham, D., Jemal, A. Cancer statistics, 2012. CA. Cancer J. Clin. 62, 10–29 (2012)

Stein, W.H., Moore, S. The free amino acids of human blood plasma. J. Biol. Chem. 211, 915–926. (1954)

Steinhardt, A.A., Gayyed, M.F., Klein, A.P., Dong, J., Maitra, A., Pan, D., Montgomery, E.A., Anders, R.A. Expression of Yes-associated protein in common solid tumors. Human Pathol. 39, 1582–1589 (2008)

Sudol, M., Harvey, K.F. Modularity in the Hippo signaling pathway. Trends Biochem. Sci. 35, 627–633 (2010)

Takahashi, K., Yamanaka, S. Induction of pluripotent stem cells from mouse embryonic and adult fibroblast cultures by defined factors. Cell 126, 663–676 (2006)

Taylor, R.C., Cullen, S.P., Martin, S.J. Apoptosis: controlled demolition at the cellular level. Mol. Cell Biol. 9, 231–241 (2008)

Ura, S., Masuyama, N., Graves, J.D., Gotoh, Y. Caspase cleavage of MST1 promotes nuclear translocation and chromatin condensation. Proc. Natl. Acad. Sci. USA 98, 10148–10153 (2001)

Valis, K., Prochazka, L., Boura, E., Chladova, J., Obsil, T., Rohlena, J., Truksa, J., Dong, L.F., Ralph, S.J., Neuzil, J. Hippo/Mst1 stimulates transcription of the proapoptotic mediator NOXA in a FoxO1-dependent manner. Cancer Res. 71, 946–954 (2011)

Vander Heiden, M.G., Cantley, L.C., Thompson, C.B. Understanding the Warburg effect: the metabolic requirements of cell proliferation. Science 324, 1029–1033 (2009)

Vermes, I., Haanen, C., Steffens-Nakken, H., Reutelingsperger, C. A novel assay for apoptosis. Flow cytometric detection of phosphatidylserine expression on early apoptotic cells using fluorescein labelled Annexin V. J. Immunol. Methods 184, 39–51 (1995)

Voet, D., Voet, J.G. Biochemistry, 3rd edition, Wiley, New York (2004)

Wang, H., Mannava, S., Grachtchouk, V., Zhuang, D., Soengas, M.S., Gudkov, A.V., Prochownik, E.V., Nikiforov, M.A. c-Myc depletion inhibits proliferation of human tumor cells at various stages of the cell cycle. Oncogene 27, 1905–1915 (2008)

Wang, L., Shi, S., Guo, Z., Zhang, X., Han, S., Yang, A., Wen, W., Zhu, Q. Overexpression of YAP and TAZ Is an Independent Predictor of Prognosis in Colorectal Cancer and Related to the Proliferation and Metastasis of Colon Cancer Cells. Human Pathol. 43, 1376–1389 (2013)

Wang, T., Marquardt, C., Foker, J. Aerobic glycolysis during lymphocyte proliferation. Nature 261, 702–705 (1976)

Wang, X.F., Dong, L., Zhao, Y., Tomasetti, M., Wu, K., Neuzil, J. Vitamin E analogues as anticancer agents: lessons from studies with alpha-tocopheryl succinate. Mol. Nutr. Food Res. 50, 675–685 (2006)

Wang, X.F., Witting, P.K., Salvatore, B.A., Neuzil, J. Vitamin E analogs trigger apoptosis in HER2/erbB2-overexpressing breast cancer cells by signaling via the mitochondrial pathway. Biochem. Biophys. Res. Commun. 326, 282–289 (2005)

Warburg, O. Injuring of Respiration the Origin of Cancer Cells. Science 123, 309–314 (1956)

Warburg, O., Wind, F., Negelein, E. The metabolism of tumors in the body. J. Gen. Physiol. 8, 519–530 (1927)

Watabe, M., Kakeya, H., Osada, H. Requirement of protein kinase (Krs/MST) activation for MT-21-induced apoptosis. Oncogene 18, 5211–5220 (1999)

Wen, W., Zhu, F., Zhang, J., Keum, Y.S., Zykova, T., Yao, K., Peng, C., Zheng, D., Cho, Y.Y., Ma, W., Bode, A.M., Dong, Z. MST1 promotes apoptosis through phosphorylation of histone H2AX. J. Biol. Chem. 285, 39108–39116 (2010)

Wiechelman, K.J., Braun, R.D., Fitzpatrick, J.D. Investigation of the bicinchoninic acid protein assay: identification of the groups responsible for color formation. Anal. Biochem. 175, 231–237 (1988)

Willecke, M., Hamaratoglu, F., Sansores-Garcia, L., Tao, C., Halder, G. Boundaries of Dachsous Cadherin activity modulate the Hippo signaling pathway to induce cell proliferation. Proc. Natl. Acad. Sci. USA 105, 14897–14902 (2008)

Wise, D.R., DeBerardinis, R.J., Mancuso, A., Sayed, N., Zhang, X.Y., Pfeiffer, H.K., Nissim, I., Daikhin, E., Yudkoff, M., McMahon, S.B., Thompson, C.B. Myc regulates a transcriptional program that stimulates mitochondrial glutaminolysis and leads to glutamine addiction. Proc. Natl. Acad. Sci. USA 105, 18782–18787 (2008)

Wise, D.R., Thompson, C.B. Glutamine Addiction: A New Therapeutic Target in Cancer. Trends Biochem. Sci. 35, 427–433 (2011)

Xu, M.Z., Yao, T.J., Lee, N.P.Y., NgI, O.L., Chan, Y.T., Zender, L., Lowe, S.W., Poon, R.T.P., Luk, J.M. Yes-associated protein is an independent prognostic marker in hepatocellular carcinoma. Cancer 115, 4576–4585 (2009)

Yu, J., Zheng, Y., Dong, J., Klusza, S., Deng, W.M., Pan, D. Kibra functions as a tumor suppressor protein that regulates Hippo signaling in conjunction with Merlin and Expanded. Dev. Cell 18, 288–299 (2010)

Yuan, Z., Lehtinen, M.K., Merlo, P., Villén, J., Gygi, S., Bonni, A. Regulation of neuronal cell death by MST1-FOXO1 signaling. J. Biol. Chem. 284, 11285–11292 (2009)

Zhang, N., Bai, H., David, K.K., Dong, J., Zheng, Y., Cai, J., Giovannini, M., Liu, P., Anders, R.A., Pan, D. The Merlin/NF2 tumor suppressor functions through the YAP oncoprotein to regulate tissue homeostasis in mammals. Dev. Cell 19, 27–38 (2010)

Zhang, X., Tang, N., Hadden, T.J., Rishi, A.K. Akt, FoxO and regulation of apoptosis. Biochim. Biophys. Acta 1813, 1978–1986 (2011)

Zhao, B., Lei, Q.Y., Guan, K.L. The Hippo-YAP pathway: new connections between regulation of organ size and cancer. Curr. Opin. Cell Biol. 20, 638–646 (2008)

Zhao, B., Li, L., Lei, Q., Guan, K. The Hippo – YAP pathway in organ size control and tumorigenesis: an updated version. Gen. Dev. 24, 862–874 (2010a)

Zhao, B., Li, L., Tumaneng, K., Wang, C., Guan, K. A coordinated phosphorylation by Lats and CK1 regulates YAP stability through SCFbeta-TRCP. Genes. Dev. 24, 72–85 (2010b)

Zhou, D., Conrad, C., Xia, F., Park, J.S., Payer, B., Yin, Y., Lauwers, G.Y., Thasler, W., Lee, J.T., Avruch, J., Bardeesy, N. Mst1 and Mst2 maintain hepatocyte quiescence and suppress hepatocellular carcinoma development through inactivation of the Yap1 oncogene. Cancer Cell 16, 425–438 (2009)

Ziosi, M., Baena-López, L.A., Grifoni, D., Froldi, F., Pession, A., Garoia, F., Trotta, V., Bellosta, P., Cavicchi, S., Pession, A. dMyc functions downstream of Yorkie to promote the supercompetitive behavior of hippo pathway mutant cells. PLoS Genet. 6, 1–11 (2010)

I agree with the lending of this work for study purposes and I ask for the proper record of the borrowers.

Name and surname with address	Number of OP	Date of rental	Note